Species-Specific, Site-Sensitive Stand Carrying Capacity Models and Future Climate Forecasting for Pacific Northwest Conifer Forests

A Dissertation
Presented in Partial Fulfillment of the Requirements for the
Degree of Doctor of Philosophy
with a
Major in Natural Resources
in the
College of Graduate Studies
University of Idaho
by

Ryan R. Heiderman

Major Professor: Mark Kimsey, Ph.D.
Committee Members: Andrew Nelson, Ph.D.; Paul Gessler, Ph.D.; Janet Rachlow, Ph.D.
Department Administrator: Charles Goebel, Ph.D.

May 2021

Authorization to Submit Dissertation

This dissertation of Ryan R. Heiderman, submitted for the degree of Doctor of Philosophy with a Major in Natural Resources and titled "Species-Specific, Site-Sensitive Stand Carrying Capacity Models and Future Climate Forecasting for Pacific Northwest Conifer Forests," has been reviewed in final form. Permission, as indicated by the signatures and dates below, is now granted to submit final copies to the College of Graduate Studies for approval.

Major Professor: Mark Kimsey Date: 2/3/2021
Mark Kimsey, Ph.D.

Committee Members: Andrew Nelson Date: 2/3/2021
Andrew Nelson, Ph.D.

Paul Gessler Date: 2/3/2021
Paul Gessler, Ph.D.

Janet Rachlow Date: 2/3/2021
Janet Rachlow, Ph.D.

Department Administrator: Charles Goebel Date: 2/19/2021
Charles Goebel, Ph.D.

Abstract

Maximum stand density index (SDI_{MAX}) models were developed for important Pacific Northwest conifers of western Oregon and Washington, USA, based on site and species influences and interactions. Inventory and monitoring data from numerous federal, state and private forest management groups were obtained throughout the region to ensure a wide coverage of site characteristics. These observations include information on tree size, number and species composition. The effects and influence on the self-thinning frontier of plot-specific factors, such as climate, topography, soils and geology, as well as species composition, were evaluated based on geographic location using a multistep modelling approach. The influence of climatic variables was explored further in the context of potential future climate scenarios. Future climate projections based on global circulation models under different representative concentration pathways were utilized in a space-for-time substitution within an ensemble learning model to understand potential shifts, both magnitude and direction, in modelled SDI_{MAX}. Further issues of model sensitivity to both spatial errors associated with input plot locations, as well as diameter cutoffs and calculations, were explored. The regional model of site-specific SDI_{MAX} will support forest managers in decision making regarding density management and species selection to more efficiently utilize site resources toward healthy, productive forests.

Acknowledgements

I wish to thank Dr. Mark Kimsey first and foremost for all his support throughout my graduate program here at the University of Idaho, and for all the great conversations we have had along the way. Also, to my committee members, Dr. Andrew Nelson, Dr. Paul Gessler and Dr. Janet Rachlow, for pushing me to think deeper and more thoroughly about my work. To Robyn Darbyshire and the U.S. Forest Service for supporting and funding this research. To all the Intermountain Forestry Cooperative members who provided inventory data used in the analyses of this project. To Drs. Jim Bockheim, Zakiya Leggett, Eric Kruger, Birl Lowery, Tom Gower, Joe Roise, Jose Stape, Ron Gehl, Rachel Cook, Janine Albaugh and to all the other mentors, professors, colleagues, teachers, family and friends who have inspired me throughout my educational journey. I wouldn't be where I find myself today without the passion, curiosity and desire to keep trying to figure out the world around me.

Dedication

To Blueberry and Muffin

Table of Contents

List of Figures

List of Tables

Chapter 1: Review of Forest Stand Carrying Capacity: Stand Density Index Modelling Methods and Application

Introduction

An understanding of density is critical for effective forest management. Density is a function of two variables, the number of plants and their size (Zeide, 2005). Through silvicultural prescriptions the density of a forest can be manipulated to achieve specific management objectives (Allen and Burkhart, 2018; Long, 1985). Many models attempt to determine the growth trajectory and mortality of a stand based on species and site-specific self-thinning lines that represent maximum carrying capacity. The maximum carrying capacity of a stand is an essential piece of information "for assessing site productivity, modelling and predicting stand dynamics, and silvicultural regulation." (Pretzsch and Biber, 2016)

Reineke (1933) described carrying capacity as the relationship between number of trees per unit area and their average diameter (dbh – diameter at breast height). When data from a sufficient number of stands with the same average dbh are obtained, the stand with the most trees per acre can be considered as having 100%, or maximum density. All other stands can be expressed as a percentage of this full density. Reineke plotted the log-log relationship of number of trees over average diameter to show the upper boundary as a straight, negative sloping line. A line was visually fit to this outer boundary and the number of trees that intersect at 10 inches is what Reineke called stand density index (SDI). There has been much discussion (Zeide, 2005, 2010; Curtis, 1970; Long and Smith, 1984; Zhang et al., 2005; Burkhart and Thome, 2012) and analysis (MacKinney and Chaiken, 1935; Sterba and Monserud, 1993; Woodall et. al, 2003; Weiskittel et. al, 2009; Vospernik and Sterba, 2015; Kimsey et. al, 2019) of the stand density index since Reineke first published his findings.

Yoda et al. (1963) showed through a variety of experiments on cultivated plants, grasses and road-side weeds that the pure stands cannot be more densely populated than a fixed limiting density and that when plant number was plotted against plant mass on a log-log relation, the slope of the self-

thinning line was “in every case nearly equal to -3/2 irrespectively of the difference in species.” Yoda’s -3/2 power law of self-thinning law, along with Reineke’s SDI, have been the basis for much forest density related research (Drew and Flewelling, 1977; Weller, 1987a; Zeide, 1987).

Species- and Site-Specific Self-thinning Lines

Reineke (1933) first described the self-thinning line utilizing log-log paper and visually fit a reference curve to the outer boundary. He concluded the slope of the line to be -1.605 and was invariant to tree species or site quality. Contrary to Reineke’s belief that the slope was constant, many subsequent investigations have revealed systematic variations in slope (Zeide, 1987). Sterba and Monserud (1993) express similar doubts by stating “Reineke’s -1.605 is a reasonable average over all species but is probably not quite right for any individual species.” In fact, MacKinney and Chaiken (1935) reanalyzed Reineke’s data for loblolly pine (*Pinus taeda)* just 2 years after his paper and found a slope of -1.7070. Since initial acceptance of the self-thinning rule, slope and intercept has been found to be much more variable (Bi et. al., 2000). Charru et. al. (2012) conclude, based on their findings of modelling the self-thinning line of 11 tree species, that “the significant between-species differences in the self-thinning allometric coefficient invalidates the hypothesis of a constant coefficient among species.” Pretzsch and Biber (2005) also find the species invariant slope questionable and caution that using the wrong slope coefficient could cause severe errors in stand density estimates.

Interestingly, Westoby (1984) pondered that “overall it is at present impossible to tell in what proportions the variation in slope among observed thinning lines is attributable to differences among species, differences among environmental conditions, or experimental error”. Many recent studies continue to explore this variation and have found species- and site-specific self-thinning lines, which are affected by important variables such as species composition, site topography, climatic inputs, soil properties and specific wood properties (Kimsey et. al., 2019; Andrews et.al., 2018; Aguirre et. al., 2018; Kweon and Comeau, 2017; Vospernik and Sterba, 2015; Zhang et. al., 2013; Weiskittel et. al.,

2009; Woodall et. al., 2005; Bi et. al, 2001). This literature review attempts to synthesize the current knowledge on controls and modelling approaches of the self-thinning boundary line.

Biological Controls of Self-thinning

As trees, in particular their canopies, grow, their demands on limited forest resources and growing space increases. This struggle between trees occurs when "the branch tips of the seedlings begin to touch and interfere with each other" and the success of individual trees depends on their ability "to keep their crowns in the light" (Frothingham, 1914). As such, the major drivers of self-thinning (i.e., density related mortality) in forest stands are growing space competition and self-tolerance. Yoda et. al. (1963) state as the overcrowded stand grows, the plant density becomes successively lower due to the competitive interaction between individuals and subsequent death of the suppressed. Beyond the initial establishment phase, increasing density with associated above- and below-ground competition diminishes growth of tree volume and diameter (Zeide, 2005). Initially, forest stand development is essentially free of intra- or interspecific competition during which time mortality is independent of density and therefore self-thinning only occurs when a site becomes fully occupied (Drew and Flewelling, 1977). Bi et. al. (2000) describe site occupancy as the extent to which the trees have occupied the growing space and utilized the available resources within the given environment for growth. They go on to describe a site as fully occupied when the stand has accumulated the maximum attainable biomass at that stand density where any further growth will incur mortality.

Leaf Shape and Crown Dimensions

Quite literally, there exists a limit of how much biomass can be packed into the canopy of a standing crop of plants, which ultimately leads to competition for space among individuals. Curtis (1970) states reduction in growth rate of the individual tree and change in distribution of growth among its parts is the manifestation of density related competition. Echoed by Zeide, (2005) "the proximity of trees and branches, their size and arrangement, distribution of foliage, form and depth of

roots, all these and many other factors bear on stand density." Westoby (1984) as well states "obvious features of ecosystems such as the quantity and spatial arrangement of plant stand crop" are important to consider when trying to understand density dynamics. Krajicek et. al. (1961) understood the importance of growing space competition and first described the crown competition factor (CCF) as an expression of stand density and is an estimate of the competition among crowns for growing space. CCF estimates the area available to the average tree in a stand in relation to the maximum area it could use if it were open grown. They demonstrated that the shape of the crown and relative self-tolerance determine the maximum densities attainable by a particular species. Dean and Baldwin (1996) present an equation of Reineke's SDI in terms of canopy metrics. They utilized the D-cubed law to express SDI in terms of mean leaf area per tree and mean live-crown ratio, and found 76% of variation of SDI in loblolly plantations could be explained as a function of these two metrics. Canopy growing space competition drives foliage to the top of crown, increasing the bending stress resulting in larger diameters and subsequent increase in SDI. Stress on the stem is also increased from smaller live crown ratios by increasing the leverage the crown exerts on the stem (Dean and Baldwin, 1996).

Longsdale and Watkinson (1983) experimented with plants of differing geometry to evaluate the differences in the self-thinning line under the hypothesis that canopy structure may have an influence on the position of the self-thinning line. They evaluated three plants of differing geometry, a dicot with tall erect stems and opposite leaves, an herbaceous dicot, and a perennial grass, and concluded that indeed plant geometry and in particular leaf shape influence self-thinning, finding the grass had a higher intercept than the dicots. Regarding trees, they state "one might expect canopy structure as well as leaf shape to be important in determining the intercept" of the self-thinning line. Harper (1977) showed that pyramidal trees have higher intercepts than round-crowned trees. Longsdale and Watkinson (1983) reason that "the pyramidal profile of conifers or, again, their narrow leaves improve the efficiency of light interception and allow close packing of plant material into a given volume of space or the development of a greater stand height before thinning commences."

Pyramidal trees are usually coniferous with narrow leaves (i.e., needles) and round-crowned are usually broad-leaved trees.

Throughout the literature, where values of SDI are reported, round-crowned hardwoods consistently report lower SDI than conifer species. For example, Andrews et al. (2018) reported mean predicted maximum SDI for northern hardwoods such as yellow birch (*Betula alleghaniensis* Britt.), sugar maple (*Acer saccharum Marsh.)* and American beech (*Fagus grandifolia* Ehrh.) to be the lowest compared to higher values for northern white cedar (*Thuja occidentalis* L.), eastern hemlock (*Tsuga candensis* (L.) Carr.) and eastern white pine (*Pinus strobus* L.). Bravo-Oviedo et al. (2018) reported a lower range of maximum SDI value for European beech (*Fagus sylvatica* L.) compared to the higher range of values for Scots pine (*Pinus sylvenstris* L.). Vospernik and Sterba (2015) found potential density of broadleaf species to be considerably lower than most pine, spruce and fir they studied with the exception of stone pine (*Pinus cembra* L.) having an unusually low max density compared to other pine species. Pretzsch and Biber (2005) found much steeper self-thinning lines for Norway spruce (*Picea abies* Karst.) and Scots pine compared to common oak (*Quercus petraea* [Mattuschka] Liebl.), although they found European beech could have a wide range of slopes, which they attribute to the self-tolerance of beech and the ability to quickly fill canopy gaps.

Shade Tolerance

There has been, and continues to be, much discussion regarding shade-tolerance and the effect on maximum SDI. Weller (1987b) found the slope of the self-thinning line to be significantly correlated with shade tolerance and concluded differences in thinning slopes are at least partly due to systematic biological differences between species. Jack and Long (1996) state, in general, shade-tolerant species have a greater intercept than intolerant species. They attribute this to the ability of shade-tolerant trees to have higher ‘packing density’ (plant biomass per growing space volume).

Assmann (1970) states the different light requirements of species in a mixed stand may produce greater assimilation efficiency in comparison to pure stands. A stand with an upper canopy of

light-demanding species and the intermediate and lower canopy of semi-shade-tolerant and shade-tolerant species, which are capable of utilizing the light that has been transmitted through the upper canopy, may produce an additive increment on density. Pretzsch and Biber (2016) found significant density gains when species associations included highly shade-tolerant species such as European Beech, or an intermediately shade-tolerant species such as Norway spruce mixed with a very light demanding species like European larch (*Larix decidua* Mill.). Pretzsch and Schutze (2016) found similar results of higher density in stands of mixed shade tolerance, which they attribute to the complementary ecological traits of light-demanding species in the upper canopy and shade-tolerant ones in the lower canopy.

Not all studies found such clear-cut relationships between shade tolerance and density. Weiskittel et. al. (2009) examined the self-thinning boundary line of three tree species of varying shade tolerance and found the steepness of the self-thinning slope did not follow shade tolerance rankings, although the extremely shade-tolerant western hemlock (*Tsuga heterophylla*) did have the steepest slope, red alder (*Alunus rubra* Bong.), a shade-intolerant hardwood had the shallowest. Kimsey et. al (2019) found steeper slopes when stands were composed of shade-intolerant ponderosa pine (*Pinus ponderosa* var. *ponderosa)* compared to stands containing intermediate Douglas-fir (*Pseudotsuga menziesii* [Mirbl] Franco var. *glauca* [Biessn.] Franco) and tolerant grand fir (*Abies grandis* [Douglas ex D. Don] Lindl. Var. *idahoensis)*. Aguierre et. al. (2018) found the "least pronounced" (i.e., shallowest) slopes in the two most shade-tolerant species of pine (*Pinus sylvestris* and *Pinus nigra)* that were studied on the Iberian Peninsula. Charru et. al. (2012) found a significant positive correlation between maximum density and shade tolerance. Vospernik and Sterba (2015) compared 10 tree species in Australia and could not find a relation of self-thinning slopes with shade tolerance. Charru et. al. (2012) found significant exceptions to the positive correlation between increasing shade tolerance and max density in Douglas-fir (*Pseudotsuga menziesii* Franco.), Scots pine and Corsican pine (*Pinus nigra* Arn. Subsp. l*aricio* (Poir.) Maire var. *Corsicana* (Loud.) Hyl.), which

"reached unexpectedly high densities given their low shade tolerance, suggesting that factors other than light resources may reduce stocking." Ducey et. al. (2017) found that in general, species with the lowest specific gravities could support the highest densities regardless of shade tolerance but that there was significant interaction of climatic variables with shade tolerance. They found that cooler temperatures are associated with the ability to sustain higher densities of shade-tolerant species. Bravo-Oviedo et. al. (2018) also found a similar interaction between climate and shade tolerance, but ultimately concluded the addition of a shade-tolerance value in the model to be non-significant.

Specific Gravity

Dean and Baldwin (1996) explored the relationship between the mechanical stress the canopy exerts on the stem and the physical properties of the wood of particular species. In their linear model, wood specific gravity accounted for 91% of the variation in maximum SDI. Woodall et. al. (2005) found plot level mean specific gravity explained 92% of the variation in maximum SDI. Andrews et. al. (2018) determined wood specific gravity to be the most important variable in hardwood maximum SDI model. Bravo-Oveido et. al. (2018) showed a significant relationship between specific gravity and stocking, in particular on colder sites. An inverse relationship between maximum SDI and increasing specific gravity is the general trend in all the aforementioned studies. Woodall et. al. (2005) explain that species with a low specific gravity are more limited in the amount of foliage they can support when compared to species with higher specific gravity. Low specific gravity tree species must have a greater density to support the maximum leaf area the site can handle, whereas high specific gravity trees can carry more foliage per tree and require lower densities to fully capture the leaf area. Ducey and Knapp (2010) conclude from their study of SDI of mixed-species forest in the northeastern US that "specific gravity can be a powerful predictor" of density but that clearly other factors are important which are "related to the competitive dynamics of trees in mixed-species forests."

Drought Tolerance

Niinemets et. al. (2006) demonstrated there are often negative correlations between drought and shade tolerance, with only 2.6-10.3% of species investigated being relatively tolerant to two environmental stresses simultaneously, indicating ecological trade-offs between tolerance to differing environmental limitations. Bravo-Oviedo et. al. (2018) found the influence of drought tolerance to be significant in their model of maximum density. Their results indicated a trade-off between drought and shade tolerance depending on site conditions and that tolerance actually reduces "the number of individuals needed to make full use of resources." Their results showed the warmer the site, the greater presence of drought tolerant species and subsequent reduction in density. Aguirre et. al. (2018) included the Martonne aridity index in their maximum density model, and found significant, specie-specific responses in all five species of pine, indicating species-specific variation in drought tolerance. The greatest improvement with the inclusion of the aridity index was to the *Pinus halepensis* model and is attributed to this species' high adaptation to water stress.

Environmental Controls of Self-thinning

The intercept and slope of the self-thinning line varies with site specific environmental factors such as topography, climate and soils. Aguierre et. al. (2018) state, at large scales, including environmental variables in a density model might be crucial in explaining the variability of the self-thinning line over large environmental gradients. Vospernik and Sterba (2015) found, in general, larger intercepts in stands grown on more productive land. Pretzsch and Biber (2005) describe the limiting boundary, or self-thinning line, as the maximum density of individuals at a given size under optimal site conditions, where any boundary lower than this line would signify a stand under suboptimal growth conditions. Kimsey et. al. (2019) suggest sites with greater growth resources are capable of not only higher growth rates but also greater maximum carrying capacity than sites with fewer resources. The presence and availability of resources is strongly influenced by site-specific environmental variables.

Climate

Water and sunlight (i.e., photosynthetically active radiation) are essential for sustaining forest ecosystems. The amount, spatial distribution and timing of precipitation and sunlight strongly influence ecosystem structure and functioning (Chapin et. al., 2011). Other factors held equal, a decrease in precipitation or an increase in temperature results in increased evapotranspiration and susceptibility to drought stress (Abtew and Melesse, 2012). Condes et. al. (2017) showed the Martonne aridity index had significant and species-specific effects on maximum carrying capacity of pure Scots pine and European beech stands. Aguirre et. al. (2018) also showed that including the Martonne aridity index in their maximum SDI model improved results for the five *Pinus* species studied. Henniger et. al. (2017) found average growing season temperature and frost-free days to be significant explanatory variables of biomass growth in the Acadian Forest Region of the USA. Andrews et. al. (2018) found important species-specific interaction of growing season precipitation, annual degree-days > 5°C and < 0°C, as well as the interactions between growing season precipitation and the mean temperature in the coldest month on maximum SDI in the same region. Kweon and Comeau (2017) found the intercept of the self-thinning line to be strongly influenced by climate variables associated with evapotranspiration and water balance in trembling aspen stands (*Populus tremuloides* Michx.). Kimsey et. al. (2019) found across all species maximum SDI intercepts increased with reductions in annual dryness index, higher summer precipitation and warmer winters. The maximum SDI model of Ducey and Woodall (2017) included three climate variables with significant interaction with species specific gravity and shade tolerance. They found minimum annual temperature and shorter growing season length are associated with higher densities of shade tolerant species.

Day Length and Light Availability

While it is clear that light levels strongly control photosynthesis, light availability also has an influence on the self-thinning rate. Westoby (1984) attributes the density limit to ultimately depend on light interception. Kays and Harper (1974) experimented on perennial ryegrass (*Lolium perenne*) *at*

different densities and light levels, and found no difference in the slope of the self-thinning line between grasses grown in full light and 70% sunlight. However, they found the self-thinning slope of grass grown under the heaviest shade conditions (30% light intensity) flattened to around -1. Longsdale and Watkinson (1982) duplicated the ryegrass experiment and found the degree of shading altered the intercept of the self-thinning line but did not affect the slope. In another experiment, Longsdale and Watkinson (1983), from their study of plant geometry and light levels, conclude there is "strong evidence that the seasonal variation in the amount and quality of incident light can significantly affect the position of the self-thinning line." Westoby (1984) comments on the typical presence of large numbers of shade tolerant plants in the forest understory, which are often assumed "to persist for long periods, making only very slow growth but not dying", until they are released. Interestingly, he argues that there are actually high mortality rates and suggests "the continuous presence of large number of such seedlings in forest understories is due to continual recruitment more than high persistence."

Topography

Moisture and sunlight are the primary drivers of tree growth but are significantly modified by slope, aspect and elevation. Topography strongly determines vegetation distribution and influences site potential in many ways. Humboldt (1807) describes (through translation) in his Essay on the Geography of Plants,

> "When one ascends from sea level to the peaks of high mountains, one can see a gradual change in the appearance of the land and in the various physical phenomena in the atmosphere."

He continues.

> "As we go further away from sea level the temperature and pressure of the air diminish. [The] altitude also influences the intensity of the sun's rays traversing the atmosphere, and the refraction of the rays as they travel through it."

The influence of elevation on temperature and precipitation is apparent (Daubenmire, 1943); however, these climatic factors are further modified by slope and aspect. A relationship between growth, elevation and aspect is based on underlying processes related to the influence of elevation and aspect on incoming solar energy and water availability (Roise and Betters, 1981). Slope and aspect are critical components influencing the amount of incident solar radiation on a site (Coops et. al, 2000). Stage (1976) determined aspect, which is further modified by slope, to be important indicators of site productivity of western white pine (*Pinus monticola* Dougl.) in northern Idaho. Kimsey et. al. (2008) examined the influence of site factors on Douglas-fir site index, and found elevation, slope and aspect to strongly impact productivity. Weiskittel et. al. (2009) found the self-thinning line of red alder in the Pacific Northwest USA to be significantly influenced by site aspect with the intercept much lower on north-facing slopes than on south-facing slopes. Kimsey et al. (2019) found within the Inland Northwestern USA, where seasonal drought is common, maximum SDI generally increased on northerly facing slopes, which have lower evapotranspiration rates and where winter snow pack tends to last longer.

Factor compensation, as explained by Cooper et. al. (1991), explains why certain vegetative communities will occur on different topographic features. Daubenmire (1980) describes a relatively xerophytic (dry) community on the south slope and a more mesophytic (moderate) community on the north slope of the Palouse Range near Moscow, Idaho. A specific example is that of Douglas-fir communities that shift from the warmer, dry, south-facing slopes of Northern Idaho, where precipitation is relatively high, to steeper north-facing slopes east of the Continental Divide in Montana where precipitation is lower and the northerly aspects retain moisture longer into the growing season (Cooper et. al., 1991).

Another important example of topography modifying climate is illustrated by frost pockets found in valley floors. Daubenmire (1980) describes frost pockets as cold air drainage down a valley into the narrow gaps where pools of cold air accumulate at night. Frost pockets allow for trees typically found at higher elevation to descend into lower altitude areas. Daubenmire (1980) gives an example of this microclimate phenomenon by describing the islands of *Thuja plicata*, which can extend down into deep valleys where they abruptly terminate at the edge of the terrace. He concludes, "clearly topographic influences on microclimate are so strong and pervasive…that references to elevation above sea level [alone] have very low value for indicating the nature of the environment".

Soils

Soils influence site quality in many ways, including water holding capacity, nutrient availability and rooting depth. The significance of water availability on site quality and carrying capacity can be directly influenced by the soils present. Kimsey et. al. (2019) found soil parent material to have an important effect on stand density, in particular the presence of a volcanic ash cap significantly increased maximum SDI for all species studied. They attribute the increase in carry capacity of ash-influenced soils to the increased water holding capacity of volcanic ash. Binkley (1984) showed the effect of soil fertility on maximum size density relationships in Douglas-fir/red alder stands. The most fertile site, as expressed by the highest site index, had the greatest maximum size-density relationship and dropped off from this ceiling with decreasing fertility.

Modelling Stand Density Index

"When examining bivariate data, scatter diagrams illustrate associative relationships…and have historically proven useful for exploring a diversity of ecological phenomena" (Scharf et al. 1998). Reineke (1933) explored such an association when he first plotted the log-log relationship of number of trees on average diameter and noticed the outer boundary assumes a straight line form. Reineke proposed SDI as a stand density assessment tool where the number of trees at the reference diameter of 10 inches is formulated as:

$$SDI = N\left(\frac{QMD}{10}\right)^{b}$$

Where N is the number of trees per unit area, QMD is quadratic mean diameter and b is the slope parameter of the self-thinning line. This index allowed for comparison of densities between stands of similar species and region, however, to compare between various species and site types, SDI should be expressed in relation to a maximum (Zeide, 2010). Maximum SDI can be expressed as the maximum density that can exist for a particular average tree size. Knowledge of the maximum SDI and the current SDI would then allow for a calculation of stocking or relative density (Drew and Flewelling, 1979). Modelling and statistical techniques have come a long way since Reineke hand fit a line, on paper, to the outer edge of his scatter plots.

Plot Selection Criteria

A key aspect in determining maximum SDI is data selection, that is, selecting plot data from stands that are currently undergoing density related mortality. Bi and Tuvey (1997) remark "a problem that has always existed in self-thinning studies is the lack of objectivity in determining which data points to include when fitting the maximum biomass-density line." Lee and Choi (2019) describe this difficulty, "a key implication is that analyzing maximum size-density relationships is difficult…when analysts cannot be sure whether sample plots are at a self-thinning frontier." Burkhart (2013) ponders on how to objectively determine which observations are at the maximum; he states "the maximum size-density relationship that results from fitting data depends on how the data are screened to determine which observations are at the maximum and what fitting procedure is applied."

Mohler et al. (1978) describes the consequences of plot selection: "First…if sampled prior [to density-induced] thinning, these plots will have a low density for their mean [size] and will fall below the thinning line toward the middle of the usual log-log diagram. Second, in some young sample plots the populations may not have attained a sufficient size for crowding to have produced a change in density…Third, if density-independent mortality is acting on the population, some plots will have a

density below what would be predicted from their mean plant [size].” They continue “inclusion of plots not fully thinning due to lack of time for growth will result in an estimated slope which is too steep…Inclusion of plots not thinning due to low initial densities may or may not change the slope but will lower the intercept. Finally, inclusion of senescent plots will result in an estimated slope which is too shallow.”

Reineke selected plots by hand-fitting a line to the outer edge of his data, this method, although considered arbitrary and subjective (Weller, 1987b; Zhang et al., 2005) is still utilized as a ‘first step’ (Burkhart, 2013) in examining data in self-thinning studies. Bi et al. (2000) describe the early methods of choosing data points that “lie close to an arbitrarily visualized upper boundary before the line is estimated, and to subjectively eliminate data points from populations that are believed to be not undergoing density-dependent mortality.” VanderSchaaf and Burkhart (2007) utilized “a visual inspection of all plots…to ensure only those observations occurring along [the] dynamic thinning line boundary were included” in their analysis. Zhang et al. (2005) in their evaluation of various techniques of plot selection demonstrated the use of the visualization technique when they “purposefully selected two data points that lay close to a visualized upper boundary for all available points” and simply fit a linear regression between the two points.

Hutchings and Budd (1981a) in deciding which plots to include, utilized repeat counts of density on their experimental plots of red clover, and only included populations “whose density appeared to be declining exponentially” in their calculations, which they admit “still requires some subjectivism.” West (1982) made use of repeated measurements of *Eucalyptus* forests in Tasmania and chose only plots from stands “having substantial and continuing competition-induced mortality and which therefore appeared to be at maximum density”, which he defined as “generally more than 1% of trees dying per year”. West and Borough (1983) make use of repeated measures and only selected plots “for which at least 10 per cent of the trees present in the plot at planting had died by the time of the measurement.” They go on to acknowledge “the value of 10 per cent was chosen arbitrarily to

indicate that ‘substantial’ mortality had occurred.” Puettmann, Hann and Hibbs (1993) used data from repeated measurement periods on stands of pure red alder and pure Douglas-fir, and only included plots in their analysis “which had no signs of past disturbance and exhibited mortality during the measurement periods.” The use of repeated measures to determine if a forest stand is undergoing self-thinning was employed by Poage et al. (2007) in hemlock-spruce stands in Alaska, where multiple observations of TPA and QMD over time were available. Only plots where the trajectory (on log-log basis) began to curve were used. Begin et al. (2001) utilized repeated measures to eliminate plots “showing an increase in density between two measures.”

Some methods have no formal statistical basis, as in Mohler et al. (1978) where in one case, field notes were relied upon to eliminate plots which had clear density-independent mortality. Prezsch and Biber (2016) made use of detailed stand history to select “only unthinned or slightly thinned plots to represent conditions at or close to maximum density” and verified this in the field by the “absence of stumps and presence of dead standing trees, both indicating approximate maximum stand density.”

Many methods have been proposed for how to overcome the subjective data selection criteria. Bi and Turvey (1997) proposed what is known as ‘the interval method’, which involves dividing the range of log density into a specified number of equal intervals, then the data points having the maximum tree size in each interval are selected. They repeated this selection method by varying the number of intervals. Soloman and Zhang (2002) only included plots with a relative density (RD) greater than 0.7, which they admit is an arbitrary threshold. Zhang et al. (2005) used an RD threshold of 0.85. Kweon and Comeau (2017) removed measurements with an RD below 0.4. Monserud, Ledermann and Sterba (2005) included only plots “showing full crown closure and an SDI (using Reineke’s slope value of -1.605) value greater than 700.” Burkhart (2013) utilized normal yield tables to screen his data with targeted values of relative spacing and stand density index (using Reineke’s slope value). Condes et al. (2017) utilized quantile regression to discard plots “located in open forests that would be of no interest for the purpose of estimating” the maximum size-density relationship.

Their method involved fitting two quantile regressions (of tau = 0.5) between basal area and an aridity index, as well as a ratio of dominant height-QMD and the aridity index. “All plots which, for a given M [the aridity index], presented values for a basal area or [height:QMD] ratio of less than half of those expected were removed from the sample”, which they determined represented plots growing at low densities.

Reyes-Hernandez et al. (2013) utilized a two-step process to determine which plots in their dataset were within the density-dependent stage of self-thinning. A model with both a linear and non-linear segment was fit to plots with at least five remeasurements, then determined if a plot had reached the self-thinning phase based on criteria regarding the slope coefficients of each segment. They also acknowledge “a visual inspection of points was also performed so that only those observations that were showing trends that are consistent with the density-dependent mortality stage of the self-thinning trajectory were used for further analysis.” VanderSchaaf and Burkhart (2008) used a similar segmented regression approach to model different phases of the trajectory to “statistically determine what observations are within the generally accepted stages and phases of stand development.”

Zhang et al. (2005) proposes one way “to avoid subjectively selecting data points is to use all available points and fit the self-thinning line by appropriate regression techniques.” More recent studies exploring the self-thinning line utilize these techniques where no, or at least minimal, plot screening is performed *a priori* and the regression methods determine which plots are at the maximum.

Modelling Methods

The standard approach to modelling the self-thinning relationship in forest stands is linear regression of the following form:

$$\log(N) = \beta_0 + \beta_1 \log(QMD)$$

Where N is the number of trees per unit area, QMD is quadratic mean diameter and β_0 and β_1 are the intercept and slope parameters to be estimated. The important features of this linear relationship are the slope of the line, which is the thinning rate, and the intercept which implicitly accounts for site level variation, including species composition and physical site properties (Andrews et al., 2018). Reineke (1933) hand fit a line utilizing log-log paper along the outer boundary of the data to determine the slope and intercept of the line. MacKinney and Chaiken (1935) reanalyzed the same data using standard statistical techniques of regression to determine the slope and intercept. These early determinations were used as the basis to determine stocking by "dividing the actual number of trees [found in the stand of interest] by the number necessary for 100% stocking" (MacKinney and Chaiken, 1935). Burkhart (2013), after screening plots he considered at maximum, fit OLS regression to determine the slope and intercept of the self-thinning line in loblolly pine plantations of the southeastern United States. Comeau et al. (2010) used OLS regression to fit self-thinning lines in Sitka spruce (*Pieca sitchensis* (Bond.) Carr.) and Douglas-fir from Great Britain and Canada by first choosing plots they deemed at the maximum, then fit the "average" line and finally, to correct the intercept, moved this line parallel upward to the plot with the highest SDI value. Pretzsch and Biber (2005) used OLS regression to find the species specific slopes of common beech, Norway spruce, Scots pine and common oak in stands determined to be 'A-grade and fully stocked'.

Many methods have been developed to model the self-thinning line with an unbiased approach to plot selection (Bi et al., 2000; Zhang, 2005; VanderSchaaf and Burkhart, 2007). The methods discussed in the previous paragraph highlight regression methods of "arbitrarily hand fitting a line above an upper boundary of data points" (Zhang, 2005) and fitting an ordinary least squares through selected data points thought to be at maximum density. Beyond hand fitting and OLS, coefficients of the self-thinning line have been estimated via frontier analysis (Bi et al., 2000; Weiskittel et al., 2009; Comeau et al., 2010; Charru et al., 2012; Kweon and Comeau, 2017; Kimsey et al., 2019), quantile regression (Ducey and Knapp, 2010; Vospernik and Sterba, 2015; Condes et al., 2017; Aguirre, del

Rio and Condes, 2018; Bravo-Oveido et al., 2018), linear quantile mixed models (Andrews et al., 2018), major axis reduction and principal component analysis (Mohler et al., 1978; Hutchings and Budd, 1981b; Begin et al., 2001), and linear mixed models (Kweon and Comeau, 2017). Some of these methods will be discussed below.

Frontier Analysis

Frontier analysis is an econometric approach to "expressing the maximum amount of output obtainable from given input" (Aigner, Lovell and Schmidt, 1977). Farrell (1957), in his pioneering work on technical efficiency, set out to provide "a satisfactory measure of productive efficiency" when he developed the efficient production function. Farrell believed the use of average productivity of labor, the common approach of the time, to be a wholly unsatisfactory measure of true efficiency. Instead, he developed a method of incorporating all combinations of inputs (not defined by the weighted averages that were currently "enjoying an extensive popular vogue") to find the measure of technical efficiency. Interestingly, in his example application to American agricultural data, he notes that the production efficiency is more than the four factors he incorporated in his model of land area, labor, materials and capital, and that undefined inputs of climate and fertility affect the differences in efficiency. Perhaps Farrell was aware of the future application of his frontier function to ecological concepts such as the maximum carrying capacity of a forest stand.

Aigner, Lovell and Schmidt (1977) built upon the theory and empirical work of Farrell, to develop a "new approach to the estimation of frontier production functions" which utilizes a two component error term, "one normal and the other from a one-sided distribution." This frontier function is considered stochastic, as opposed to deterministic, due to the two-part error term which allows some observations to lie above the maximum boundary and is expressed as:

$$\varepsilon_i = v_i + u_i$$

Where v_i and u_i are unobservable random errors (Battese and Corra, 1977). v_i is assumed identically and independently distributed as normal with mean of 0 and variance as σ_v^2. This error term is interpreted as the random effects of both favorable and unfavorable conditions which affect performance, as well as any associated measurement error. The error term u_i, is the non-positive disturbance function assumed half-normal and distributed independently of v_i with variance as σ_u^2. This error term is interpreted as the deviation from the maximum output. When u_i is equal to 0, the output, or trajectory has reached maximum.

With respect to the self-thinning boundary, the first error term is the result of the site factors discussed previously such as climate and topography, as well as the characteristics of the tree species present such as size (QMD), crown architecture, specific gravity and tolerance to shade, drought and cold temperatures. This error term also encompasses any measurement error associated with these factors. The second error term reflects the fact that a stands trajectory has not reached the maximum boundary line, that is any observation not on the self-thinning boundary line will have u_i<0.

The maximum stand density index model can be formulated as follows

$$lnN = \beta_0 + \beta_1 lnQMD + \beta_i n_i + \varepsilon_i$$

Where *N* is trees per unit area, *QMD* is quadratic mean diameter –a measure of average tree size, β_0 is the intercept of the self-thinning line, β_1 is the slope of the self-thinning line, and β_i are model coefficients for the i^{th} site or species-specific covariate, n_i represents the value of the i^{th} site or species-specific covariate and ε_i is as defined above. The model utilizes all observations and is solved by maximum likelihood estimation with the error parameter assumptions as described above.

The variance parameter of the stochastic frontier function is:

$$\sigma^2 = \sigma_v^2 + \sigma_u^2$$

The variance ratio parameter is given by:

$$\gamma = \frac{\sigma_u^2}{\sigma_u^2+\sigma_v^2}$$

Where γ lies between 0 and 1. The value of γ can be interpreted as to the applicability of a stochastic frontier function. For example, if γ = 0 then the variance σ_u^2 = 0 and thus there would be no need to include u_i in the error term which would then allow the model to be estimated simply with OLS (Battese and Coelli, 1992). As γ approaches 1, the greater validity of the parameter estimations given by the stochastic frontier function. Weiskittel et al. (2009) reported γ values approaching 1 when using stochastic frontier analysis to model stand density of Douglas-fir, red alder and western hemlock in the pacific northwest and concluded the use of stochastic frontier analysis was warranted. Kimsey et al. (2019) modelled the maximum stand density for several conifer species of the inland northwest and found γ values near 1 in all models tested and concluded the use of stochastic frontier regression was appropriate. Kweon and Comeau (2017) reported γ values between 0.804 and 0.854 in their results of modeling the self-thinning boundary line of trembling aspen stands in Canada but did not comment on the implication of these values. Charru et al. (2012) utilized stochastic frontier analysis to model the self-thinning line of 11 temperate and Mediterranean tree species in France and reported γ values approaching 1 for many of the species models tested.

Quantile Regression

Koenker and Bassett (1978) proposed a robust method to estimate linear models using regression quantiles in cases where the use of ordinary least squares would be too sensitive to outliers and long tailed or non-Gaussian error distributions. Cade and Noon (2003) note that a "regression model with heterogeneous variances implies that there is not a single rate of change that characterizes changes in the probability distributions." Koenker and Hallock (2001) echo this notion when they state that the effect of covariates "may not be constant across the conditional distribution of the independent variable." Quantile regression allows for an estimation of the relationship of explanatory variables at any quantile of the response variable including near the upper bounds (Zhang et al., 2005),

which is where stands at maximum density will lie. Quantile regression has the benefit of not requiring subjective prescreening of plots at some assumed maximum density (Ducey and Knapp, 2010) and instead is fit to the "original unmodified data" (Scharf et al., 1998), where a chosen quantile (q - a percentage) splits the data where q observations fall below the line and 1-q fall above the line (Bravo-Oviedo et al., 2018). Where ordinary least squares regression provides an estimate of central tendency (the mean) by minimizing the squares of the residuals, quantile regression is fit by minimizing the sum of asymmetrically weighted least absolute values of the residuals (Koenker and Hallock, 2001)

The conditional median function is found with the 0.5 quantile, but any quantile of the dependent variable from 0 to 1 can be used which forces a certain percentage of observations to sit above and below the line. Scharf et al. (1998) note "the choice of which quantile best represents the boundaries of the data is an arbitrary one and must be made by the investigator." Vospernik and Sterba (2015) reasoned quantile regression was appropriate in their work with Norway spruce, European larch and European beech because the self-thinning line is a limiting boundary where the extreme is important and tested quantiles of 0.9, 0.95 and 0.99, and chose the highest quantile that had significant parameters. Condes et al. (2017) fit maximum size density relationships of Scots pine and European beech using quantiles of 0.95, 0.975 and 0.99 but made no mention on which was best suited for the data. However, they do comment that as the quantile value approaches 1, the fitting can become very sensitive to extreme values "especially for small datasets or if there are several co-variables in the models" and that a constant quantile should be utilized when comparing the self-thinning line between species or between models with different variables (Condes et al., 2017). Bravo-Oveido et al., (2018) tested multiple quantiles near 1 for models of relative density and utilized Schwarz's Bayesian Information Criteria (BIC) to determine that quantile 0.975 produced the model of best fit.

Quantile selection can be made based on which produces realistic results in accordance with published stocking recommendations. Aguirre et al. (2018) investigating the maximum size density relationship of pine species in Spain chose a quantile of 0.975 as a compromise between 0.95 which

found “excessively low maximum stand densities” compared to previous studies of similar species, and 0.99 which “resulted in models that did not fit properly to the data.” Ducey and Knapp (2010) selected quantiles that produced results which agreed with A-line stocking of the species of interest. For example, they used a quantile of 0.85 in their eastern white pine model because it was the closest in agreement with published density guidelines on the species. Ducey and Woodall (2017) used published density management guideline and stocking diagrams when fitting quantile regression models to maximum size density relationships for red pine (*Pinus resinosa*) in the Lake States and found a quantile of 0.90 as the closest match.

Linear Quantile Mixed Models

A mixed model approach to quantile regression can allow for each observation to have a ‘location shift effect’ (Koenker, 2004). Andrews et al. (2018) used linear quantile mixed models to estimate the slope and intercept coefficients of the self-thinning line of 15 tree species in the Acadian Region of North America. This approach utilizes the concepts of quantile regression discussed previously but allows for a random effects parameter. The model can be written as:

$$lnN = (\beta_0 + k_i) + \beta_1 lnQMD$$

Where *N* and *QMD* are defined as before, and β_0 and β_1 are the fixed parameters of intercept and slope and now the addition k_i as the random effect of the of the i^{th} plot on intercept. The slope is kept constant for individual species. Andrews et al. (2018) reason the use of the individual plot estimates of intercept will account for site-level factors and the “near infinite variation in species composition” which influences SDI. Each observation now has a corresponding fixed slope determined by dominant species on the plot, and a unique, random deviation from the overall intercept. The influence of site and species-specific effects are determined in a second step after random plot intercepts are used to calculated unique plot level maximum SDI.

As to which approach is best or most appropriate, many of these methods have addressed the concerns of objectively selecting plots to fit the self-thinning line and issues with extreme outliers, but the superiority of one method over the other depends on the questions asked of the data and the utility of the results. Burkhart (2013) sums this up well when he states "quantifying stand density has been and remains one of the most vexing problems confronting modelers of forest stand dynamics, and a completely satisfactory measure has not yet been advanced."

Modelling Site and Species Effects

To understand the influence of site and species-specific effects on the self-thinning line, the modelling methods discussed above often introduce site and species specific covariates to the model (Kimsey et al., 2019; Aguirre, del Rio and Condes, 2018). Another method is a two-stage approach where first the intercept and slope are fit to the observations and then relationships between calculated plot or stand specific SDI_{MAX} are determined through various statistical methods such as linear and non-linear regression (Woodall et al., 2005; Dean and Baldwin, 1996) and regression trees (Andrews et al., 2018).

As discussed previously, site quality is influenced by many environmental factors such as climate and topography. Measures of these influential factors are introduced as covariates into the modelling process. The inclusion of climate and topographic variables as covariates is a common approach to understanding the influence on the maximum size-density relationship. Climate variables such as mean annual temperature, mean annual precipitation, frost free period and a whole host of other easily derived climate metrics, as well as topographic variables expressed as transformations of slope and aspect measures, have been found to be significant in explaining variation in maximum SDI.

One approach to determine the influence of site quality on maximum stand density is by wrapping all the factors influencing site quality into one variable. This has been accomplished by introducing site index (SI) to the model as a covariate (Zhang et al., 2013; Bi, 2001). Zhang et al. (2013) found SI to be significant with quantile regression, showing a SDI_{MAX} for ponderosa pine in

California to be 860 TPH at SI of 10 m and 1330 TPH with SI of 50 m. Bi (2001) introduced a relative site index measure into a maximum SDI model of *Pinus radiata* in Australia using stochastic frontier analysis. Ge et al. (2017) used SI intervals to group plots from China fir (*Cunninghamia lanceolata* (Lamb.) Hook) plantations into five categories of site quality and then produced a different maximum SDI model for each. Weiskittel (2009) introduced SI, as well as measures of species basal area proportion and a variable indicating if the stand was planted or natural, directly into a stochastic frontier model of maximum SDI in Douglas-fir, western hemlock and red alder stands of the Pacific Northwest.

An indicator of how many and which species are present in a forest stand is an important consideration in modeling maximum stand density due to differing tolerance, crown architecture and a number of other variables which play a role in how trees interact and grow as a stand. Introducing species basal area proportion as a covariate into the model can account for the mixing of species with differing qualities. Woodall et al. (2005) give the example of how inappropriately applying the maximum SDI of a pure lodgepole pine (*Pinus contorta*) stand (around 2640 TPH) to a stand with only 51% lodgepole and the rest mixed species could result in a deviation of true maximum SDI of the mixed stand by more than 1000 stems, a very large difference. Kimsey et al. (2019) found significant increases in maximum SDI when shifting from pure stands of Douglas-fir or ponderosa pine to mixed stands. This increase was attributed to a mixing of more tolerant species, as shown by the relatively small increase between pure stands of shade tolerant grand fir and mixed stands of grand fir.

The correlation of site and species-specific factors can be done without the addition of covariates by analyzing the relationship of the calculated SDI to the variable of interest. Dean and Baldwin (1996) in a two-stage approach first found plot level SDI and then used linear regression to fit the relationship of SDI as a function of foliage density and live crown ratio and found 76% of the variation in SDI could be explained by these two variables. Woodall et al. (2005) after finding the 99th

percentile SDI used linear regression to estimate the relationship with mean specific gravity and found a strong negative correlation with R^2 of 0.9216.

Andrews et al. (2018) used a two-stage approach in an attempt to determine the influence of species and site characteristics on maximum stand density. First the self-thinning line was fit with plot specific random intercepts and overall fixed slope which allowed for a unique maximum SDI to be calculated for each observation. The next step was to use a random forest approach to determine the influence of the specific plot level species and site characteristics. Random forest is an ensemble regression method of multiple decision trees (Breiman, 2001). This approach found the most important explanatory variables, such as specific gravity, leaf longevity, annual degree-days less than 0°C, various interactions between temperature and precipitation, for each species-specific model.

Measures of Size

Why use diameter as the predictor of density? The choice of diameter by Reineke, and others, was "a major innovation" in describing density (Zeide, 2010) as it was historically common to use average or dominant height as the main descriptor of a forest. The number of trees per unit area, along with some dominant height, had been a simple and easy to measure expression of density but gave no detail on the size or spatial arrangement of the trees (Burkhart and Thome, 2012). Basal area per unit area, as well, conveys little about the frequency and size distribution of the trees (Chisman and Schumacher, 1940). Basal area, calculated as the cross-sectional area of tree stems at dbh, has the same components as Reineke's SDI, that is diameter raised to a power. With basal area, that power is 2 – the squared radius of a tree stem at 4.5 feet. If basal area is used as a measure of density, it states that number of trees is inversely proportional to squared diameter (Zeide, 2010). In determining the slope of the self-thinning line, as demonstrated in the numerous studies cited throughout this review, it is found to not be a squared relationship but one closer to Reineke's -1.605 or Yoda's -3/2. While trees per area and basal area are considered density measures, they do not, taken alone, express degree of crowding (Curtis, 2010).

Ultimately, density induced mortality is driven by increasing crown width, which is the plant part that takes up most of the space occupied by a tree (Zeide, 2005). Any meaningful descriptor of density should account for the occupancy of space by the tree crowns. Curtis (1982) states diameter-based expressions of density are useful predictors because diameter is "not intrinsically correlated with age and site" and is "directly related to average crown development." Chisman and Schumacher (1940) understood the correlation between diameter and crown when they developed the 'Tree-Area Ratio' as an equation for expressing the ground area allocation of a single tree in terms of its diameter. Krajicek et al. (1961) demonstrated the strong relationship between diameter and crown width in their study on crown competition factor. Bonnor (1964) showed, in stands of lodgepole pine, the relationship between crown width and height was similar at all densities. This is the familiar allometric relationship between plant parts, that is, plants of the same species have a particular shape independent of their size or state of development (Drew and Flewelling, 1977). It is this strong correlation between diameter and crown width, at any development stage, that explain why diameter is the best choice to describe density.

Curtis (1971) concluded that diameter-based measures have the "common advantage of avoiding the frequently bothersome and inaccurate estimation of age and site index." West (1982) compared 17 different measures of density of eucalyptus stands in Tasmania using the most basic approach of diameter as well as the more complex methods involving basal area, volume and height, and concluded that although the different approaches are related mathematically there is little gain achieved in the more complex models. Lee and Choi (2019) evaluated diameter, height and volume as predictors of the size-density relationship in Korean red (*Pinus densiflora*) and white pine (*Pinus koraiensis*) and Japanese larch (*Larix kaempferi*), and concluded even though volume had slightly higher correlation, that diameter was the best predictor because it fit the models well and is easily measurable. They also concluded height was the least descriptive because it is affected by site conditions. Burkhart (2013) who similarly investigated the use of diameter, volume and height in his

study of planted loblolly pine concluded that stem diameter had "a modest but consistent advantage" for describing the number of trees in self-thinning plots.

Which diameter?

Reineke (1933) used average diameter by basal area in his equation. This diameter is mathematically equivalent to what is known as the quadratic mean diameter. It is quadratic because of the squared function and is different than the arithmetic mean diameter, which is a measure of central tendency. The quadratic mean gives greater weight to larger trees (Curtis and Marshall, 2000). Reineke developed his SDI equation from data of even-aged forests and QMD was sufficient in that there was not much variance in the diameter distribution of these stands. Reineke's SDI equation is:

$$SDI = N\left(\frac{QMD}{10}\right)^{b}$$

Where N is the number of trees per unit area, QMD is diameter of average basal area, and b is the calculated slope of the self-thinning line which he determined was 1.605. Zeide (1983) points out that the use of QMD in Reineke's SDI equation is 'not technically correct' and instead recommends what he calls "Reineke's diameter" or D_R.

$$D_R = \bar{d}\left[1 + \frac{(b-1)b}{2} * C^2\right]^{1/b}$$

Where $\bar{d}$ is the arithmetic mean, b is the slope of the self-thinning which should lie somewhere between 1, which would produce the arithmetic mean, and 2, which would produce the quadratic mean (1.6 is a good approximation for b), and C^2, which is the coefficient of variation of the diameter distribution.

Stage (1968) demonstrated that SDI "can be computed tree by tree within a stand" by subdividing the contribution of each tree to SDI in an additive equation. Long and Daniel (1990) suggested the general summation expression as:

$$SDI = \sum \left(\frac{DBH_i}{10}\right)^b$$

Where DBH_i is the diameter of the ith tree in the stand and b is the slope of the self-thinning line, again 1.6 is a good approximation. They reason the summation method is more appropriate for stands with non-normal diameter distributions over QMD because of the skewness in diameters and the way "growing stock is partitioned among the various size classes" (Long and Daniel, 1990). Burkhart and Thome (2012) echo this concern where Reineke's equation and the summation equation give almost identical values of SDI in an even-aged monoculture with a unimodal and symmetric diameter distribution, but when each is applied to a stand with a more complex, inverse shaped diameter distribution, the values are considerably different. Chisman and Schumacher (1940) were critical of SDI for this very reason when they argued "the number of trees in a stand may be associated with an entirely different distribution of diameters than that of a normal stand having the same average." Woodall (2003) notes the summation method should only be applied to uneven-aged stands and one needs to be aware of the diameter distribution and the effect on SDI interpretation.

Shaw (2000) showed proof that Zeide's (1983) calculation of D_R is equivalent to the summation method proposed by Stage (1968) and Long and Daniel (1990). The summation method allows for the determination of how much each diameter class contributes to relative stand density and this information is lost when using QMD. Shaw (2000) deems this information critical to informed management decisions regarding manipulation of stand structure and concludes summation is the superior method of calculating SDI in irregular structured stands. Woodall et al. (2005) make a similar conclusion "the only way to appropriately determine SDI in stands with non-normal DBH distributions is to determine the SDI for individual DBH classes and then add them for the entire stand." Ducey and Larson (2003) argue that the summation SDI and Reineke's SDI should be considered different indices altogether and state there is no "superiority of any particular index". They reason that "while additivity is useful, and simplifies many issues of mensuration and

interpretation…mathematical theory alone cannot settle whether one index is superior to another". They conclude, this question of which method is superior, is an important research need for "guidance on what density index is best for a given species and management context."

Andrews et al. (2018) used D_R when modeling maximum SDI in the Acadia region of North America. Kimsey et al. (2019), Aguirre et al. (2018), Charru et al. (2012), Comeau et al. (2010), Condes et al. (2017), del Rio et al. (2001), Kweon and Comeau (2017), Lee and Choi (2019), Poage et al. (2007), Pretzsch (2005), Weiskittel (2009) used standard QMD. Bravo-Oviedo et al. (2018), Ducey and Knapp (2010), Long and Daniel (1990), Woodall et al. (2005), Woodall et al. (2006) used the summation method.

Diameter cutoffs

The lower limit of diameter measurements can have considerable impact on the calculation of SDI. This is demonstrated in the case studies presented by Curtis (2010) where he shows the common problem in applying SDI to a stand with a shade-tolerant understory that is essentially managed as even-aged. The stand in the 'Black Rock' example has a very pronounced bimodal diameter distribution where nearly all the volume is in the overstory of Douglas-fir, and has a hemlock understory comprising only 8% of the basal area. He used three methods of diameter cutoff in calculating SDI - only including trees in the overstory, including all trees greater than or equal to 1.6 inches and including all trees greater than or equal to the diameter cutoff calculated by the D40/4 rule (the mean diameter of the 40 largest trees divided by 4) which was about 8.5 inches in this case. These diameter cutoffs yielded SDI values (calculated with QMD) of 272, 545 and 274 respectively. Even the use of the summation SDI yielded values of 270, 411 and 271 respectively. The understory contributes little to the overall volume or basal area of the stand but has a huge effect on the number of trees. Curtis (2010) makes some conclusions and recommendations:

- In general trees less than 1.6 inches should be excluded, or in the case of older stands a more subjective cutoff might be used – the D40/4 is one such method recommended
- When a stand has numerous small stems in the understory and is clearly distinguishable from the main canopy, the understory should be excluded
- The summation approach to SDI is less affected by numerous understory trees or an irregular diameter distribution and is preferred to the standard QMD approach.

Condes et al. (2017) used data from five different European National Forest Inventories and restricted to only plots with QMD between 10 and 55 cm in order to avoid plots in older stands where harvests are more frequent, as well as eliminating plots from younger stands which have not reached canopy closure or were under sampled due to diameter cutoffs in the sampling design. Aguirre et al. (2018) followed a similar protocol for their work on the maximum size-density relationship of *Pinus* species in Spain and only included plots with QMD between 10 and 50 cm to avoid under-sampled and harvested stands. Salas-Eljatib and Weiskittel (2018) in their study of carrying capacity of *Northofagus* forests in Chile used a diameter cutoff of 5 cm possibly because this was the sampling protocol of the data source. Charru et al. (2012) "for the sake of caution," rejected plots with QMD less than 15 cm to avoid including stands not undergoing self-thinning. Their dataset consisted of plots with multiple repeat measurements so they went a step further than the 'arbitrary' 15 cm cutoff and utilized mortality metrics to determine if plots were sufficiently in the self-thinning stage. This procedure led to an increase of the diameter threshold of 1 to 5 cm, depending on the species and also caused them to set an upper threshold between 33 and 50 cm, again depending on the species. Comeau et al. (2010) used the interval method to select only plots in the top 10 percent SDI within each 5 cm interval starting at 10 cm QMD. Kimsey et al. (2019) only included plots with a minimum QMD of 2.54 cm. Weiskittel et al. (2009) did not designate a diameter cutoff and had plots with QMD range of 0.7 cm to 73.6 cm. Zhang et al. (2013) only described removing trees with heights less than 1.37 m

and provided summary statistics of the dataset with QMD between 8.2 cm and 54.5 cm in FIA plots and 10.1 cm to 86.1 cm in research plots.

QMD is typically available as standard stand summary statistics and will "probably continue" to be used in the calculation of SDI (Shaw, 2000). One major drawback to using stand or plot summarized data where only QMD is given can come when the diameter distribution and cutoff in the sampling design may be unknown.

One curiously lacking descriptor in the protocol of many published studies on the self-thinning line is whether dead trees are removed or included in the analysis. During this literature review few sources were found which specifically mention how trees marked as dead were treated. Ducey and Knapp (2010) mention dead trees were removed from the dataset. Ducey et al. (2017) state only live trees were included in analysis. It might seem obvious to exclude dead trees but it should be explicitly stated given that many datasets include dead trees and if not removed could strongly bias results.

Utilization of the Stand Density Index

Density management of a forest stand involves the manipulation and control of growing stock to achieve desired objectives (Long, 1985). Manipulation of growing stock allows for the selection of desired species, the lengthening or shortening of a rotation and the potential to maximize the yield of selected products (Bickford et al., 1957). Stand density index has the benefit of being a standard by which sites can be compared independent of stand age or site quality (Williams, 1996; Long, 1985). The maximum stand density for a species on a given site is "an essential piece of information for assessing site productivity, modelling and predicting stand dynamics and silvicultural regulation." (Pretzsch and Biber, 2016) Westoby (1984) describes self-thinning as informative about stand dynamics, as a pattern of biomass rising over a period then collapsing. Avery and Burkhart (2002) describe growth models as typically requiring descriptors of stand density. Maximum SDI allows for

the constraint of growth models, where equations consist of expansion and decline, that is positive and negative factors (Zeide, 2005).

Zeide (2005) stated it is “not possible” to determine optimal thinning levels without an ability to describe density. Stand density is an important tool in silviculture, most commonly as a guide to thinning and stand density control, and relates to suppression mortality, crown development and risk of windfall and snow breakage (Curtis, 2010). The ability to predict when natural, density-related mortality will begin to quickly increase is useful to determine the optimal timing and level of thinning regimes of a stand (del Rio et al., 2001). Knowledge of the maximum SDI allows for the determination of relative density (RD) (Drew and Flewelling, 1979), a critical component of any silvicultural treatment (Woodall et al., 2005). SDI and RD have been used to develop density-management diagrams (DMDs) which are useful for planning stand management activities such as thinning (Tappeiner et al., 2015). DMDs are developed for many commercially important species and serve as a tool for regulating and scheduling density management activities and are “a practical application of the self-thinning rule and its properties.” (Begin et al., 2001). DMDs are built under basic assumptions regarding density-dependent behavior of forest stands including self-thinning and competition responses (Jack and Long, 1996). These diagrams, as developed by Drew and Flewelling (1979), contain three relationships:

1. The maximum size-density line
2. Lower bound of imminent competition-mortality
3. The line at a relative density to expect crown closure

Drew and Flewelling (1979) describe the practical application of density management diagrams – stands growing below the line of crown closure are not fully utilizing the site and therefore density can be increased without drop in growth; maximum tree size can be obtained by managing stands close to the crown closure line; a stand managed between the lower bound of imminent competition mortality and at an RD of around 0.40 will achieve high total stand growth but will be

distributed among smaller individual trees compared with a stand managed at lower densities; and finally stands should not be allowed to move into the zone of imminent competition, or density-dependent mortality until shortly before a final harvest. Condes et al. (2017) acknowledge understanding of density is crucial for silviculture and forest modelling but they take it further by stating "clear information regarding size-density relationships under given climatic conditions can contribute significantly to the development of regionally appropriate and more precise silvicultural guidelines for shaping stand density management diagrams."

Climate Forecasting for Density Management

The influence of climatic variables on the self-thinning line has been demonstrated through empirical modeling of the size-density relationship of various tree species and forest ecosystems around the world. These models are built with historical data to which the forests have been exposed to over the course of stand development. Many of these models find the amount and timing of precipitation, and the interaction with temperature to be highly influential (Kimsey et al., 2019; Andrews et al., 2018; Ducey et al., 2017) As concerns about the potential impact of climate change grow, forest managers must be ready to deal with the possibility of increased variability and uncertainty involving future climate scenarios (Puettmann, 2010). Future climate projections built from general circulation models (GCMs) under different representative concentration pathways (RCPs) can be utilized to predict the impact of these changes on the carrying capacity of forests. Understanding this potential impact will allow for the development of mitigation and adaptation strategies.

Ducey et al. (2017) developed a maximum stocking model for important tree species in the lake states region of the US. Their model incorporated the AN81d dataset from the PRISM Climate Group which consists of calculated climate variables from 1981 through 2012. The climate variables are extracted for each specific plot location. It is noted that their FIA plot locations were 'dithered' or fuzzed from the true plot location to protect land owner confidentiality. They conclude their model

may “present a path forward for development of future forest stocking metrics in the face of climate change and tree range shift scenarios” but do not provide examples of this utilization. Kimsey et al. (2019) used thirty-year normal from 1961-1990 developed by the USFS Moscow Forest Sciences Laboratory extracted to unfuzzed plot locations and concluded “model sensitivity to climatic gradients may be useful for future assessment of climate change effects on maximum stand density.” Aguirre et al. (2018) developed a climate-dependent model of maximum size-density relationships based on data from meteorological stations between 1951 and 1999. They did not utilize future climate scenarios but concluded their model “could be used for management decision support and even to predict possible consequences of climate change.” Brunet-Navarro et al. (2016) developed climate-sensitive self-thinning lines for four *Pinus* species on the Iberian Peninsula utilizing historical meteorological station precipitation and temperature data for each plot from 1951-1999. They calculated self-thinning lines for individual species at the lowest, mean and highest levels of precipitation and temperature levels to show the impact and range as a function of these climate variables. They acknowledge they did not evaluate “specific climate change scenarios” but that general inferences could be made about each species and how they might respond under wetter/dryer or warmer/cooler conditions. They recommend future work relating self-thinning lines under future climate scenarios.

Andrews et al. (2018) took the further step of applying their model with data for potential future climate scenarios. Their model was built using 30-year climate normal dataset from 1961-1990 developed by the USFS Moscow Forest Science Laboratory. They then applied future climate scenarios from 2060 and 2090 using prediction from multiple GCMs using the RCP6 scenario. The RCP6 was selected because it represents a likely case or a mid-range scenario of future climate change. They found future scenarios predict significant and steep decreases in individual species maximum SDI and revealed shifts northward of where high maximum SDI ranges were located. Rehfeldt et al. (2006) developed range maps of forest communities based on climate relationships. They utilized normalized climate data from 1961-1990 at both point locations (latitude and longitude)

as well as a gridded surface. They updated their plant-climate relationship surfaces with IS92a climate scenario using the Canadian Centre for Climate Modeling and Analysis GCM (HadCM3GGa1) for periods beginning in 2030, 2060 and 2090. They found climate changes would shift ranges by increasing montane forest and grasslands at the expense of subalpine, alpine and tundra communities.

Yue et al. (2016) developed a dynamic environment-sensitive site index model (DESIM) to assess change scenarios for Norway spruce stands in Germany. Although not specifically looking at the effect on density, they utilized four projected change scenarios during the next 100 years including a no change in temperature (control scenario) and increase in mean growing season temperature by 1°C, 2°C and 4°C. DESIM allowed site potential for a given stand to vary as a consequence of environmental changes over time. Their results, although not consistent across their study region, indicated decreases in forest site productivity at the higher scenarios and modest increases in productivity at the lowest scenario. The approach of Yue et al. (2016) differed from that of Andrews et al. (2019) and Rehfeldt et al. (2016) in that it was not 'space-for-time' substitution of historic condition for future condition model parameters but was a dynamic longitudinal approach where predictions can be made on a continuum of time-sensitive change into the future.

Conclusion

Maximum stand density index serves as a tool for silvicultural prescriptions, in particular timing and levels of thinning and other density control measures such as planting and species selection. Stocking, or relative density, is determined by the ratio of current stand density to the potential maximum. Many environmental and biological factors control the self-thinning trajectory of a stand and determine the maximum carrying capacity. Empirical modeling efforts attempt to determine site and species dependent maximum values for many tree species and regional forest ecosystems. Climate sensitive models may support the development of strategies for dealing with potential future climate change. Regionally specific models can aid forest managers in decision making now and in the future to promote healthy, sustainable and productive forests.

References

Abtew, W. and A. Melesse. 2012. Evaporation and Evapotranspiration: Measurements and Estimations. Springer, New York, ISBN 978-94-007-4736-4

Aguirre, A., del Río, M and Condes, S. 2018. Intra- and inter-specific variation of the maximum size-density relationship along an aridity gradient in Iberian pinewoods. *Forest Ecology and Management*, 411, 90-100. https://doi.org/10.1016/j.foreco.2018.01.017

Aigner, D., Lovell, C and Schmidt, P. 1977. Formulation and estimation of stochastic frontier production function models. *Journal of Econometrics*, 6, 21-37. https://doi.org/10.1016/0304-4076(77)90052-5

Allen, M and Burkhart, H. 2018. Growth-density relationships in loblolly pine plantations. *Forest Science*, 65:3, 250-264. https://doi.org/10.1093/forsci/fxy048

Andrews, C., Weiskittel, A., Amato, A. W. D., and Simons-legaard, E. (2018). Forest Ecology and Management Variation in the maximum stand density index and its linkage to climate in mixed species forests of the North American Acadian Region. *Forest Ecology and Management*, 417, 90–102. https://doi.org/10.1016/j.foreco.2018.02.038

Assmann, E. 1970. The principles of forest yield study: Studies in the Organic Production, Structure, Increment and Yield of Forest Stands. Pergamon Press, Oxford, New York, ISBN 978-0-08-006658-5.

Burkhart, HE, Avery, TE and Bullock, PB. 2019. Forest Measurements. Waveland Press, Inc. ISBN:1-4786-3618-1

Battese, G. and Coelli, T. 1992. Frontier production functions, technical efficiency and panel data: With application to paddy farmers in India. J Prod Anal 3, 153–169 (1992). https://doi.org/10.1007/BF00158774

Battese, G. and Corra, G. 1977. Estimation of a production frontier model: with application to the pastoral zone of eastern Australia. *Australian Journal of Agricultural Economics* 21, 169–179. https://doi.org/10.1111/j.1467-8489.1977.tb00204.x

Bégin, E., Bégin, J., Bélanger, L., Rivest, L. and Tremblay, S. 2001. Balsam fir self-thinning relationship and its constancy among different ecological regions. *Canadian Journal of Forest Research*, 31:6, 950-959. https://doi.org/10.1139/x01-026

Bi, H and Turvey, N. 1997. A method of selecting data points for fitting the maximum biomass-density line for stands undergoing self-thinning. *Australian Journal of Ecology*, 22, 356-359. https://doi.org/10.1111/j.1442-9993.1997.tb00683.x

Bi, H., Wan, G. and Turvey, N. 2000. Estimating the self-thinning boundary line as a density-dependent stochastic biomass frontier. *Ecology*, 81:6, 1477-1483. https://doi.org/10.2307/177300

Bi, H. 2001. The self-thinning surface. *Forest Science*, 47:3, 361-370. https://doi.org/10.1093/forestscience/47.3.361

Bickford, C. 1957. Stocking, normality, and measurement of stand density. *Journal of Forestry*, 55:2, 99-104. https://doi.org/10.1093/jof/55.2.99

Binkley, D. 1984. Importance of size—density relationships in mixed stands of Douglas-fir and red alder. *Forest Ecology and Management*, 9:2, 81-85. https://doi.org/10.1016/0378-1127(84)90075-6

Bonnor G. 1964. The influence of stand density on the correlation of stem diameter with crown width for lodgepole pine. *The Forestry Chronicle*, 40:3, 347–349. https://doi.org/10.5558/tfc40347-3

Bravo-Oviedo, A., Condés, S., del Río, M., Pretzsch, H. and Ducey, M. 2018. Maximum stand density strongly depends on species-specific wood stability, shade and drought tolerance, *Forestry: An International Journal of Forest Research*, 91:4, 459–469, https://doi.org/10.1093/forestry/cpy006

Breiman, L. 2001. Random forests. *Machine Learning*, 45: 5–32. https://doi.org/10.1023/A:1010933404324

Brunet-Navarro, P., Sterck, F., Vayreda, J, Martinez-Vilalta, J. and Mohren, G. 2016. Self-thinning in four pine species: an evaluation of potential climate impacts. *Annals of Forest Science*, 733, 1025-1034. https://doi.org/10.1007/s13595-016-0585-y

Burkhart, H. and Tomé, M. 2012. Chapter 8: Quantifying stand density, in Modeling Forest Trees and Stands. Springer, New York, ISBN 978-90-481-3170-9

Burkhart, H. 2013. Comparison of maximum size–density relationships based on alternate stand attributes for predicting tree numbers and stand growth. *Forest Ecology and Management*, 289, 404-408. https://doi.org/10.1016/j.foreco.2012.10.041

Cade, B and Noon, B. 2003. A gentle introduction to quantile regression for ecologists. *Frontiers in Ecology and the Environment*, 1:8, 412-420. https://doi.org/10.2307/3868138

Chapin, F, Matson, P. and Vitousek, P. 2011. Principles of Terrestrial Ecosystem Ecology, Springer, New York, ISBN 9781441995032

Charru, M., Seynave, I., Morneau, F., Rivoire, M. and Bontemps, J. 2012. Significant differences and curvilinearity in the self-thinning relationships of 11 temperate tree species assessed from forest inventory data. *Annals of Forest Science*, 69, 195-205. https://doi.org/10.1007/s13595-011-0149-0

Chisman, H and Schumacher, F. 1940. On the tree-area ratio and certain of its applications. *Journal of Forestry*, 38:4, 311-317. https://doi.org/10.1093/jof/38.4.311

Comeau, P., White, M., Kerr, G. and Hale, S. 2010. Maximum density–size relationships for Sitka spruce and coastal Douglas-fir in Britain and Canada. *Forestry: An International Journal of Forest Research*, 83:5, 461-468. https://doi.org/10.1093/forestry/cpq028

Condés, S., Vallet, P., Bielak, K., Bravo-Oviedo, A., Coll, L., Ducey, M., Pach, M., Pretzsch, H., Sterba, H., Vayreda, J., and del Río, M. 2017. Climate influences on the maximum size-density relationship in Scots pine (*Pinus sylvestris* L.) and European beech (*Fagus sylvatica* L.) stands. *Forest Ecology and Management*, 385, 295-307. https://doi.org/10.1016/j.foreco.2016.10.059

Cooper, S., Neiman, K. and Roberts, D. 1991. Forest habitat types of northern Idaho: a second approximation. General Technical Report INT-236, 143. https://doi.org/10.2737/INT-GTR-236

Coops, N., Waring, R. and Moncrieff, J. 2000. Estimating mean monthly incident solar radiation on horizontal and inclined slopes from mean monthly temperatures extremes. *International Journal of Biometeorology* 44, 204–211. https://doi.org/10.1007/s004840000073

Curtis, R. and Marshall, D. 2000. Why quadratic mean diameter? *Western Journal of Applied Forestry*, 15, 137-139.

Curtis, R. 1970. Density measures: an interpretation. *Forest Science*, 61:4, 403-414. https://doi.org/10.1093/forestscience/16.4.403

Curtis, R. 1971. A tree area power function and related stand density measures of Douglas-fir. *Forest Science*, 17:2, 146-159. https://doi.org/10.1093/forestscience/17.2.146

Curtis, R. 1982. A simple index of stand density for Douglas-fir. *Forest Science*, 28:1, 92-94, https://doi.org/10.1093/forestscience/28.1.92

Curtis, R. 2010. Effects of diameter limits and stand structure on relative density indices: a case study. *Western Journal of Applied Forestry*, 25:4, 169-175. http://doi.org/10.1093/wjaf/25.4.169

Daubenmire, R. 1943. Vegetation zonation in the Rocky Mountains. *The Botanical Review*, 9:6, 325-393, https://doi.org/10.1007/BF02872481

Daubenmire, R. 1980. Mountain topography and vegetation patterns. *Northwest Science*, 54:2, 146-152.

Dean, T. and Baldwin, V. 1996. The relationship between Reineke's stand-density index and physical stem mechanics. *Forest Ecology and Management*, 81, 25-34. https://doi.org/10.1016/0378-1127(95)03666-0

del Río, M., Montero, G. and Bravo, F. 2001. Analysis of diameter–density relationships and self-thinning in non-thinned even-aged Scots pine stands. *Forest Ecology and Management*, 142, 79-87. https://doi.org/10.1016/S0378-1127(00)00341-8

Drew, R and Flewelling, J. 1977. Some recent Japanese theories of yield-density relationships and their application to Monterey pine plantations. *Forest Science*, 23:4, 517-534. https://doi.org/10.1093/forestscience/23.4.517

Drew, R. and Flewelling, J. 1979. Stand density management: an alternative approach and its application to Douglas-fir plantations. *Forest Science*, 25:3, 518-532. https://doi.org/10.1093/forestscience/25.3.518

Ducey, M. and Knapp, R. 2010. A stand density index for complex mixed species forests in the northeastern United States. *Forest Ecology and Management*, 260:9, 1613-1622. https://doi.org/10.1016/j.foreco.2010.08.014

Ducey, M. and Larson, B. 2003. Is there a correct stand density index? An alternate interpretation. *Western Journal of Applied Forestry*, 18:3, 179-184. https://doi.org/10.1093/wjaf/18.3.179

Ducey, M., Woodall, C. and Bravo-Oviedo, A. 2017. Climate and species functional traits influence maximum live tree stocking in the Lake States, USA. *Forest Ecology and Management*, 385, 51-61. https://doi.org/10.1016/j.foreco.2016.12.007

Farrell, M. 1957. The measurement of productive efficiency. *Journal of the Royal Statistical Society*, 120:3, 253-281. https://doi.org/10.2307/2343100

Frothingham, E. 1914. White pine under forest management. Bulletin 13, US Department of Agriculture, Washington, DC

Ge, F., Zeng, W., Ma, W and Meng, J. 2017. Does the slope of the self-thinning line remain a constant value across different site qualities? – An implication for plantation density management. *Forests*, 8:10, 355. https://doi.org/10.3390/f8100355

Harper, J. 1977. Population Biology of Plants. Academic Press, London. ISBN 0123258502

Hennigar, C., Weiskittel, A, Allen, H and MacLean, D. Development and evaluation of a biomass increment based index for site productivity. *Canadian Journal of Forest Research*, 47:3, 400-410. https://doi.org/10.1139/cjfr-2016-0330

Humboldt, A and Bonpland, A. 1807. Essay on the Geography of Plants. The University of Chicago Press, Chicago, ISBN 0-226-36066-0

Hutchings, M and Budd, C. 1981a. Plant self-thinning and leaf area dynamics in experimental and natural monocultures. *Nordic Society Oikos*, 36:3, 319-325. https://doi.org/10.2307/3544629

Hutchings, M and Budd, C. 1981b. Plant competition and its course through time. *BioScience*, 31:9, 640-645. https://doi.org/10.2307/1308637

Jack, S. and Long, J. 1996. Linkages between silviculture and ecology: An analysis of density management diagrams. *Forest Ecology and Management*, 86, 205–220. https://doi.org/10.1016/S0378-1127(96)03770-X

Kays, S and Harper, J. 1974. The regulation of plant and tiller density in a grass sward. *Journal of Ecology*, 62, 97-105. https://doi.org/10.2307/2258882

Kimsey, M, Moore, J and McDaniel, P. 2008. A geographically weighted regression analysis of Douglas-fir site index in north central Idaho. *Forest Science*, 54:3, 356-366. https://doi.org/10.1093/forestscience/54.3.356

Kimsey, M., Shaw, T. and Coleman, M. 2019. Site sensitive maximum stand density index models for mixed conifer stands across the Inland Northwest, USA. *Forest Ecology and Management*, 433, 396-404. https://doi.org/10.1016/j.foreco.2018.11.013

Koenker, R and Bassett, G. 1978. Regression quantiles. *Econometrica*, 46, 33-50. https://doi.org/10.2307/1913643

Koenker, R. and Hallock, K. 2001. Quantile Regression. *Journal of Economic Perspectives*, 15:4, 143-156. https://doi.org/10.1257/jep.15.4.143

Koenker, R. 2004. Quantile regression for longitudinal data. *Journal of Multivariate Analysis*, 91, 74-89. https://doi.org/10.1016/j.jmva.2004.05.006

Krajicek, J., Brinkman, K. and Gingrich, S. 1961. Crown competition – a measure of density. *Forest Science*, 7, 35-42. https://doi.org/10.1093/forestscience/7.1.35

Kweon, D. and Comeau, P. 2017. Effects of climate on maximum size-density relationships in Western Canadian trembling aspen stands. *Forest Ecology and Management*, 406, 281-289. https://doi.org/10.1016/j.foreco.2017.08.014

Lee, D. and Choi, J. 2019. Evaluating maximum stand density and size–density relationships based on the Competition Density Rule in Korean pines and Japanese larch. *Forest Ecology and Management*, 446, 204-123. https://doi.org/10.1016/j.foreco.2019.05.017

Long, J. and Daniel, T. 1990. Assessment of growing stock in uneven-aged stands. *Western Journal of Applied Forestry*, 5:3, 93-96. https://doi.org/10.1093/wjaf/5.3.93

Long, J. and Smith, F. 1984. Relation between size and density in developing stands: a description and possible mechanisms. *Forest Ecology and Management*, 7:3, 191-206. https://doi.org/10.1016/0378-1127(84)90067-7

Long, J. 1985. A practical approach to density management. *The Forestry Chronicle*, 61, 23-27. https://doi.org/10.5558/tfc61023-1

Lonsdale, W and Watkinson, A. 1982. Light and self-thinning. *New Phytologist*, 90:3, 431-445. https://doi.org/10.1111/j.1469-8137.1982.tb04476.x

Lonsdale, W and Watkinson, A. 1983. Plant geometry and self-thinning. *Journal of Ecology*, 71, 285-297. https://doi.org/10.2307/2259977

MacKinney A. and Chaiken L. 1935. A method of determining density of loblolly pine stands. Technical Note No. 15. USDA Forest Service, Appalachian Forest Experiment Station, Asheville, NC. https://doi.org/10.5962/bhl.title.127546

Mohler, C., Marks, P. and Sprugel, D. 1978. Stand structure and allometry of trees during self-thinning of pure stands. *Journal of Ecology*, 66:2, 599-614. https://doi.org/10.2307/2259153

Monserud, R., Ledermann, T., and Sterba, H. 2005. Are self-thinning constraints needed in a tree-specific mortality model. Forest Science. 50:6, 848-858. https://doi.org/10.1093/forestscience/50.6.848

Niinemets, Ü and Valladares, F. 2006. Tolerance to shade, drought, and waterlogging of temperate northern hemisphere trees and shrubs. *Ecological Monographs*, 76:4, 521-547. https://doi.org/10.1890/0012-9615(2006)076[0521:TTSDAW]2.0.CO;2

Poage, N., Marshall, D. and McClellan, M. 2007. Maximum stand-density index of 40 western hemlock-Sitka spruce stands in southeast Alaska. *Western Journal of Applied Forestry*, 22:2, 99-104. https://doi.org/10.1093/wjaf/22.2.99

Pretzsch, H and Biber, P. 2005. A re-evaluation of Reineke's rule and stand density index. *Forest Science*, 51:4, 304-320. https://doi.org/10.1093/forestscience/51.4.304

Pretzsch, H. and Biber, P. 2016. Tree species mixing can increase maximum stand density. *Canadian Journal of Forest Research*, 46:10, 1179-1193. https://doi.org/10.1139/cjfr-2015-0413

Pretzsch, H. and Schütze, G. 2016. Effect of tree species mixing on the size structure, density, and yield of forest stands. *European Journal of Forest Research*, 135, 1–22. https://doi.org/10.1007/s10342-015-0913-z

Puettmann, K., Hann, D. and Hibbs, D. 1993. Evaluation of the size-density relationships for pure red alder and Douglas-fir stands. *Forest Science*, 39, 7-27. https://doi.org/10.1093/forestscience/39.1.7

Puettmann, K. 2011. Silvicultural challenges and options in the context of global change: "Simple" fixes and opportunities for new management approaches. *Journal of Forestry*, 109:6, 321-331. https://doi.org/10.1093/jof/109.6.321

Rehfeldt, G., Crookston, N., Warwell, M. and Evans, J. 2006. Empirical analyses of plant-climate relationships for the western United States. *International Journal of Plant Sciences*, 167:6, 1123-1150. https://doi.org/10.1086/507711

Reineke, L. 1933. Perfecting a stand-density index for even-aged forests. *Journal of Agricultural Research*, 46:7, 627-638.

Reyes-Hernandez, V., Comeau, P. and Bokalo, M. 2013. Static and dynamic maximum size–density relationships for mixed trembling aspen and white spruce stands in western Canada. *Forest Ecology and Management*, 289, 300-311. https://doi.org/10.1016/j.foreco.2012.09.042

Roise, J and Betters, D. 1981. An aspect transformation with regard to elevation for site productivity models. *Forest Science*, 27:3, 483-486. https://doi.org/10.1093/forestscience/27.3.483

Salas-Eljatib, C and Weiskittel, A. 2018. Evaluation of modeling strategies for assessing self-thinning behavior and carrying capacity. *Ecology and Evolution*, 8, 10768-10779. https://doi.org/10.1002/ece3.4525

Scharf, F., Juanes, F. and Sutherland, M. 1998. Inferring ecological relationships from the edges of scatter diagrams: Comparison of regression techniques. *Ecology*, 79:2, 448-460. https://doi.org/10.1890/0012-9658(1998)079[0448:IERFTE]2.0.CO;2

Shaw, J. 2000. Application of stand density index to irregularly structured stands. *Western Journal of Applied Forestry*, 15, 40-42. https://doi.org/10.1093/wjaf/15.1.40

Solomon, D and Zhang, L. 2002. Maximum size–density relationships for mixed softwoods in the northeastern USA. *Forest Ecology and Management*, 155, 163-170. https://doi.org/10.1016/S0378-1127(01)00556-4

Stage, A. 1968. A tree-by-tree measure of site utilization for grand fir related to stand density index. USDA Forest Service Research Note INT-77, Intermountain Forest and Range Experiment Station, Ogden, Utah

Stage, A., 1976. An expression for the effect of aspect, slope, and habitat type on tree growth. *Forest Science,* 22, 457–460. https://doi.org/10.1093/forestscience/22.4.457

Sterba, H. and Monserud, R. 1993. The maximum density concept applied to uneven-aged mixed-species stands. *Forest Science*, 39:3, 432-452. https://doi.org/10.1093/forestscience/39.3.432

Tappeiner, J., Bailey, J., Harrington, T. and Maguire, D. 2015. Silviculture and Ecology of Western U.S. Forests, Oregon State University Press, Corvallis, OR ISBN 978-0-87071-803-8

VanderSchaaf, C. and Burkhart, H. 2007. Comparison of methods to estimates Reineke's maximum size-density relationship species boundary line slope. *Forest Science*, 53:3, 435-442. https://doi.org/10.1093/forestscience/53.3.435

VanderSchaaf, C. and Burkhart, H. 2008. Using segmented regression to estimate stages and phases of stand development. *Forest Science*, 54:2, 167-175. https://doi.org/10.1093/forestscience/54.2.167

Vospernik, S. and Sterba, H. 2015. Do competition-density rule and self-thinning rule agree? *Annals of Forest Science*, 72, 379-390. https://doi.org/10.1007/s13595-014-0433-x

Weiskittel, A. Gould, P. and Temesgen, H. 2009. Sources of variation in the self-thinning boundary line for three species of varying levels of shade tolerance. *Forest Science*, 55, 84-93. https://doi.org/10.1093/forestscience/55.1.84

Weller, D. 1987a. Self-thinning exponent correlated with allometric measures of plant geometry. *Ecology*, 68:4, 813-821. https://doi.org/10.2307/1938352

Weller, D. 1987b. A reevaluation of the -3/2 power rule of plant self-thinning. *Ecological Monographs*, 57, 23-43. https://doi.org/10.2307/1942637

West, P. and Borough, C. 1983. Tree suppression and the self-thinning rule in a monoculture of *Pinus radiate* D. Don. *Annals of Botany*, 52:2, 149-158. https://doi.org/10.1093/oxfordjournals.aob.a086560

West, P. 2011. Comparison of stand density measures in even-aged regrowth eucalypt forest of southern Tasmania. *Canadian Journal of Forest Research*, 13, 22-31. https://doi.org/10.1139/x83-004

Westoby, M. 1984. The self-thinning rule. *Advances in Ecological Research*, 14, 167-225. https://doi.org/10.1016/S0065-2504(08)60171-3

Williams, R. 1996. Stand density index for loblolly pine plantations in north Louisiana. *Southern Journal of Applied Forestry*, 20:2, 110-113. https://doi.org/10.1093/sjaf/20.2.110

Woodall, C., Miles, P. and Vissage, J. 2005. Determining maximum stand density index in mixed species stands for strategic-scale stocking assessments. *Forest Ecology and Management*, 216, 367-377. https://doi.org/10.1016/j.foreco.2005.05.050

Woodall, C., Perry, C. and Miles, P. 2006. The relative density of forests in the United States. *Forest Ecology and Management*, 226, 368-372. https://doi.org/10.1016/j.foreco.2006.01.032

Woodall, C., Fiedler, C., and Milner, K. 2003. Stand density index in uneven-aged ponderosa pine stands. *Canadian Journal of Forest Research*, 33, 96-100. https://doi.org/10.1139/X02-168

Yoda, K., Kira, T., Ogawa, H., and Hozumi, K. 1963. Self-thinning in overcrowded pure stands under cultivated and natural conditions. *Journal of Biology*, 14, 107-129.

Yue, C., Kahle, H., von Wilpert, K. and Kohnle, U. 2016. A dynamic environment-sensitive site index model for the prediction of site productivity potential under climate change. *Ecological Modelling*, 337, 48-62. https://doi.org/10.1016/j.ecolmodel.2016.06.005

Zeide, B. 1983. The mean diameter for stand density index. *Canadian Journal of Forest Research*, 13:5, 1023-1024. https://doi.org/10.1139/x83-135

Zeide B. 1987. Analysis of the 3/2 power law of self-thinning. *Forest* Science, 33:2, 517–537. https://doi.org/10.1093/forestscience/33.2.517

Zeide B. 2005. How to measure stand density. *Trees*, 19,1–14. https://doi.org/10.1007/s00468-004-0343-x

Zeide, B. 2010. Comparison of self-thinning models: an exercise in reasoning. *Trees*, 24, 1117-1126. https://doi.org/10.1007/s00468-010-0484-z

Zhang, L., Bi, H., Gove, J. and Heath, L. 2005. A comparison of alternative methods for estimating the self-thinning boundary line. *Canadian Journal of Forest Research*, 35:6, 1507-1514. https://doi.org/10.1139/X05-070

Zhang, J., Oliver, W. and Powers, R. 2013. Reevaluating the self-thinning boundary line for ponderosa pine (*Pinus ponderosa*) forests. *Canadian Journal of Forest Research*, 43:10, 963-971. https://doi.org/10.1139/cjfr-2013-0133

Chapter 2: A Species-Specific, Site-Sensitive, Maximum Stand Density Index Model for Pacific Northwest Conifer Forests

Forthcoming in Canadian Journal of Forest Research

Introduction

Forest stand density is a function of two variables: the number of trees and their size (Zeide, 2005). Initially, forest stand development is essentially free of intra- or inter-specific competition, during which time mortality is independent of density (Drew and Flewelling, 1977). As trees, in particular their canopies, grow, demand on limited forest resources and growing space increases, causing density to become successively lower due to the competitive interaction between individuals and subsequent death of the suppressed (i.e. density related mortality) (Yoda et al., 1963). A site is fully occupied when the stand has accumulated the maximum attainable biomass at a given stand density where any further growth will incur mortality (Bi et al., 2000). As such, the major drivers of self-thinning in forest stands are self-tolerance and the ability of individuals to acquire site resources through competition for above- and below-ground growing space.

The maximum stand density (SDI_{MAX}), or carrying capacity, for a species on a given site is an essential piece of information for assessing site productivity, modelling and predicting stand dynamics and silvicultural regulation (Pretzsch and Biber, 2016). Through silvicultural prescriptions, the density of a forest can be manipulated to achieve specific management objectives (Allen and Burkhart, 2018). Manipulation of growing stock allows for the selection of desired species, the lengthening or shortening of a rotation and the potential to maximize the yield of selected products (Bickford et al., 1957). The ability to predict when natural, density-related mortality will begin to quickly increase is useful to determine the optimal timing and level of thinning regimes of a stand (del Rio et al., 2001). The timing of key events such as crown closure and the onset of density dependent mortality can be anticipated at various levels of density relative to the maximum attainable carrying capacity (Long, 1985).

The determination of regional and species-specific SDI_{MAX} values for guiding forest management decisions has been, and continues to be, an important subject in forestry research (Zeide, 2010). Reineke (1933) plotted the log-log relationship of number of trees against average diameter to show the upper boundary as a straight, negative sloping line. A line was visually fit to this outer boundary and the number of trees that intersect at 10 inches is what Reineke called stand density index, where the highest number of trees is considered the maximum attainable density or SDI_{MAX}. Stand density index has the benefit of being a standard by which sites can be compared independent of stand age or site quality (Williams, 1996). The traditional approach to modelling the self-thinning relationship in forest stands has been to use the Reineke equation of the following form:

[1] $$\log(N) = \beta_0 + \beta_1 \log(QMD)$$

Where N is the number of trees per unit area, QMD is the quadratic mean diameter and β_0 and β_1 are the intercept and slope parameters to be estimated. The important features of this linear relationship are the slope of the line, which is the self-thinning rate, and the intercept, which implicitly accounts for site level variation, including species composition and physical site properties (Andrews et al., 2018). Reineke concluded the slope of the line to be -1.605 and to be invariant to tree species or site quality. Contrary to this belief in a constant slope, many subsequent investigations have revealed systematic variations in slope (Zeide, 1987). Although Reineke's -1.605 is a reasonable average over all species, it is probably not quite right for any individual species (Sterba and Monserud, 1993). Many models attempt to determine the growth trajectory and mortality of a stand based on species and site-specific self-thinning lines that represent maximum carrying capacity.

The intercept and slope of the self-thinning line (Equation 1) varies with site-specific environmental factors such as topography, climate and soils. Aguirre et al. (2018) state, at large scales, including environmental variables in a density model might be crucial in explaining the variability of the self-thinning line over large environmental gradients. Vospernik and Sterba (2015) found, in general, larger intercepts in stands grown on more productive land. Pretzsch and Biber (2005) describe

the limiting boundary, or self-thinning line, as the maximum density of individuals at a given size under optimal site conditions, where any boundary lower than this line would signify a stand under suboptimal growth conditions.

The presence and availability of resources is directly determined by site-specific environmental variables. The amount, spatial distribution and timing of precipitation and sunlight strongly influences ecosystem structure and functioning (Chapin et al., 2011). Numerous studies have incorporated important climate variables in stand density index modelling efforts (Andrews et al., 2018; Condes et al., 2017; Kweon and Comeau, 2017). Moisture and sunlight are the primary drivers of tree growth but are significantly modified by site topography (i.e. slope, aspect and elevation), as well as soil and geologic properties. A relationship between growth, elevation and aspect is based on underlying processes related to the influence of elevation and aspect on incoming solar energy and water availability (Coops et al., 2000; Roise and Betters, 1981; Stage, 1976). Topographic variables have proven important in driving many stand density index models (Kimsey et al., 2019; Weiskittel et al., 2019). Soils influence site quality in many ways, including water holding capacity, nutrient availability and rooting depth. The significance of water availability on site quality and carrying capacity can be directly influenced by the soils present. Binkley (1984) showed the most fertile site, had the greatest maximum size-density relationship and dropped off from this ceiling with decreasing fertility. Kimsey et al. (2019) found soil parent material to have an important effect on stand density; in particular, the presence of fine-textured volcanic tephra significantly increased maximum SDI for all species studied. They attribute the increase in carrying capacity on ash-influenced soils to its increased water holding capacity.

Stand composition (i.e. species presence) has been shown to influence the size-density trajectory. Pretzsch (2014) demonstrated how stands of species with varying physiological and morphological traits lead to more efficient, denser crown packing. Pretzsch and Biber (2016) showed average stand density was higher in mixed species stands compared with pure stands, attributing the

increase to complementary ecological traits. Woodall et al. (2005) give an example of how inappropriately applying the maximum SDI of a pure lodgepole pine (*Pinus contorta*) stand (around 2640 trees per hectare (TPH)) to a stand with only 51% lodgepole could result in a deviation of true maximum SDI of the mixed stand by more than 1000 stems. Kimsey et al. (2019) found significant increases in maximum SDI when shifting from pure stands of Douglas-fir or ponderosa pine (*Pinus ponderosa* [Douglas ex C. Lawson] var. *ponderosa*) to mixed stands. This increase was attributed to a mixing of more tolerant species, as shown by the relatively small increase between pure stands of shade tolerant grand fir and mixed stands of grand fir.

To understand the influence of these biological and environmental effects on the self-thinning line, site- and species-specific covariates are explored in the modelling process. Andrews et al. (2018) used a two-stage approach to determine the influence of species and site characteristics on maximum stand density in mixed-species forests of the North American Acadian Region. First, the self-thinning line was fit with plot-specific random intercepts and overall fixed slope which allowed for a unique maximum SDI to be calculated for each observation. The next step was to use a random forest approach to determine the influence of the specific plot level species and site characteristics. Weiskittel and Kuehne (2019), exploring similar mixed species forests of New England, USA, also used a multi-step approach where first, a size-density relationship was fit with linear quantile mixed models to estimate slope and plot-specific intercepts, then random forest was utilized to determine the most influential plot-level biotic and abiotic variables. The important variables were then added to the base model in a stepwise fashion until a final model was chosen.

This research project sought to determine whether these proposed methods utilized in other regional modelling efforts are capable of producing accurate SDI_{MAX} region-wide models for Pacific Northwest conifer forests and to evaluate if these methods could offer a path towards a standardized approach to nationwide modelling efforts. The overall goal of this study was to utilize the available data and modelling methodologies in the literature, to develop maximum stand density index models

for important Pacific Northwest conifer species of western Oregon and Washington based on site- and species-specific influences and interactions.

Materials and Methods

Study Area

This analysis covers over 13.6 million hectares of Pacific Northwest forests in western Oregon and Washington, USA, spreading from the southern Klamath Mountains, north along the crest of the Cascade Range, west through the Willamette Valley and Puget Trough to the Coastal and Olympic ranges reaching the Pacific Ocean. These forests are dominated by coastal Douglas-fir (*Pseudotsuga menziesii* (Mirb.) Franco) stands, western hemlock (*Tsuga heterophylla* (Raf.) Sarg.) and western red cedar (*Thuja plicata* Donn ex. D. Don) climaxes (Franklin and Waring, 1980). Forest land ownership is diverse and comprises a mixture of federally-owned National Forests and Parks, tribal lands, state and local government-owned forests and private forest and timberland held by individuals and timber management organizations. Elevation averages 550 meters and varies from sea level to over 4390 meters at the top of Mount Rainer. Geology and soils are found in highly varied and complex patterns with extensive influence of volcanic activity (Franklin and Dyrness, 1988). Thirty-year (1961-1990) annual mean precipitation averaged 221 cm with a range from 54 to 631 cm. The percentage of precipitation during the growing season (May-September) averages 15% with a range of 7.5 to 29%. Mean annual temperature from this same period averaged 9.3 ºC with a range from 1 to 13.1 ºC.

Data

Plot data were obtained through a collaborative network of public and private forest land management organizations. Inventory and monitoring plot data represented a range of fixed and variable radius sampling methods, each geolocated to allow extraction of desired attributes from spatial layers containing various physiographic metrics. Plot location information, including United States Forest Service (USFS) Forest Inventory and Analysis (FIA) and Field Sampled Vegetation (FSVeg) records, was provided as unfuzzed coordinates. When exact plot location was unavailable,

data were rolled up to the stand level (stand shapefiles supplied by data provider) and a stand centroid location was utilized (<10% of the dataset). Each plot record included number of trees per hectare (TPH), quadratic mean diameter (QMD) and proportion of basal area (BA) by major species groups. Data sources provided species basal area proportions for six species groups: Douglas-fir, western hemlock, western red cedar, red alder (*Alnus rubra* Bong.), and two other categories of conifer and hardwood. Data screening removed plots with less than 2.54 cm QMD and 24.7 TPH to establish a consistent threshold of diameter and number of trees. Only trees marked as living were included in plot-level estimates. The final dataset consisted of 168,220 unique observations representing the varied range of forest ecotypes across the Pacific Northwest (Figure 2.1). The data were broken into two distinct subsets, the first (n=155,083) are those plots containing at least 10% Douglas-fir by BA, and the second (n=13,137) consisting of plots with at least 10% western hemlock by BA which contained no Douglas-fir BA proportion. Summary statistics on plot data shown in Table 2.1. Although dominated by western hemlock, the later dataset had a significant BA proportion in secondary species of Pacific silver fir (*Abies amabilis*), which is rolled into the Other Conifer basal area proportion. This second subset of plots was concentrated in the wetter, climax forest conditions with less extreme heating events found in the Coast Range, Olympic Peninsula and Northern Cascades; however, each subset covered the range of the study area. These datasets will be referred to as DF-Mix and HemFir,

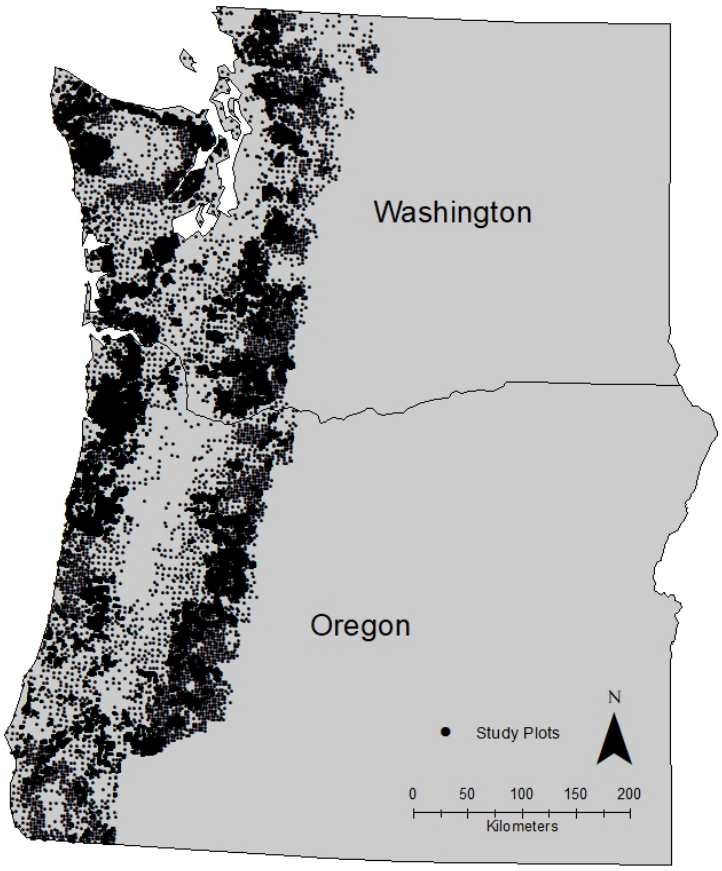

Figure 2.1 Study locations across western Washington and Oregon, USA (n = 168,220). Map was developed in R (R Core Team, 2020) with state boundaries from the U.S. Census Bureau TIGER/Line Shapefiles.

Table 2.1 Stand summary characteristics from plot record data used in this study

Variable	Mean	SD	Minimum	Maximum
DF-Mix (n = 155,083)				
Quadratic mean diameter (QMD; cm)	29.3	15.0	2.54	160.5
No. of stems (TPH; trees ha^{-1})	1,196.0	2,102.4	24.7	56,656.7
HemFir (n = 13,137)				
Quadratic mean diameter (QMD; cm)	27.6	16.6	2.54	131.3
No. of stems (TPH; trees ha^{-1})	1,623.8	2,602.2	25.1	38,182.4

respectively, throughout this paper. Species basal area proportions for each of the two datasets are found in Table 2.2.

Table 2.2 Basal area proportion (%) breakdown of plot data used in this study

Variable	Mean	SD	Minimum	Maximum
DF-Mix				
Douglas-fir	0.77	0.27	0.10	1
Western hemlock	0.09	0.18	0	0.90
Red alder	0.05	0.15	0	0.90
Western red cedar	0.02	0.07	0	0.90
Other conifer	0.04	0.12	0	0.90
Other hardwood	0.03	0.11	0	0.90
HemFir				
Douglas-fir	0	0	0	0
Western hemlock	0.68	0.30	0.10	1
Red alder	0.13	0.23	0	0.90
Western red cedar	0.04	0.12	0	0.90
Other conifer	0.13	0.23	0	0.90
Other hardwood	0.02	0.09	0	0.90

Topographic attributes were derived from U.S. Department of Agriculture (USDA) and National Resource Conservation Service (NRCS) National Elevation Data 30-m digital elevation models. Slope and aspect were derived using the 'raster' package (Hijmans, 2020) available through R 4.0 (R Core Team, 2020). Trigonometric transformations of slope and aspect were utilized to express the influence of these features on climate factors such as moisture and temperature (Roise and Betters, 1981). Spatial maps of soil parent materials were derived from U.S. Geological Service (USGS) 1:24,000 geology maps and surficial volcanic ash mantles from the NRCS soil survey geographic

database (SSURGO). Major geologic groupings and presence-absence of ash influence were determined similarly to the methods described by Kimsey et al. (2019).

Thirty-year (1961-1990) annual, seasonal and monthly climate normals were obtained through the ClimateNA v6.11 (Wang et al., 2016) software package using plot-specific latitude, longitude and elevation. These climate data contained directly calculated and derived variables, as well as various interactions resulting in over 230 climate variables assigned to each record. Some of these important climatic variables can be seen in Table 2.3.

Table 2.3 Site summary characteristics of plot locations used in this study

Variable	Mean	SD	Minimum	Maximum
DF-Mix				
LAT (º)	45.18	1.47	42	49
LON (º)	-123.07	0.72	-124.65	-120.73
ELEV (m)	517.20	311.46	0	2,098
SLOPE (º)	18.62	10.41	0	59.43
ASPECT (º)	183.37	102.98	0	360
MAT (ºC)	9.36	1.30	2.3	13.1
MCMT (ºC)	2.56	1.61	-6.3	7.4
MWMT (ºC)	16.90	1.33	11.2	21.5
MAP (cm)	214.74	75.22	54.4	571.4
GSP (cm)	32.33	11.44	7.8	85.5
RH (%)	66.15	3.73	52	78
PRATIO	0.15	0.03	0.075	0.29
MAPMCMT	8.25	3.68	-14.23	24.07
HemFir				
LAT (º)	46.08	1.18	42.70	49
LON (º)	-123.39	0.79	-124.70	-120.77
ELEV (m)	400.18	337.61	0	1,574
SLOPE (º)	17.99	10.76	0	56.82
ASPECT (º)	183.82	113.59	0	360
MAT (ºC)	9.01	1.21	2.4	11.9
MCMT (ºC)	2.73	1.75	-6.5	7.0
MWMT (ºC)	15.74	0.86	12.3	20.6
MAP (cm)	267.78	68.72	58.9	630.9
GSP (cm)	42.45	9.87	13.1	92.9
RH (%)	68.99	2.49	55	79
PRATIO	0.16	0.03	0.10	0.26
MAPMCMT	7.25	4.55	-12.03	22.01

*LAT – latitude, LON – longitude, ELEV – elevation, MAT – mean annual temperature, MCMT – mean temperature in the coldest month, MWMT – mean temperature in the warmest month, MAP – mean annual precipitation, GSP – growing season precipitation (May – September), RH – mean annual relative humidity, PRATIO – ratio of GSP to MAP, MAPMCMT – interaction between MAP and MCMT (MAP*MCMT)/1000

Modeling Maximum Stand Density

The data analysis process involved a multistep approach utilizing linear quantile mixed models and random forest in a variable selection process, followed by the development of an SDI_{MAX} model using stochastic frontier analysis.

Following the findings of Salas-Eljatib and Weiskittel (2018), linear quantile mixed models (LQMM) were developed with the 'lqmm' package (Geraci, 2014) within the R programming environment (R Core Team, 2020) to estimate the random plot-specific intercepts and fixed species-specific slope of the self-thinning line based on the Reineke (1933) equation:

[2] $$lnTPH = (\beta_0 + k_i) + \beta_1 * lnQMD$$

Where *TPH* is trees per hectare, *QMD* is quadratic mean diameter in cm, β_0 and β_1 are fixed effects parameters and k_i is the estimated random effect for plot record i. The random intercept parameter produced unique individual plot-level intercept values. The inclusion of a random intercept in the mixed model framework accounts for individual plot-level variance which is influenced by many inherent location factors such as site quality and the myriad possible species compositions found across the study region (Andrews et al., 2018).

Scharf et al. (1998) note that the decision of which quantile best represents the boundary of the data is an arbitrary one and must be made by the investigator. As in Andrews et al. (2018), values from the 90th through the 99th quantile were compared to determine which percentile to utilize. The 95th was chosen as the values produced were reasonable while removing the sensitivity of highly influential observations found at the higher quantiles, as well as unreasonably low values produced at the lower quantiles. Resulting from equation [2], plot-level SDI_{MAX} values for plot i can be calculated as:

[3] $$SDI_{MAX} = \exp((\beta_0 + k_i) + \beta_1 * \ln(25.4))$$

Individual plot SDI_{MAX} values resulting from the application of equation [3] were then utilized to explore variable influence. Due to the large number of explanatory variables assigned to each plot

record, random forest (RF) analysis (Breiman, 2001) with the R package 'randomForest' (Liaw and Wiener, 2002) was used as a variable selection process. RF is a machine learning algorithm which constructs an ensemble of decision trees. RF was utilized to understand variable importance in predicting SDI_{MAX} and determine the most influential variables to be considered in the final predictive model. RF was ran under multiple algorithm parameters utilizing a grid search tuning method to determine the best combination with a final run of 2500 trees trying approximately 1/3 of the variables at each node with an 80/20 training/testing split for cross validation. Variable importance plots (varImpPlot) display ranked variables on two criteria based on error and node purity measured by the Gini importance index.

The top variables selected from the random forest analysis were then explored using stochastic frontier analysis (SFA). SFA is an econometric approach to express the maximum output obtainable from a given input (Aigner et al., 1977). The frontier function is considered stochastic, as opposed to deterministic, due to the two-part error term which allows some observations to lie above the maximum boundary line. The maximum stand density index model can be formulated as follows:

[4] $$lnTPH = \beta_0 + \beta_1 lnQMD + \beta_i n_i + \varepsilon_i$$

where:

[5] $$\varepsilon_i = v_i + u_i$$

TPH is number of trees per hectare, QMD is quadratic mean diameter, β_0 is the intercept of the self-thinning line, β_1 is the slope of the self-thinning line, β_i are model coefficients for the i^{th} site or species-specific covariate, n_i represents the value of the i^{th} site or species-specific covariate, where v_i and u_i are unobservable random errors (Battese and Corra, 1977). v_i is assumed identically and independently distributed as normal with mean of 0 and variance as σ_v^2. This error term is interpreted as the random effects of both favorable and unfavorable conditions, which affect performance, as well as any associated measurement error. The error term u_i is the non-positive disturbance function

assumed half-normal and distributed independently of v_i with variance as σ_u^2. This error term is interpreted as the deviation from the maximum output. When u_i is equal to 0, the output has reached maximum.

With respect to the self-thinning boundary, the first error term v_i is the result of the site factors discussed previously such as climate and topography, as well as the characteristics of the tree species present such as size (QMD), crown architecture, specific gravity and tolerance to shade, drought and cold temperatures. This error term also encompasses any measurement error associated with these factors. The second error term reflects the fact that a stand's trajectory has not reached the maximum boundary line; that is, any observation not on the self-thinning boundary line will have u_i<0. The model utilizes all observations and is solved by maximum likelihood estimation with the error parameter assumptions as described above.

The variance parameter of the stochastic frontier function is:

[6] $$\sigma^2=\sigma_v^2 + \sigma_u^2$$

The variance ratio parameter is given by:

[7] $$\gamma = \frac{\sigma_u^2}{\sigma_u^2+\sigma_v^2}$$

Where γ lies between 0 and 1. The value of γ can be interpreted as to the applicability of a stochastic frontier function. For example, if γ = 0 then the variance σ_u^2 = 0 and thus there would be no need to include u_i in the error term which would then allow the model to be estimated simply with OLS (Battese and Coelli, 1992). As γ approaches 1, the greater the validity of the parameter estimations found by the stochastic frontier function.

SFA was run using PROC QLIM in SAS 9.4 (SAS Institute Inc., 2012) specified as a half normal, production model with the natural log of TPH as the endogenous variable. The top explanatory variables shown as important from the RF analysis were sequentially added and/or

removed depending on AIC score and γ values. Multicollinearity was assessed among the top variables that were considered in the selection process through Pearson Correlation Coefficients using the CORR procedure in SAS.

Independent Validation of Maximum Stand Density Index Model

Final model results were compared against published SDI_{MAX} of similar species and region to evaluate reasonableness of predictions and self-thinning line parameter values for slope and intercept. Also, stand growth trajectories of independent, long-term monitoring datasets were utilized to evaluate the predicted self-thinning trajectory. Published tables of remeasured TPH and QMD data from the Levels of Growing Stock (LOGS) Douglas-fir thinning studies (Curtis et al., 1997) and from western hemlock growth and yield trials (Hoyer and Swanzy, 1986) were utilized as independent datasets. Stand data was plotted along with the site-specific self-thinning line extracted from the predicted values at the location of these studies. Performance was evaluated based on the trajectory of these data points relative to the predicted self-thinning line.

Results

Quantile Regression

LQMM at the 95th quantile with random plot-level intercepts yielded predicted self-thinning slope and intercept of -1.607 (SE=0.013) and 12.3 (SE=0.045) for DF-Mix, and -1.544 (SE=0.017) and 12.227 (SE=0.060) for HemFir. The random effects covariance was 0.068 for DF-Mix and 0.096 for HemFir. Mean predicted SDI_{MAX} was 1220 TPH (SD=119) with a range from 464 to 1719 TPH for DF-mix and mean predicted SDI_{MAX} was 1396 TPH (SD=151) with a range of 540 to 1916 TPH for HemFir.

Influential Variables

The RF analysis was utilized for variable selection among the > 250 biotic, climatic, geologic and topographic factors assigned to each record. Each of the two variable importance measures (Error and Gini Index) was considered; however, the top 50 variables were fairly consistent between each

measure of importance with 40 of the top 50 in each measure being identical for the DF-Mix dataset and 35 of 50 for the HemFir dataset. The most influential variables were measures of basal area proportions for the following species: western hemlock (WH_BA), red alder (RA_BA), western red cedar (RC_BA) and two 'other' categories of conifer (OtherC_BA) and hardwood (OtherH_BA), location information (latitude, longitude and elevation), topographic transformations and many climatic variables and their interactions describing precipitation and temperature. Similar, but not identical, variables were selected to test in the SFA between the DF-Mix and HemFir datasets.

Stochastic Frontier Regression

To begin the process, an initial model of predicting ln(TPH) with the single variable ln(QMD) served as the base model. The base model for DF-Mix and HemFir was considered as having 100% of each species basal area proportion, respectively. Then, through an iterative process, variables were introduced to the model and kept or removed based on variable significance ($p < 0.0001$) as well as AIC score.

The final models (Table 2.4) had a γ of 0.924 for the DF-Mix dataset and 0.940 for the HemFir dataset, indicating SFA was appropriate for modeling the self-thinning boundary line. The self-thinning slope was -1.517 for DF-Mix model and -1.461 for HemFir model.

Table 2.4 Summary of frontier model parameters and variance estimates for DF-Mix and HemFir. Reineke model only includes intercept and slope, whereas full model includes all chosen species and site variables. Standard errors shown in parenthesis. All variables significant ($p < 0.0001$).

Model	Variables	Intercept	Slope	gamma	AIC
DF-Mix Reineke	log(QMD)	12.182 (0.009)	-1.531 (0.003)	0.915	250321
DF-Mix Full	all	12.202 (0.016)	-1.517 (0.003)	0.924	239957
HemFir Reineke	log(QMD)	12.014 (0.033)	-1.430 (0.010)	0.919	26624
HemFir Full	all	9.754 (0.177)	-1.461 (0.009)	0.940	26147

The final DF-Mix model had the following structure:

$$SDI_{MAX} = \exp(\beta_0 + (\beta_1 * \ln(25.4)) + (\beta_2 * WH_{BA}) + (\beta_3 * RA\_BA)$$
$$+ (\beta_4 * RC\_BA) + (\beta_5 * OtherC\_BA) + (\beta_6 * OtherH\_BA) + (\beta_7 * LAT) + (\beta_8 * Elev)$$
$$+ (\beta_9 * tan\_slope\_sin\_aspect) + (\beta_{10} * \cos\_aspect) + (\beta_{11} * PRATIO)$$
$$+ (\beta_{12} * MAPMCMT) + (\beta_{13} * ASH\_Absent) + (\beta_{14} * ASH\_Andic) + (\beta_{15} * ROCK\_type))$$

The final HemFir model had the following structure:

$$SDI_{MAX} = \exp(\beta_0 + (\beta_1 * \ln(25.4)) + (\beta_2 * RA\_BA) + (\beta_3 * RC\_BA) + (\beta_4 * OtherH\_BA)$$
$$+ (\beta_5 * LAT) + (\beta_6 * tan\_slope\_sin\_aspect) + (\beta_7 * PRATIO) + (\beta_8 * RH)$$
$$+ (\beta_9 * TD) + (\beta_{10} * ASH\_Absent) + (\beta_{11} * ROCK\_type))$$

The RF variable importance gave high rankings to many of the interaction terms between temperature and precipitation. Often these terms had high multicollinearity. When multiple variables deemed important showed high correlation, only the variable which produced the higher likelihood ratio was kept in the model. For example, in the DF-Mix dataset, RF variable importance showed interactions of both growing season precipitation (GSP) and mean annual precipitation (MAP) with the mean coldest month temperature (MCMT) as having large influence. These two interaction variables, GSPMCMT and MAPMCMT have a Pearson Correlation Coefficient of 0.98264, therefore, although both were significant in model development, only MAPMCMT was kept in the model because it produced the larger log likelihood ratio and thus the lower AIC score. Latitude (LAT), which was kept in both the DF-Mix and HemFir model, and had the highest Pearson Correlation Coefficient with PRATIO at 0.58 and 0.52 for each model respectively. Elevation (ELEV), which was kept in the DF-Mix model, had a Pearson Correlation Coefficient of -0.58 with MAPMCMT. These terms (Latitude and Elevation) were kept in the model as they account for other regional, spatial processes such as genetic adaptations of bud phenology and emergence, as well as the effect of day

length patterns on other biological developments (St. Clair et al., 2005). No other terms in either model had a Pearson Correlation Coefficient greater than +/- 0.5.

In application, if a stand is either pure Douglas-fir or western hemlock, then the DF-Mix and HemFir models imply 100% basal area proportion of those species respectively, with other species' basal area proportion values set to 0. As a stand diverges from pure, the additional species basal area proportion coefficients are introduced. To predict the SDI_{MAX} for a stand of 80% Douglas-fir, 15% western hemlock and 5% other hardwood, 0.15 and 0.05 would be inserted for the values of WH_BA and OtherH_BA respectively, and the remaining 80% Douglas-fir is built into the intercept, with the RA_BA, RC_BA and OtherC_BA taking a value of 0. The HemFir model inherently has 0% Douglas-fir basal area and therefore has no coefficient for this species. In the DF-Mix model, mixing of all other species groups increased carrying capacity. In the HemFir model, additional hardwood species mixing has a negative effect on carrying capacity, while the addition of western red cedar, a tolerant species, increased carrying capacity.

Climatic variables were influential in both models (Figure 2.2). PRATIO, the ratio of growing season precipitation to annual precipitation (GSP/MAP), was the single most influential climatic variable in each model. The DF-Mix and HemFir model each showed a strong positive effect of having more precipitation during the growing season relative to the annual total. The DF-Mix model included an interaction term between mean annual precipitation and mean temperature in the coldest month (MAPMCMT), which had a negative effect on carrying capacity. This interaction term signified cooler environments receiving the same precipitation relative to warmer sites can support a higher carrying capacity. Relative humidity (RH) and temperature difference (TD) each had a positive effect on HemFir carrying capacity. The forests which support these climax stands tend to be wetter throughout the year. The TD term was driven mainly by cooler winters rather than hotter summer months, showing these forests have less extreme heating events and can tolerate the lower temperatures of the winter months.

Elevation had a positive effect in the DF-Mix model showing that higher elevations support greater carrying capacity. While elevation was shown to be an influential variable in the RF analysis of

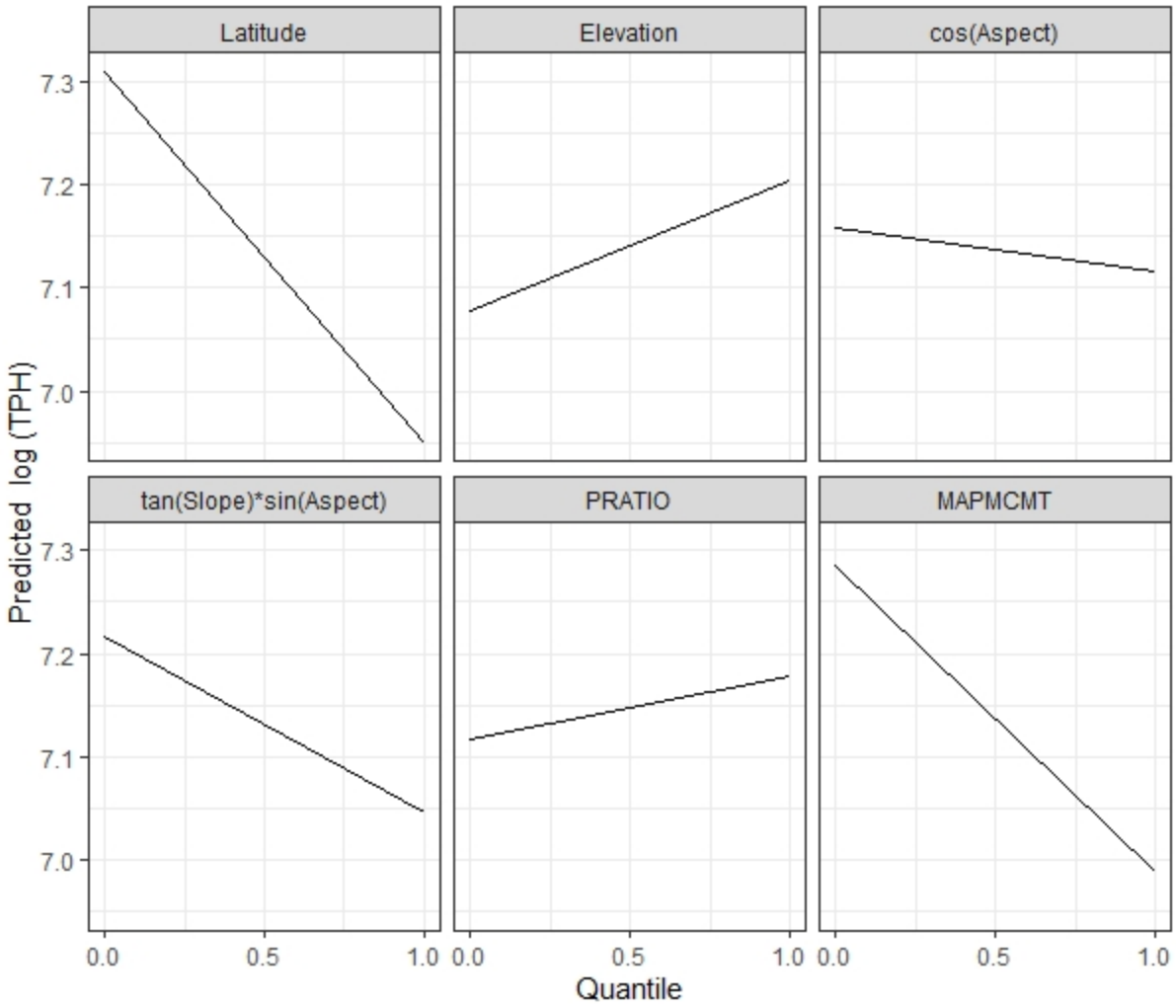

Figure 2.2 Site effects on DF-MIX predicted maximum density index for the 10th and 90th quantile of each individual site variable while keeping other site variables constant at the 50th quantile. QMD is indexed to 25.4cm and Douglas-fir basal area proportion held constant at 100%.

the HemFir dataset, this variable continuously dropped out during the model building process and was not included in the final HemFir model. Latitude had a negative effect in both models showing, with other variables held constant, the forests of the northern latitudes have lower carrying capacity than southern forests. With approximately 7 degrees of latitude between the most southerly and most northerly plot in each dataset, this effect may be capturing the difference in day length with respect to

sun angle. The cosine of aspect, a measure of north-south slope effect, had a slight negative effect on DF-Mix carrying capacity as the topography shift from southerly to northerly. The interaction of tangent of slope and sine aspect, a modification of the east-west slope effect, had a negative effect on SDI_{MAX} in both models, giving steeper, eastern facing slopes a greater carrying capacity than steeper, western facing slopes. This variable had little effect on flatter topography.

Ash influence (ASH_ANDIC), or lack thereof (ASH_ABSENT), was influential in both models. The absence of any underlying volcanic ash negatively affected carrying capacity in each the DF-Mix and HemFir models. In the DF-Mix model, the presence of andic soil properties increased carrying capacity significantly. Parent materials of sandstone and glacial outwash had a negative effect on DF-Mix and HemFir models respectively. The geologic and soil variables are binary and receive a value of 1 (present) or 0 (absent) when applying the model.

Evaluation of Model Performance

The site specific SDI_{MAX} models developed here were compared against published reference curves. Self-thinning slope and intercepts of the 50^{th} and 95^{th} quantile of growing conditions for each model were determined and plotted against published reference values (Figure 2.3). Results from modeling the 95^{th} percentile of modeled SDI_{MAX} values for the DF-Mix and HemFir plot data showed 1,728 TPH and 1,952 TPH, respectively.

When applying the model across the species ranges (expected to make up at least 10% basal area) within the study area (Figure 2.4), mean SDI_{MAX} values were 1,234 TPH for DF-Mix with 100% Douglas-fir basal area and 2,068 TPH for HemFir with 100% western hemlock basal area. Predicted SDI_{MAX} values at the 0.05 and 0.95 percentiles ranged from 1,065 to 1,459 TPH for pure Douglas-fir stands and 1,579 to 2,644 TPH for pure western hemlock stands. Long (1985) reported SDI_{MAX} values of 1,450 and 1,950 for stands of pure Douglas-fir and western hemlock, respectively.

Repeat measurements of control plots from two long-term studies were available to evaluate the modelled self-thinning lines. The first dataset was from the Levels of Growing Stock (LOGS) Douglas-fir thinning trials. The LOGS study had seven sites available in the study region including Francis (Hoyer et al., 1996), Hoskins (Marshall and Curtis, 2002), Rocky Brook (Curtis and Marshall,

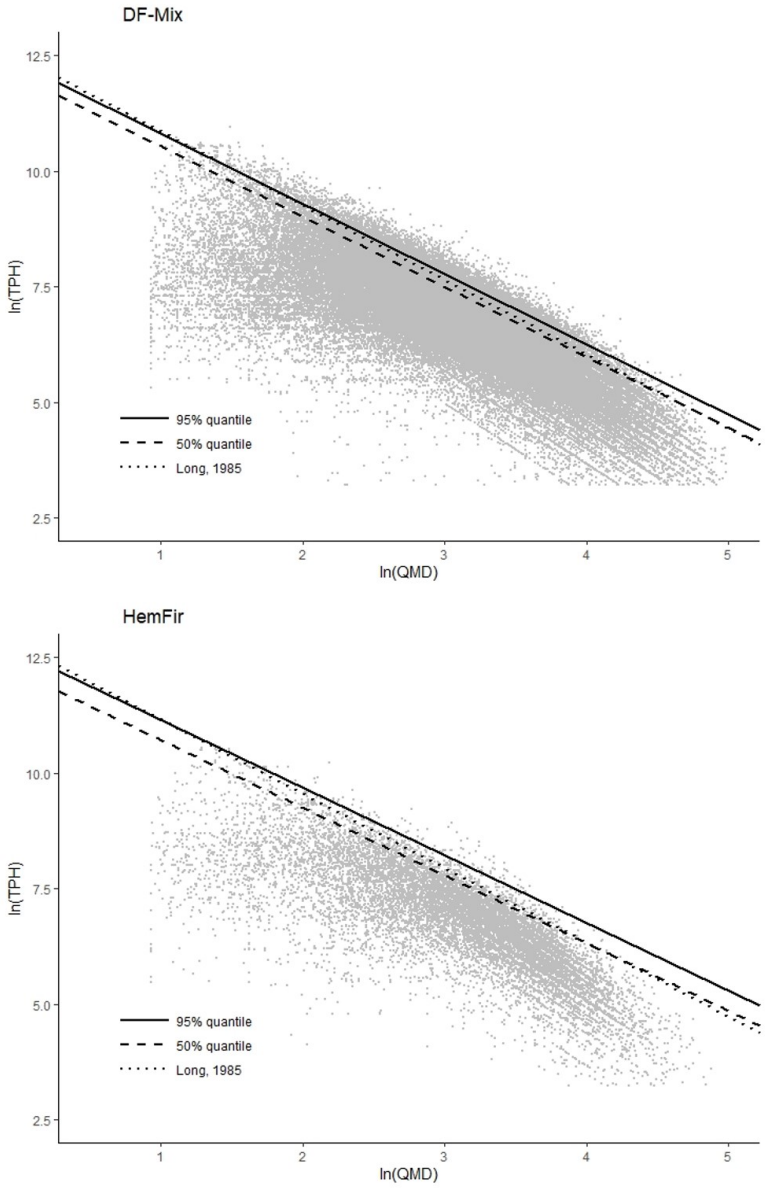

Figure 2.3 Maximum stand density index frontiers of the 95th (solid line) and 50th (dashed line) quantile of optimal site characteristics. Established regional species-specific maximum density lines (dotted lines) are shown from Long (1985). Dots represent plot specific size-density relationships.

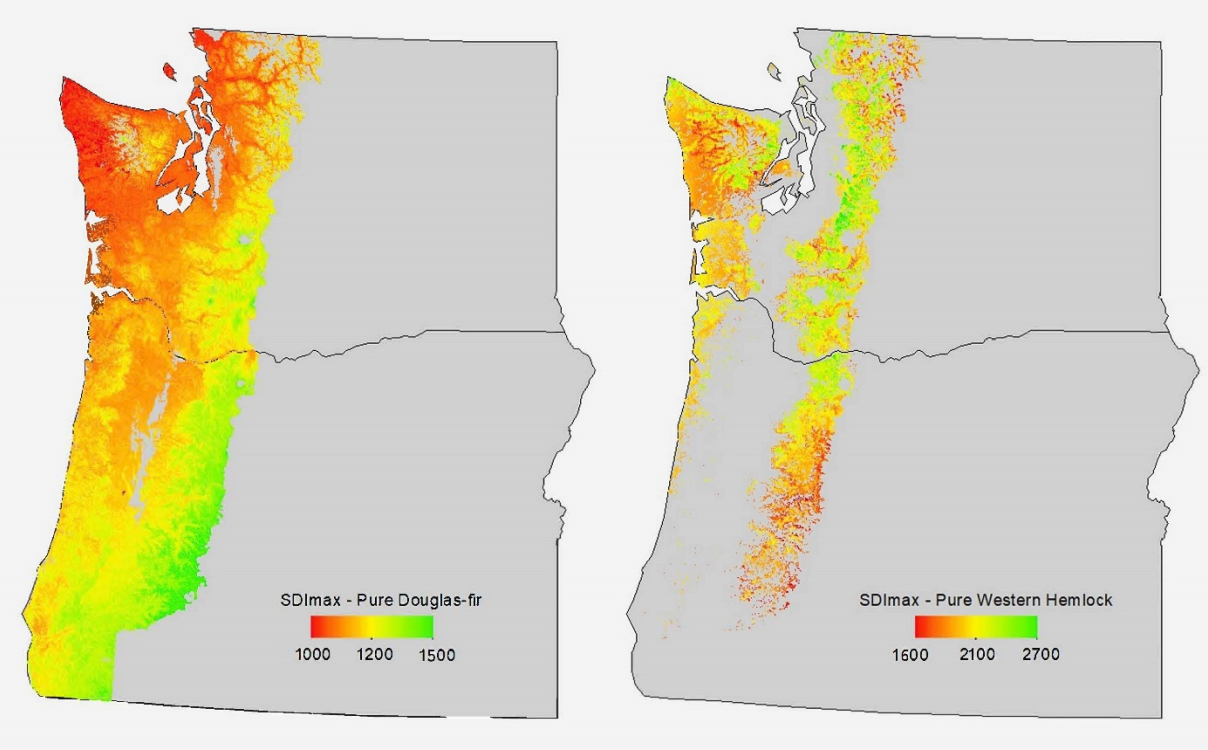

Figure 2.4 Regional models applied to expected species ranges within the study area with basal area input at 100% for each Douglas-fir and western hemlock within the DF-Mix and HemFir models respectively. Units represent trees per hectare indexed to 25.4 cm. Output limited to specie range with expected basal area proportion of at least 10%. Map was developed in R (R Core Team, 2020) from 1km raster tiles with state boundaries from the U.S. Census Bureau TIGER/Line Shapefiles.

2009a), Iron Creek (Curtis and Marshall, 2009b), Skykomish (King et al., 2002), Clemons (King et al., 2002) and Stampede Creek (Curtis and Marshall, 2002). The LOGS study had one western hemlock plot that was also used for evaluating the HemFir model. Data from tables published in these reports were digitized and site-specific SDI_{MAX} values and self-thinning curves were extracted for each location. Plot location information was provided by Oregon State University's Center for Intensive Planted-forest Silviculture group (D. Mainwaring, personal communication). The second dataset came from two western hemlock thinning trials (Clallam Bay and Cascade Head) which were part of a growth and yield study with detailed results published by Hoyer and Swanzy (1986). This report contained detailed location information to extract modelled SDI_{MAX} values at these sites. The results (Figure 2.5) of plotting stand development of these repeat measures datasets against model-predicted, site-specific self-thinning lines showed an overall good fit of the stand trajectory.

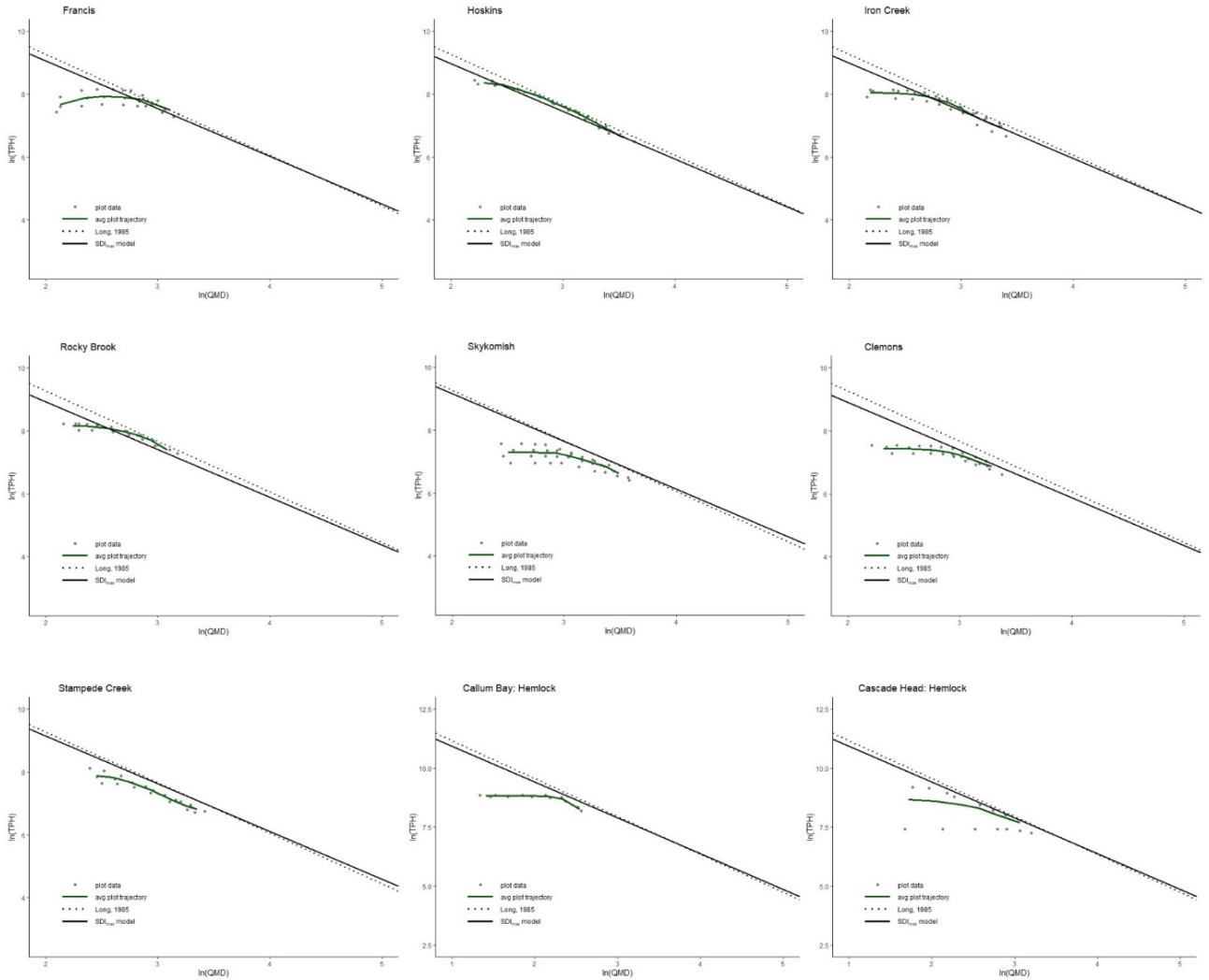

Figure 2.5 Independent validation of regional models using long-term, repeat measures data from the LOGS (Curtis, 1997) and western hemlock spacing trials (Hoyer and Swanzy, 1986). Measured stand size-density trajectories are plotted against the site-specific modeled SDI_{MAX} self-thinning line. The available dataset (grey dots) with established regional species-specific maximum density frontiers (dotted lines) (Long, 1985).

Discussion

Controlling stand density through silvicultural prescriptions is one of the oldest and most commonly used methods for achieving forest management goals (Allen and Burkhart, 2018). Knowledge of stand carrying capacity under given climatic and physiographic conditions is crucial for developing regionally appropriate management guidelines (Condes et al., 2017). Results from this SDI_{MAX} modelling analysis have shown the systematic differences of the self-thinning line with respect to varying species composition and site-specific environmental factors. Within the complex landscape of the Pacific Northwest, these results demonstrate the variability of site carrying capacity and the need for site adapted reference values of maximum density.

Reineke's original analysis utilized only the measures of tree size and number from even-aged monocultures, with no assessment on the impact of environmental factors. It was interesting to note the LQMM analysis on only tree size and number of the DF-mix dataset, which was dominated by records from stands of pure or nearly pure Douglas-fir (median values of 87% Douglas-fir BA proportion) produced a self-thinning slope of -1.607 compared to Reineke's -1.605. While the self-thinning slope may have been similar solely based on the relationship between tree size and number, the subsequent analysis involving environmental variables and, in particular the introduction of species mixing, produce systematic differences in the slope and intercept values.

Utilizing the variable importance results from the random forest analysis provided a convenient means of dealing with the large number of potential explanatory variables. This machine learning approach allowed for the identification of predictors to introduce into the regression model. While random forest could have potentially been used as the predictive model, we opted for stochastic frontier regression which allowed for the assignment of coefficients to specific variables. The ability to display the model form with variables and assigned coefficient facilitated technology transfer and application of this model amongst industry partners.

The results from stochastic frontier regression show a divergence from the self-thinning slope from -1.605 proposed by Reineke and still utilized for determining SDI today. Stands dominated by Douglas-fir showed a shallower slope of -1.517, while stands of hemlock-fir showed an even shallower slope of -1.461. Although not universal (Vospernik and Sterba, 2015; Charru et al., 2012), shade-tolerance of species is often thought to have an effect on the self-thinning line (Weller, 1987; Jack and Long, 1996; Pretzsch and Biber, 2016; Kimsey et al., 2019). This is often attributed to the higher 'packing density' and ability for shade-tolerant species to fill canopy gaps (Pretzsch, 2014). The results presented here show not only a flatter slope for the more shade-tolerant HemFir compared to DF-Mix, but also higher SDI_{MAX} values with greater species mixing with complementary ecological traits. For example, in the DF-Mix model, SDI_{MAX} increases as a stand moves away from pure, intermediate shade-tolerant Douglas-fir toward a mix with more shade-tolerant western hemlock and western red cedar.

As expected, climate played a significant role in the determination of site-specific SDI_{MAX} in both the DF-mix and HemFir models. Consistency of precipitation, as PRATIO, throughout the growing season had a large positive effect on carrying capacity. This metric signals the droughtiness of the site, with the model showing forests receiving balanced precipitation throughout the year as supporting a greater carrying capacity. Extreme heating events caused a drop in carrying capacity with milder conditions allowing for greater SDI_{MAX} in HemFir sites. Throughout the study region, cooler temperatures and greater precipitation allowed for higher carrying capacity. Adapting a species mix at the appropriate density, given expected climatic conditions, can allow for optimization of the stand to capture and utilize site resources.

The influence of particular underlying soil parent material was seen in both models. DF-Mix sites on sandstone negatively affecting site carrying capacity. Sandstone-derived soils contain more than 50% sand-sized particles predominantly of quartz and often have low base cation status and nutrient reserve (Buol et al., 2003). HemFir carrying capacity was negatively affected by soils of

unconsolidated glacial materials. Glacial-derived soils in the Pacific Northwest are often younger, shallower, less clay-rich with lower nitrogen content and rapid drainage compared to igneous or sedimentary derived soils (Littke et al., 2011).

Site carrying capacity increases when DF-Mix and HemFir stands are found on soils with presence of volcanic ash. As well, DF-Mix stands growing on sites in absence of volcanic ash influence were found to have lower carrying capacity throughout the study region. Soils associated with the volcanic ash tend to have greater nutritional and water holding capacity and have been shown to significantly affect growth and mortality (Coleman et al., 2014, Kimsey et al., 2011)

The range of SDI_{MAX} values are in line with results from other published studies from the region (Long, 1985; Weiskittel et al., 2009). The higher reported values for the DF-mix dataset relative to Long (1985) or Reineke (1933) is mainly driven by species mixing. Where stands with a mixture of more shade-tolerant species increases the overall density relative to a stand composed of only less tolerant species. Overall, model evaluation against the long-term datasets demonstrated the importance of site-specific assessment of carrying capacity. There was strong agreement within the Clemons and Iron Creek sites, with the growth trajectory tracking along the predicted self-thinning line. While not unexpected, some sites tracked slightly below, never quite reaching the self-thinning line. These stands tended to self-thin before reaching previously published curves or would curve away from published lines back toward a lower level. Individual stands seldom travel along their self-thinning frontier but are more likely to converge toward them during the self-thinning phase (Vospernik and Sterba, 2015). A one-size-fits-all approach to assigning a maximum stand density index solely based on species is not appropriate as can be seen by the varying self-thinning trajectories of these datasets.

The methodology used in this approach was similar to recent analysis and modelling efforts in other regions (Kimsey et al., 2019; Andrews et al., 2018; Ducey et al., 2017). The results presented here show that while the variables chosen for inclusion in the final models may vary between different

regions and forest types, the methodology is transferable. The ability to explore a large number of site and species-specific variables, and determine the most influential for model inclusion, is key to developing regionally specific models as variable influence varies between different forested ecosystems. Understanding the influence of climate variables in particular can allow for possible future climate conditions to be assessed within this maximum stand density index modelling framework.

Conclusion

Site-sensitive, species-specific maximum stand density index models were developed for forest stands of the coastal Pacific Northwest, USA. Many environmental (climate, topography, underlying soil parent material/ash influence) and biological factors (species mixing) control the self-thinning trajectory of a stand and determine the maximum carrying capacity. Stocking, or relative density, is determined by the ratio of current stand density to the potential maximum and may be utilized to predict certain phases of stand development, in particular the onset of density dependent mortality. Maximum stand density index serves as a tool for silvicultural prescriptions, including timing and levels of thinning and other density control measures such as initial spacing at planting and species selection. Regionally appropriate models can aid forest managers in decision-making to promote healthy, sustainable and productive forests.

References

Aguirre, A., del Río, M and Condes, S. 2018. Intra- and inter-specific variation of the maximum size-density relationship along an aridity gradient in Iberian pinewoods. *Forest Ecology and Management*, 411, 90-100. https://doi.org/10.1016/j.foreco.2018.01.017

Aigner, D., Lovell, C and Schmidt, P. 1977. Formulation and estimation of stochastic frontier production function models. *Journal of Econometrics*, 6, 21-37. https://doi.org/10.1016/0304-4076(77)90052-5

Allen, M and Burkhart, H. 2018. Growth-density relationships in loblolly pine plantations. *Forest Science*, 65(3), 250-264. https://doi.org/10.1093/forsci/fxy048

Andrews, C., Weiskittel, A., Amato, A. W. D., and Simons-legaard, E. 2018. Variation in the maximum stand density index and its linkage to climate in mixed species forests of the North American Acadian Region. *Forest Ecology and Management*, 417, 90–102. https://doi.org/10.1016/j.foreco.2018.02.038

Battese, G. and Coelli, T. 1992. Frontier production functions, technical efficiency and panel data: With application to paddy farmers in India. J Prod Anal 3, 153–169 (1992). https://doi.org/10.1007/BF00158774

Battese, G. and Corra, G. 1977. Estimation of a production frontier model: with application to the pastoral zone of eastern Australia. *Australian Journal of Agricultural Economics* 21, 169–179. https://doi.org/10.1111/j.1467-8489.1977.tb00204.x

Bi, H., Wan, G. and Turvey, N. 2000. Estimating the self-thinning boundary line as a density-dependent stochastic biomass frontier. *Ecology*, 81(6), 1477-1483. https://doi.org/10.2307/177300

Bickford, C. 1957. Stocking, normality, and measurement of stand density. *Journal of Forestry*, 55(2), 99-104. https://doi.org/10.1093/jof/55.2.99

Binkley, D. 1984. Importance of size—density relationships in mixed stands of Douglas-fir and red alder. *Forest Ecology and Management*, 9(2), 81-85. https://doi.org/10.1016/0378-1127(84)90075-6

Breiman, L. 2001. Random Forests. *Machine Learning*. 45, 5-32. https://doi.org/10.1023/A:1010933404324

Buol, S., Southard, R., Graham, R. and McDaniel, P. 2003. Soil Genesis and Classification. Iowa State University Press, Ames, Iowa. ISBN 0-8138-2873-2

Chapin, F, Matson, P. and Vitousek, P. 2011. Principles of Terrestrial Ecosystem Ecology, Springer, New York, ISBN 9781441995032

Charru, M., Seynave, I., Morneau, F., Rivoire, M. and Bontemps, J. 2012. Significant differences and curvilinearity in the self-thinning relationships of 11 temperate tree species assessed from forest inventory data. *Annals of Forest Science*, 69, 195-205. https://doi.org/10.1007/s13595-011-0149-0

Coleman, M., Shaw, T., Kimsey, M. and Moore, J. 2014. Nutrition of Douglas-fir in the Inland Northwest. *Soil Science Society of America Journal*, 78(S1), S11-S22. https://doi.org/10.2136/sssaj2013.08.0327nafsc

Coops, N., Waring, R. and Moncrieff, J. 2000. Estimating mean monthly incident solar radiation on horizontal and inclined slopes from mean monthly temperatures extremes. *International Journal of Biometeorology* 44, 204–211. https://doi.org/10.1007/s004840000073

Condés, S., Vallet, P., Bielak, K., Bravo-Oviedo, A., Coll, L., Ducey, M., Pach, M., Pretzsch, H., Sterba, H., Vayreda, J., and del Río, M. 2017. Climate influences on the maximum size-density relationship in Scots pine (*Pinus sylvestris* L.) and European beech (*Fagus sylvatica* L.) stands. *Forest Ecology and Management*, 385, 295-307. https://doi.org/10.1016/j.foreco.2016.10.059

Curtis, R., and Marshall, D. 2002. Levels-of-growing-stock cooperative study in Douglas-fir: report No 14 – Stampede Creek: 30-year results. Research Paper PNW-RP-543. Portland, OR. USDA, Forest Service, Pacific Northwest Research Station 90pp.

Curtis, R., and Marshall, D. 2009a. Levels-of-growing-stock cooperative study in Douglas-fir: report No 18 – Rocky Brook: 1963-2006. Research Paper PNW-RP-578. Portland, OR. USDA, Forest Service, Pacific Northwest Research Station 90pp.

Curtis, R., and Marshall, D. 2009b. Levels-of-growing-stock cooperative study in Douglas-fir: report No 19 – Iron Creek: 1966-2006. Research Paper PNW-RP-580. Portland, OR. USDA, Forest Service, Pacific Northwest Research Station 84pp.

Curtis, R., Marshall, D. and Bell, J. 1997. LOGS A pioneering example of silvicultural research in coast Douglas-fir. *Journal of Forestry*. 95(7), 19-25. https://doi.org/10.1093/jof/95.7.19

del Río, M., Montero, G. and Bravo, F. 2001. Analysis of diameter–density relationships and self-thinning in non-thinned even-aged Scots pine stands. *Forest Ecology and Management*, 142, 79-87. https://doi.org/10.1016/S0378-1127(00)00341-8

Drew, R and Flewelling, J. 1977. Some recent Japanese theories of yield-density relationships and their application to Monterey pine plantations. *Forest Science*, 23(4), 517-534. https://doi.org/10.1093/forestscience/23.4.517

Ducey, M., Woodall, C. and Bravo-Oveido, A. 2017. Climate and species functional traits influence maximum live tree stocking in the Lake States, USA. *Forest Ecology and Management*. 386, 51-61. https://doi.org/10.1016/j.foreco.2016.12.007

Franklin, J and Dyrness, C. 1988. Natural vegetation of Oregon and Washington. Oregon State University Press. 468 pp.

Franklin, J and Waring, R. 1980. Distinctive features of the northwestern coniferous forest: Development, Structure, and Function. In: Forests: Fresh Perspectives from Ecosystem Analysis, Proceedings, 40th annual biological colloquium. Oregon State University Press. 59-86.

Geraci, M. 2014. Linear Quantile Mixed Models: The 'lqmm' package for Laplace Quantile Regression. *Journal of Statistical Software*. 57(3), 1-29. http://dx.doi.org/10.18637/jss.v057.i13

Hijmans, R. 2020. 'raster': Geographic data analysis and modeling. R package version 3.3-13. https://CRAN.R-project.org/package=raster

Hoyer, G., Anderson, N. and Marshall, D. 1996. Levels-of-growing-stock cooperative study in Douglas-fir: report No 13 – the Francis study: 1963-1990. Research Paper PNW-RP-488. Portland, OR. USDA, Forest Service, Pacific Northwest Research Station 91pp.

Hoyer, G and Swanzy J. 1986. Growth and yield of western hemlock in the Pacific Northwest following thinning near the time of initial crown closing. Research Paper PNW-RP-365. Portland, OR. USDA, Forest Service, Pacific Northwest Research Station 52pp. https://doi.org/10.5962/bhl.title.94172

Jack, S. and Long, J. 1996. Linkages between silviculture and ecology: An analysis of density management diagrams. Forest Ecology and Management, 86, 205–220. https://doi.org/10.1016/S0378-1127(96)03770-X

Kimsey, M, Moore, J and McDaniel, P. 2008. A geographically weighted regression analysis of Douglas-fir site index in north central Idaho. *Forest Science*, 54(3), 356-366. https://doi.org/10.1093/forestscience/54.3.356

Kimsey, M., Garrison-Johnston, M. and Johnson, L. 2011. Characterization of volcanic ash-influenced soils across a geoclimatic sequence. *Soil Science Society of America Journal*, 75(1), 267-279. https://doi.org/10.2136/sssaj2010.0092

Kimsey, M., Shaw, T. and Coleman, M. 2019. Site sensitive maximum stand density index models for mixed conifer stands across the Inland Northwest, USA. *Forest Ecology and Management*, 433, 396-404. https://doi.org/10.1016/j.foreco.2018.11.013

King, J., Marshall, D. and Bell, J. 2002. Levels-of-growing-stock cooperative study in Douglas-fir: report No 17 – the Skykomish study: 1961-93; the Clemons study, 1963-94. Research Paper PNW-RP-548. Portland, OR. USDA, Forest Service, Pacific Northwest Research Station 120pp.

Kweon, D. and Comeau, P. 2017. Effects of climate on maximum size-density relationships in Western Canadian trembling aspen stands. *Forest Ecology and Management*, 406, 281-289. https://doi.org/10.1016/j.foreco.2017.08.014

Liaw, A. and Wiener, M. 2002. Classification and Regression by randomForest. *R News*. 2(3), 18-22.

Littke, K., Harrison, R., Briggs, D. and Grider, A. 2011. Understanding soil nutrients and characteristics in the Pacific Northwest through parent material origin and soil nutrient regimes. *Canadian Journal of Forest Research*. 41, 2001-2008. https://doi.org/10.1139/X11-115

Long, J. 1985. A practical approach to density management. *The Forestry Chronicle*, 61, 23-27. https://doi.org/10.5558/tfc61023-1

Marshall, D., and Curtis, R. 2002. Levels-of-growing-stock cooperative study in Douglas-fir: report No 15 – Hoskins: 1963-1998. Research Paper PNW-RP-537. Portland, OR. USDA, Forest Service, Pacific Northwest Research Station 80pp.

Pretzsch, H. 2014. Canopy space filling and tree crown morphology in mixed-species stands compared with monocultures. *Forest Ecology and Management*, 327, 251-264. http://dx.doi.org/10.1016/j.foreco.2014.04.027

Pretzsch, H and Biber, P. 2005. A re-evaluation of Reineke's rule and stand density index. *Forest Science*, 51(4), 304-320. https://doi.org/10.1093/forestscience/51.4.304

Pretzsch, H. and Biber, P. 2016. Tree species mixing can increase maximum stand density. *Canadian Journal of Forest Research*, 46(10), 1179-1193. https://doi.org/10.1139/cjfr-2015-0413

R Core Team. 2020. R: A language and environment for statistical computing. R Foundation for Statistical Computing, Vienna, Austria. https://www.R-project.org

Reineke, L. 1933. Perfecting a stand-density index for even-aged forests. *Journal of Agricultural Research*, 46(7), 627-638.

Roise, J and Betters, D. 1981. An aspect transformation with regard to elevation for site productivity models. *Forest Science*, 27(3), 483-486. https://doi.org/10.1093/forestscience/27.3.483

SAS Institute, Inc, 2012. SAS/STAT 9.4 Use's Guide. SAS Institute Inc., Cary, NC.

Salas-Eljatib, C and Weiskittel, A. 2018. Evaluation of modeling strategies for assessing self-thinning behavior and carrying capacity. *Ecology and Evolution*, 8, 10768-10779. https://doi.org/10.1002/ece3.4525

Scharf, F., Juanes, F. and Sutherland, M. 1998. Inferring ecological relationships from the edges of scatter diagrams: Comparison of regression techniques. *Ecology*, 79(2), 448-460. https://doi.org/10.1890/0012-9658(1998)079[0448:IERFTE]2.0.CO;2

St. Clair, J., Mandel, N. and Vance-Borland, K. 2005. Genecology of Douglas-fir in western Oregon and Washington. *Annals of Botany*. 96, 1199-1214. https://doi.org/10.1093/aob/mci278

Stage, A., 1976. An expression for the effect of aspect, slope, and habitat type on tree growth. *Forest Science,* 22, 457–460. https://doi.org/10.1093/forestscience/22.4.457

Sterba, H. and Monserud, R. 1993. The maximum density concept applied to uneven-aged mixed-species stands. *Forest Science*, 39(3), 432-452. https://doi.org/10.1093/forestscience/39.3.432

Vospernik, S. and Sterba, H. 2015. Do competition-density rule and self-thinning rule agree? *Annals of Forest Science*, 72, 379-390. https://doi.org/10.1007/s13595-014-0433-x

Wang, T., Hamann, A., Spittlehouse, D. and Carrol, C. 2016. Locally downscaled and spatially customizable climate data for historical and future periods for North America. *PLoS ONE*. 11(6), 1-17. https://doi.org/10.1371/journal.pone.0156720

Weiskittel, A. Gould, P. and Temesgen, H. 2009. Sources of variation in the self-thinning boundary line for three species of varying levels of shade tolerance. *Forest Science*, 55, 84-93. https://doi.org/10.1093/forestscience/55.1.84

Weiskittel, A. and Kuehne, C. 2019. Evaluating and modeling variation in site-level maximum carrying capacity of mixed-species forest stands in the Acadian Region and northeastern North America. *The Forestry Chronicle*. 95(3), 171-182. https://doi.org/10.5558/tfc2019-026

Weller, D. 1987. A reevaluation of the -3/2 power rule of plant self-thinning. *Ecological Monographs*, 57, 23-43. https://doi.org/10.2307/1942637

Williams, R. 1996. Stand density index for loblolly pine plantations in north Louisiana. *Southern Journal of Applied Forestry*, 20(2), 110-113. https://doi.org/10.1093/sjaf/20.2.110

Woodall, C., Miles, P. and Vissage, J. 2005. Determining maximum stand density index in mixed species stands for strategic-scale stocking assessments. *Forest Ecology and Management*, 216, 367-377. https://doi.org/10.1016/j.foreco.2005.05.050

Yoda, K., Kira, T., Ogawa, H., and Hozumi, K. 1963. Self-thinning in overcrowded pure stands under cultivated and natural conditions. *Journal of Biology*, 14, 107-129.

Zeide B. 1987. Analysis of the 3/2 power law of self-thinning. *Forest* Science, 33(2), 517–537. https://doi.org/10.1093/forestscience/33.2.517

Zeide B. 2005. How to measure stand density. *Trees*, 19,1–14. https://doi.org/10.1007/s00468-004-0343-x

Zeide, B. 2010. Comparison of self-thinning models: an exercise in reasoning. *Trees*, 24, 1117-1126. https://doi.org/10.1007/s00468-010-0484-z

Chapter 3: Pacific Northwest Conifer Forest Stand Carrying Capacity Projections Under Future Climate Scenarios

Introduction

Forest stands are generally adapted to the historic, environmental conditions which they have been exposed to throughout stand development. Changes to temperature, humidity, and timing and amount of precipitation are all predicted to occur in the near and distant future (IPCC, 2013). General Circulation Models (GCMs) with different greenhouse gas emissions scenarios (RCPs) project various changes to these important climate variables (Wang et al., 2016). These potential changes will impact biogeochemical cycles between forests and the environment, which may lead to changes in forest growth, survival and structure (Chmura et al., 2011). The development of adaptive forest management strategies for potential future climatic conditions may provide resilience to a changing environment.

Forests of the Pacific Northwest, in particular, rely on water storage in snowpack and soils during summer droughts common to the Mediterranean climate experienced in the region (Franklin and Waring, 1980). Even without changes to the total amount of precipitation, earlier snowmelt and decline in precipitation falling as snow, is reducing this critically important water reservoir, further intensify water stress (Harpold, 2016). The manipulation and control of growing stock, in the form of density management, could be a key silvicultural tool to increase forest resilience to environmental change. Reducing stand density increases water and other resources available to the residual trees, and in turn, results in increased tree vigor and a greater ability to handle drought, and damage from insects and disease (Puettmann, 2011). Tree species and forest types that may be more vulnerable to changes in temperature or precipitation patterns, in particular overstocked stands or those with high levels of competition, should be targeted for density management manipulations (Chmura et al., 2011).

An understanding of current and potential future responses of forests are necessary to facilitate the development of silvicultural management options for adaptation to any degree of future change (Dolanc et al., 2013). The response a forest may have to a changing climate will ultimately depend on

local, site-specific conditions. Decision makers should target the most vulnerable sites, life stages, traits and processes to increase forest adaptability (Chmura et al., 2011). For example, Puettman (2011) finds special concern should be given toward areas where species grow at a moisture-limited range of conditions. Gleason et al. (2021) found the negative impacts of declining snowpack to be exacerbated by high stand density in ponderosa pine stands and recommend reducing stand density as a mitigation strategy to promote resilience to snow droughts. Fernandes et al. (2016) found thinning in pine stands increased the resilience to climate variations by increasing water use efficiency and promoted targeted (i.e., under appropriate timing) density reduction as an effective adaptive silviculture strategy under a changing climate.

Knowledge of where vulnerable species and forest types are found, such as areas with drought concerns, will facilitate where climate adaptation management efforts should be directed. Some management adjustments might include modifying harvest schedules and thinning regimes, or choosing different species or genetics when replanting (Millar et al., 2007). Capturing mortality before the initiation of self-thinning (i.e., density dependent mortality) requires temporal knowledge of when limiting conditions will begin to impact stand development.

It has been demonstrated through empirical statistical analysis that climatic conditions affect the carrying capacity (SDI_{MAX}) of a forest stand, which may be predicted through modelling efforts. Due to the climatic sensitivity of SDI_{MAX}, this index may be used to assess climate change adaptation and mitigation efforts (Brunet-Navarro, 2016). One approach to understanding how future conditions may affect modelled SDI_{MAX} is to utilize projected climatic conditions in place of historic climate data used to build the original models, referred to as space-for-time substitution (Yue et al., 2016). While these statistical models are correlative, and not necessarily suited to make mechanistic interpretations, they do allow the relative importance of climatic predictor variables to be assessed (Rehfeldt et al., 2016).

Statistical analysis techniques such as ensemble learning methods (i.e., random forest and stochastic gradient boosting) allow for the effect of many variables and their interactions on the target function to be assessed (Iverson et al., 2008; Friedman, 2001). Non-parametric, ensemble learning methods are ideal for large datasets with a multi-dimensional variable space with no prior distribution assumed between dependent and independent variables (Andrews et al., 2018). The ability of a model to incorporate many variables has proved useful in projecting effects of climate change on trees and forests (Chmura et al., 2016).

Future scenarios are often outside the range of any contemporary climate profile. These projections may be considered extramural (Rehfeldt et al., 2006) or no-analog conditions (Puettmann, 2011). Thus, any predictions made by models relying on future projections are not defensible. Rehfeldt et al. (2016) found among most of the biotic communities they examined, the majority of the landscape was projected into an extramural condition by the year 2100, with some reaching over 85%. Climate conditions were considered extramural if any one of the predictor variables at a location was outside the range of contemporary conditions. With this in mind, interpretations regarding the direction and magnitude of change may still be valid to consider. Exploring a variety of timescales and emissions scenarios can give a summary of the expected range and variability of any future changes.

The goal of this study is to understand the relationship between SDI_{MAX} and future climatic conditions across the Pacific Northwest forest region. Specific objectives are to: (1) utilize linear quantile mixed models (LQMM) to determine the self-thinning boundary of important forest types and tree species, (2) determine climatic variable influence and importance utilizing gradient boosting methodology (GBM) to predict SDI_{MAX}, (3) estimate potential future directional shifts in SDI_{MAX} under various climate projections using GCMs and different RCPs and (4) understand what proportion of the future projections for the study area falls into extramural or no-analog conditions.

Materials and Methods

Plot Data: Inventory Datasets

Forest inventory plot data for this project were provided by a collaborative network of public and private land management agencies. Each plot record contained the important tree metrics of quadratic mean diameter (QMD), number of trees per hectare (TPH) and proportion of basal area (BA) by major species group. Each record contained precise plot coordinates, which allowed for the extraction of important site-specific, environmental variables from geospatial layers. Data screening removed plots with less than 2.54 cm QMD and 24.7 TPH to establish a consistent threshold of diameter and number of trees. Only trees marked as living were included in plot-level estimates. The final dataset consisted of 168,220 unique observations representing the varied range of forest ecotypes across the Pacific Northwest. Plot records were subset to fall into one of two categories, the first (n=155,083) are those plots containing at least 10% Douglas-fir by BA, and a second (n=13,137) consisting of plots with at least 10% western hemlock BA which contained no Douglas-fir proportion. This second subset of data points was concentrated in the more niche environments in the Coast Range, Olympic Peninsula and Northern Cascades where wetter, climax forest conditions with less extreme weather events are found. These datasets will be referred to as DF-Mix and HemFir, respectively.

Topographic Data

Topographic attributes were derived from U.S. Department of Agriculture (USDA) and National Resource Conservation Service (NRCS) National Elevation Data 30-m digital elevation models. Slope and aspect were derived using the ‘raster’ package (Hijmans, 2020) available through R 4.0 (R Core Team, 2020). Trigonometric transformations of slope and aspect were utilized to express the influence of these features on climate factors such as moisture and temperature (Roise and Betters, 1981). Spatial maps of soil parent materials were derived from USGS 1:24,000 geology maps and surficial volcanic ash mantles from the NRCS soil survey geographic database (SSURGO). Major

geologic groupings and presence-absence of ash influence were determined similarly to the methods described by Kimsey et al. (2019).

Climatic Data

Climate data were obtained through the ClimateNA v6.11 software package using plot-specific latitude, longitude and elevation. ClimateNA downscales historical and future climate data layers into scale-free (not gridded but directly estimable for any location) point estimates of climate values for the entire North American continent (Wang et al., 2016). These climate data contain directly calculated and derived variables, as well as various interactions resulting in over 230 climate variables available for extraction. Future projections within ClimateNA are based on GCMs of the Climate Model Intercomparison Project 5 (CMIP5). This analysis utilizes the 15 CGM ensemble, composed of the following Atmosphere-Ocean General Circulation Models: ACCESS1-0 (Australia), CCSM4 (National Center for Atmospheric Research, USA), CESM1-CAM5 (University Center for Atmospheric Research, USA), CNRM-CM5 (France), CSIRO-Mk3-6-0 (Australia), CanESM2 (Canada), GFDL-CM3 (Geophysical Fluid Dynamics Lab, USA), GISS-E2R (Goddard Institute of Space Studies, USA), HadGEM2-ES (United Kingdom), INM-CM4 (Russia), IPSL-CM5A-MR (France), MIROC-ESM (Japan), MIROC5 (Japan), MPI-ESM-LR (Germany) and MRI-CGCM3 (Japan). The future projections incorporate different greenhouse gas concentration trajectories or RCPs. This analysis selected two RCPS: RCP4.5, a medium stabilization scenario where emissions peak in 2040's with radiative forcing pathways stabilizing at 6 W/m^2 (~650 ppm CO_2) after 2100, and RCP8.5, a very high emission scenario with rising radiative forcing pathway leading to 8.5 W/m^2 (~1370 ppm CO_2) by the end of the century (Vuuren et al., 2011). Each 15GCM ensemble and RCP scenario were summarized into 30-year time future periods referred to hereafter as 2050s (2041-2070) and 2080s (2071-2100).

From each of the DF-Mix and HemFir datasets, four different future climate scenarios were built. While keeping the tree and topographic data constant, future climate variables were extracted for

each plot location for the four climate scenarios RCP4.5 in period 2050s, RCP4.5 in period 2080s, RCP8.5 in period 2050s and RCP8.5 in period 2080s. These additional climate extractions resulted in five scenarios for each DF-Mix and HemFir dataset: the historic dataset and four future scenarios. Comparisons of predicted SDI_{MAX} between the future and the historic climate scenarios were evaluated.

Statistical Analysis – LQMM and GBM

To understand the influence of climate on forest stand carrying capacity, first the maximum size density relationship (SDI_{MAX}) must be estimated. Following the findings of Salas-Eljatib and Weiskittel (2018), linear quantile mixed models (LQMM) were developed with the 'lqmm' package (Geraci, 2014) within the R programming environment (R Core Team, 2020) to estimate the random plot-specific intercepts and fixed species-specific slope of the self-thinning line based on the Reineke (1933) equation:

$$lnTPH = (\beta_0 + k_i) + \beta_1 * lnQMD$$

where β_0 and β_1 are fixed effects parameters and k_i is the estimated random effect for plot record i. The random intercept parameter produced unique individual plot-level intercept values, thus giving each record a unique SDI_{MAX}.

The next step introduces site-specific variables by linking the estimated SDI_{MAX} to climatic and other environmental properties found at each plot location. Utilizing the ensemble learning technique gradient boosting methodology, variable influence and importance was assessed. Stochastic gradient boosting (GBM) makes use of an additive gradient descent 'boosting' algorithm which builds successively improved prediction trees (Friedman, 2001). Each dataset, DF-Mix and HemFir, was split 70/30 into training and testing sets. The test set was held back from model development and used as independent validation of model fit. The R packages 'gbm' (Greenwell et al., 2020) and 'caret' (Kuhn, 2020) were used to determine influence of environmental variables through tuning a GBM model. The

GBM model was tuned using a grid search method, where the various parameters were optimized toward the best predictive model. GBM constructs an ensemble of prediction trees in a 'greedy stepwise' manner and is noted for being robust to collinearity of variables (Hastie, Tibshirani and Friedman, 2008). A first run included all variables. Then, variable importance, the relative influence of variables on prediction, was examined to reduce the number of variables in the model to only the most influential. A relative influence of 0.25 was chosen to remove non-informative variables from the first run predictor set. Simplifying the predictor set results in a more parsimonious model, without degradation of model fit (Elith, Leathwick and Hastie, 2008). Final models were selected based on 5-fold, cross-validated mean absolute error (MAE). MAE for both training and testing data was assessed to prevent overfitting. The final number of model built trees producing the lowest error on testing data without overfitting was chosen.

Additional Regionwide Datasets

In addition to the inventory plot driven datasets, a 1-kilometer hexagonal grid was placed across the entire study region and then clipped to each Douglas-fir and western hemlock ranges. Species ranges were determined from FIA interpolated basal area maps, where if at least 10% of total basal area found at any given location was of the species of interest that location was considered in range. The grid across the entire regionwide area was then clipped to the ranges creating two regionwide datasets for DF-Mix (n= 151,299) and HemFir (n= 80,974).

The same topographic and climate variables were extracted to each plot location, including the four future scenarios. The final GBM model for DF-Mix and HemFir were then applied to the regional grid datasets for SDI_{MAX} predictions to allow climate change scenarios to be evaluated across the entire study region. Two basal area proportion scenarios were explored, one based on pure (100% basal area proportion) Douglas-fir or western hemlock composition; and a second based on species averages calculated from the original inventory plot datasets (Table 3.1).

Table 3.1 Species basal area proportions from the inventory datasets.

Variable	Mean	SD	Minimum	Maximum
DF-Mix				
Douglas-fir	0.77	0.27	0.10	1
Western hemlock	0.09	0.18	0	0.90
Red alder	0.05	0.15	0	0.90
Western red cedar	0.02	0.07	0	0.90
Other conifer	0.04	0.12	0	0.90
Other hardwood	0.03	0.11	0	0.90
HemFir				
Douglas-fir	0	0	0	0
Western hemlock	0.68	0.30	0.10	1
Red alder	0.13	0.23	0	0.90
Western red cedar	0.04	0.12	0	0.90
Other conifer	0.13	0.23	0	0.90
Other hardwood	0.02	0.09	0	0.90

Extramural Conditions

Future climate projections under the various scenarios were compared to the historic conditions to understand how much of the landscape falls into extramural conditions under future projections. Utilizing the regionwide datasets, all climate variables included in the DF-Mix and HemFir final models were evaluated for extramural status by comparing each of the future scenario predictions to the historic at the same location. A variable value falls outside the range of the historical climate data is marked as extramural. Two instances were evaluated, first, whether any of the variables at a given point fell outside the range, and second, what proportion of the variables at any given point fell outside the range. Each was evaluated as falling within the absolute range as well as within 5% and 10% of the absolute range.

Results

Maximum size-density relationship

The LQMM analysis fit a self-thinning outer boundary line to the 95th quantile of data points. This resulted in a self-thinning slope of -1.608 and -1.544 for the DF-Mix and HemFir datasets, respectively. The random intercept produced mean predicted SDI_{MAX} of 1220 TPH (SD=119) with a 1

to 99% quantile range from 840 to 1450 TPH for DF-mix and mean predicted SDI_{MAX} of 1396 TPH (SD=151) with a range of 941 to 1681 TPH for HemFir.

GBM model performance and variable influence on SDI_{MAX}

The final GBM model for the DF-mix dataset had 4202 trees and included 86 variables with a training and testing mean absolute error of 72.5 and 77.5 TPH, respectively. The most influential variable was the Douglas-fir basal area proportion, followed by other species basal area proportions, in particular western hemlock. Site characteristics of the various slope and aspect transformations, elevation, and the latitude and longitude at plot locations were important and highly ranked. Influential climate variables included interactions between the various measures of precipitation and temperature.

The final GBM model for the HemFir dataset had 1915 trees and included 106 predictor variables with a training and testing mean absolute error of 77.0 and 104.2 TPH, respectively. The top variable was the basal area proportion of western hemlock, followed by the slope and aspect transformations, elevation and latitude and longitude of the plot location. The most influential climate variables were similar to those included in the DF-Mix model and included various measures of precipitation timing and amount, as well as interactions of precipitation with temperature. The number of degree days > 5ºC (DD5) and < 18 5ºC (DD_18) both annually and seasonally were common variables included in the model. The summer season Hargreaves climatic moisture deficit (CMD) ranked as a highly influential variable as well. The most influential variables of the chosen final GBM models for SDI_{MAX} predictions are shown in Figure 3.1 and Figure 3.2 for DF-Mix and HemFir, respectively.

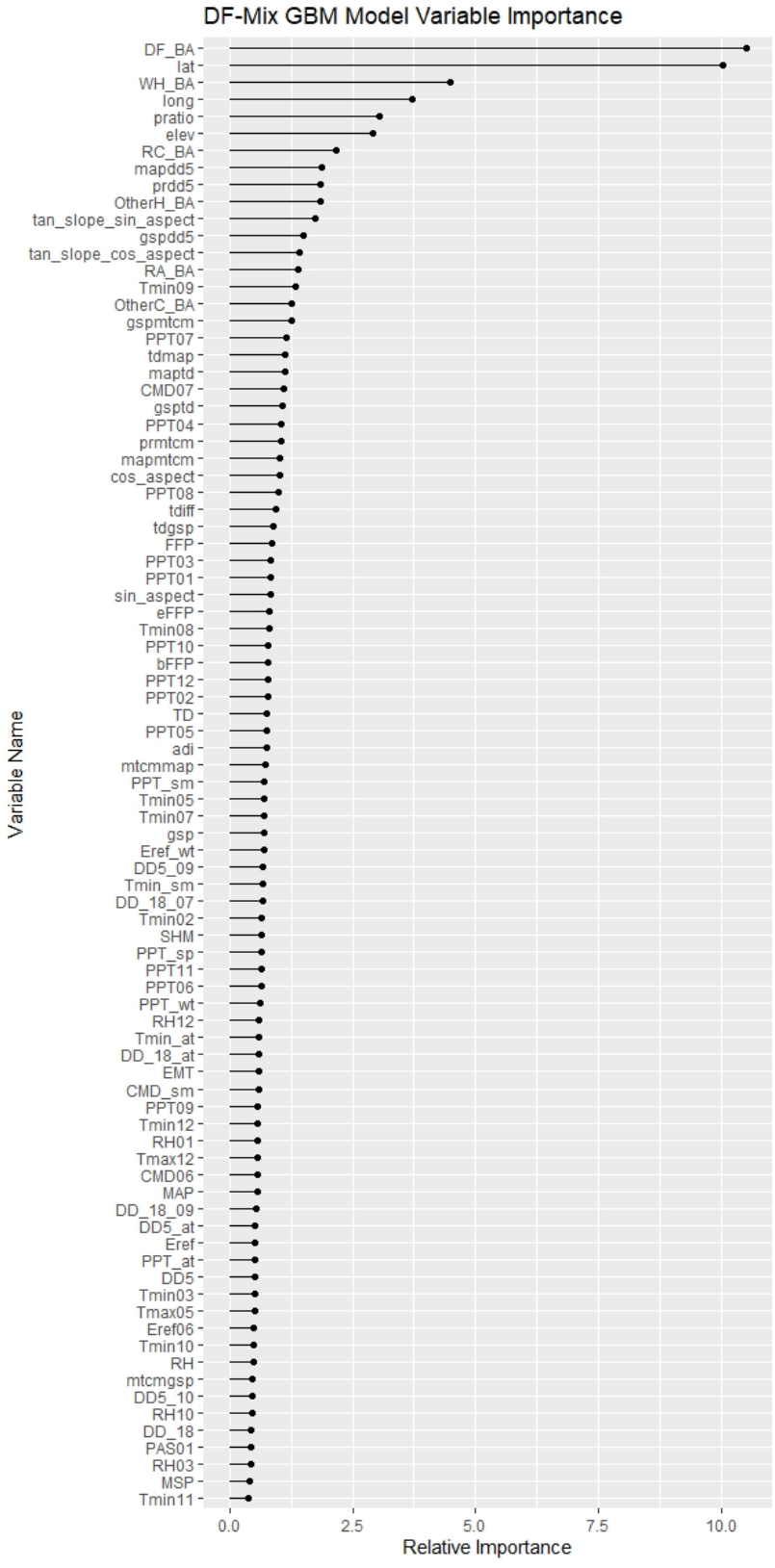

Figure 3.1 Relative variable importance for the gradient boosting model for the DF-Mix dataset.

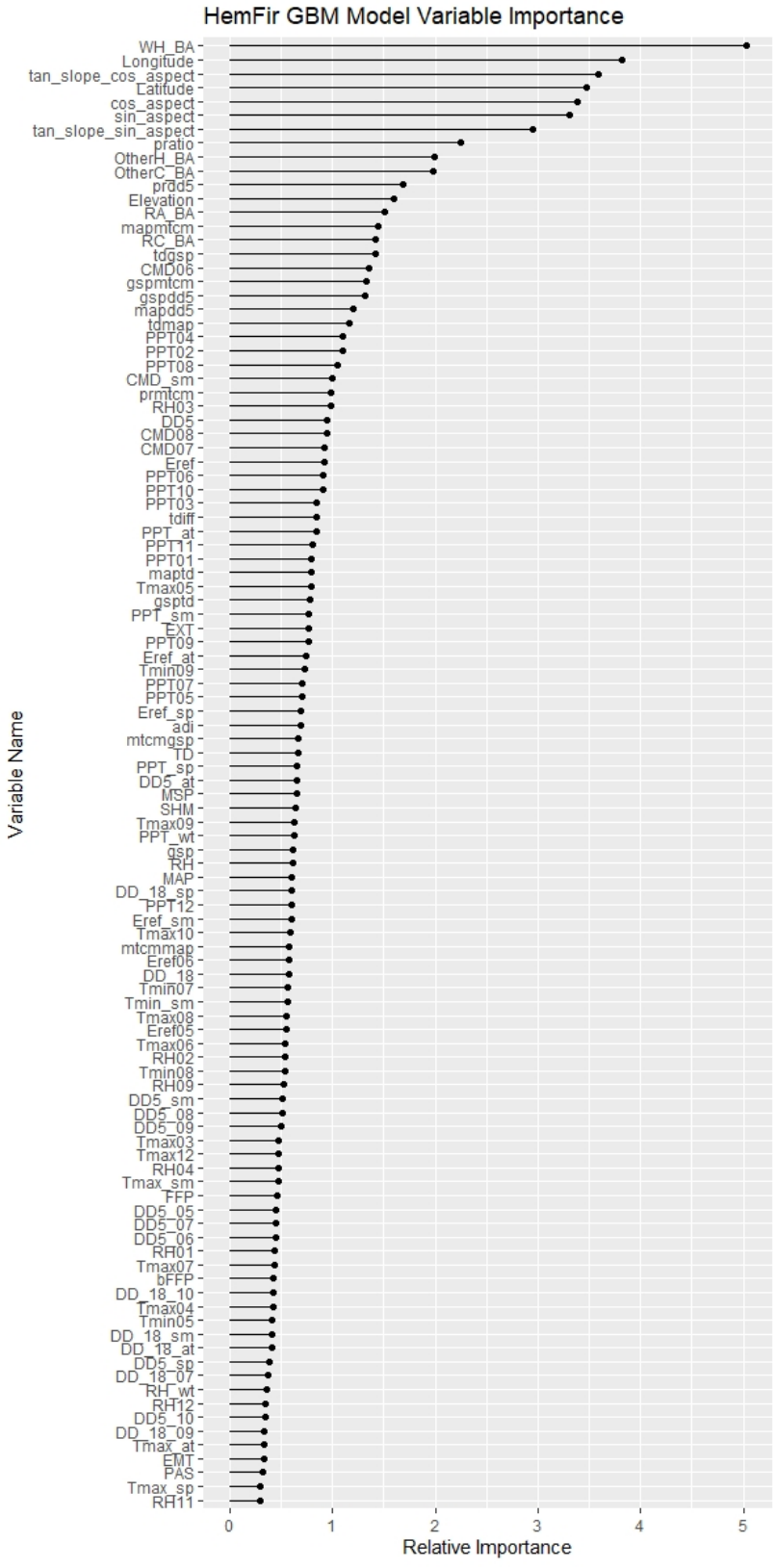

Figure 3.2 Relative variable importance for the gradient boosting model for the HemFir dataset.

Future GBM model predictions: Inventory Datasets

The future scenario inventory datasets were run through the final GBM model to produce predicted SDI_{MAX} under future climate conditions in the 2050's and 2080's. Both the DF-Mix and the HemFir datasets saw the average SDI_{MAX} value shift downward under all scenarios (Table 3.2 and 3.3).

Table 3.2 Predicted $SDIM_{AX}$ values (mean, 1 and 99 percentiles) and standard deviations for each inventory dataset of DF-Mix and HemFir.

	DF-Mix				HemFir			
Prediction Scenario	Mean	SD	1%	99%	Mean	SD	1%	99%
Current	1220	53	1067	1327	1396	79	1151	1540
RCP 4.5 - 2050's	1143	72	991	1287	1287	74	1121	1452
RCP 4.5 - 2080's	1121	80	953	1282	1275	73	1116	1444
RCP 8.5 - 2050's	1115	83	937	1281	1280	71	1126	1447
RCP 8.5 - 2080's	1071	90	880	1251	1256	68	1099	1415

Table 3.3 Average ratios of predicted SDI_{MAX} under each future scenario relative to the current SDI_{MAX} under past climate conditions.

	DF-Mix				HemFir			
Prediction Scenario	Mean	SD	1%	99%	Mean	SD	1%	99%
Current	1.01	0.09	0.86	1.35	1.01	0.10	0.84	1.34
RCP 4.5 - 2050's	0.95	0.11	0.76	1.32	0.93	0.12	0.73	1.35
RCP 4.5 - 2080's	0.93	0.11	0.74	1.31	0.92	0.12	0.72	1.35
RCP 8.5 - 2050's	0.92	0.11	0.73	1.30	0.93	0.12	0.73	1.35
RCP 8.5 - 2080's	0.89	0.11	0.69	1.25	0.91	0.12	0.71	1.33

A majority of the records under all scenarios moved in the negative direction with ranges increasing under greater emission scenarios further into the future (Table 3.4).

Table 3.4 Proportion of inventory records which had a negative change in predicted SDI_{MAX}.

Scenario	DF-Mix	HemFir
RCP 4.5 - 2050's	78%	78%
RCP 4.5 - 2080's	81%	80%
RCP 8.5 - 2050's	83%	80%
RCP 8.5 - 2080's	88%	83%

Although the majority of SDI_{MAX} projections decreased under future conditions, there was a range of positive and negative change (Table 3.5). A small proportion of sites are projected to have favorable climatic changes which may led to increases in carrying capacity. Overall, the DF-Mix locations are projected to be slightly more resilient under the RCP 4.5 scenarios compared to the HemFir sites but under the RC P8.5 scenarios it is the reverse, with HemFir fairing marginally better overall compared to the DF-Mix sites. Not unexpectedly, the 2080's under RCP8.5 saw the most dramatic shifts in SDI_{MAX} relative to current with an average 11.4 and 8.9% shift downward in the mean predicted SDI_{MAX} for DF-Mix and HemFir scenarios, respectively.

Table 3.5 Average percent change in SDI_{MAX} for inventory datasets. Overall is the mean percent change. If + is the average change for records which showed positive change. If – is the average change for records which showed negative change.

	DF-Mix			HemFir		
Scenario	Overall	If +	If-	Overall	If +	If-
RCP 4.5 - 2050's	-5.4%	9.4%	-9.7%	-6.6%	10.8%	-11.4%
RCP 4.5 - 2080's	-7.2%	9.5%	-11.0%	-7.5%	10.9%	-12.0%
RCP 8.5 - 2050's	-7.8%	9.6%	-11.5%	-7.1%	10.8%	-11.7%
RCP 8.5 - 2080's	-11.4%	9.8%	-14.2%	-8.9%	10.9%	-12.9%

Future GBM model predictions: Regionwide Datasets

The regionwide datasets under future scenarios followed similar patterns of results as the inventory datasets. Both the DF-Mix and HemFir datasets under each the 100% pure basal area and the average species basal area scenarios saw overall majority decreases in SDI_{MAX} under all future climate projections (Table 3.6 and 3.7).

Table 3.6 Predicted SDI_{MAX} values (mean, 1 and 99 percentiles) and standard deviation for each regionwide dataset of DF-Mix and HemFir for each basal area scenario.

Prediction Scenario	DF-Mix				HemFir			
	Mean	SD	1%	99%	Mean	SD	1%	99%
	100% Douglas-fir Basal Area				100% Western Hemlock Basal Area			
Current	1162	54	983	1257	1349	78	1129	1503
RCP 4.5 - 2050's	1078	81	894	1251	1260	85	1081	1427
RCP 4.5 - 2080's	1055	85	874	1250	1248	81	1085	1417
RCP 8.5 - 2050's	1047	87	865	1247	1249	79	1087	1417
RCP 8.5 - 2080's	1001	84	826	1217	1227	69	1085	1388
	Avg Species Basal Proportion							
Current	1226	49	1093	1326	1427	55	1280	1546
RCP 4.5 - 2050's	1184	62	1034	1314	1368	64	1236	1489
RCP 4.5 - 2080's	1172	63	1027	1312	1359	63	1234	1485
RCP 8.5 - 2050's	1168	64	1022	1310	1361	62	1237	1487
RCP 8.5 - 2080's	1139	68	982	1293	1343	55	1232	1463

Table 3.7 Average ratios (mean, 1 and 99 percentiles) and standard deviations of predicted SDI_{MAX} under each future climate scenarios relative to the current SDI_{MAX} under past climate conditions.

Prediction Scenario	DF-Mix				HemFir			
	Mean	SD	1%	99%	Mean	SD	1%	99%
	100% Douglas-fir Basal Area				100% Western Hemlock Basal Area			
Current	1	0	1	1	1	0	1	1
RCP 4.5 - 2050's	0.93	0.07	0.79	1.09	0.94	0.07	0.80	1.09
RCP 4.5 - 2080's	0.91	0.07	0.77	1.10	0.93	0.07	0.80	1.08
RCP 8.5 - 2050's	0.90	0.07	0.77	1.10	0.93	0.07	0.80	1.08
RCP 8.5 - 2080's	0.86	0.07	0.72	1.07	0.91	0.07	0.78	1.08
	Avg Species Basal Proportion							
Current	1	0	1	1	1	0	1	1
RCP 4.5 - 2050's	0.97	0.04	0.88	1.06	0.96	0.04	0.87	1.05
RCP 4.5 - 2080's	0.96	0.04	0.87	1.06	0.95	0.04	0.86	1.04
RCP 8.5 - 2050's	0.95	0.04	0.87	1.06	0.95	0.04	0.87	1.04
RCP 8.5 - 2080's	0.93	0.05	0.83	1.05	0.94	0.04	0.85	1.04

The scenarios with 100% basal area of Douglas-fir and western hemlock had greater magnitude in both positive and negative shifts in SDI_{MAX} compared to the average basal area scenarios. The pure basal area scenarios had greater proportion of sites seeing a downward shift of SDI_{MAX} compared to the average species basal area scenarios under all future climate projections (Table 3.8).

Table 3.8 Proportion of regionwide records which had a negative change in predicted SDI_{MAX}.

	DF-Mix		HemFir	
Scenario	100% DF BA	Avg BA	100% Hem BA	Avg BA
RCP 4.5 - 2050's	87%	85%	83%	85%
RCP 4.5 - 2080's	89%	88%	86%	88%
RCP 8.5 - 2050's	90%	89%	86%	88%
RCP 8.5 - 2080's	96%	93%	89%	94%

Although, when the datasets are split between records seeing increases and decreases (Table 3.9), the pure basal area locations had greater shifts in both directions compared to the mixed basal area scenarios, with the DF-Mix sites being of greater magnitude than the HemFir sites.

Table 3.9 Average percent change in SDI_{MAX} for regionwide datasets. Overall is the mean percent change. If + is the average change for records which showed positive change. If – is the average change for records which showed negative change.

	DF-Mix						HemFir					
	100% DF BA			Avg BA			100% Hem BA			Avg BA		
Scenario	Overall	If +	If-	Overall	If +	If-	Overall	If +	If-	Overall	If +	If-
RCP 4.5 - 2050's	-7.1%	3.6%	-8.6%	-3.4%	2.1%	-4.4%	-6.4%	3.4%	-8.4%	-4.1%	1.9%	-5.2%
RCP 4.5 - 2080's	-9.1%	4.0%	-10.7%	-4.4%	2.3%	-5.3%	-7.2%	3.3%	-9.0%	-4.7%	1.8%	-5.6%
RCP 8.5 - 2050's	-9.7%	4.1%	-11.2%	-4.7%	2.4%	-5.6%	-7.2%	3.3%	-8.9%	-4.6%	1.8%	-5.5%
RCP 8.5 - 2080's	-13.7%	5.2%	-14.5%	-7.1%	2.3%	-7.8%	-8.7%	3.3%	-10.2%	-5.9%	2.2%	-6.4%

Extramural Conditions

Extramural, or no-analog conditions, were found within all future scenarios. The percent of locations which had at least one variable falling outside the absolute range found in the historic climate conditions ranged from 49% of locations in the 2050's under RCP4.5 scenario to 97% in the 2080's under RCP8.5 scenario for the DF-Mix regionwide dataset and 38% to 99% for the HemFir mix under the same scenarios, respectively (Table 3.10). For the same time period and RCP scenarios, the average percent of all variables at each location falling outside the absolute range of historic climate conditions ranged from 7% to 45% for the DF-Mix and 7% to 46% for the HemFir, with these percentages dropping by roughly half when expanding the absolute range by 10% (Table 3.11).

Table 3.10 Percent of records with at least one variable that is extramural. Three categories of extramural are shown: Abs - at least one variable was outside the absolute range of current climate, 5% - where at least one variable is outside of a 5% of the absolute range and 10% - where at least one variable is outside 10% of the absolute range.

	DF-Mix			HemFir		
	Percent of records having at least one variable fall outside…			Percent of records having at least one variable fall outside…		
Scenario	Abs Current Range	5% of Current Range	10% of Current Range	Abs Current Range	5% of Current Range	10% of Current Range
RCP 4.5 - 2050's	49%	28%	12%	38%	24%	13%
RCP 4.5 - 2080's	71%	54%	31%	63%	46%	32%
RCP 8.5 - 2050's	75%	59%	37%	68%	51%	36%
RCP 8.5 - 2080's	97%	95%	91%	99%	97%	94%

Table 3.11 Average proportion of explanatory variables for each record which fall outside the range of historic climate conditions. Three categories of extramural are show: Abs - the proportion of variables outside the absolute range of current climate, 5% - average proportion of variables outside of 5% of the absolute range and 10% - average proportion of variables outside 10% of the absolute range.

	DF-Mix			HemFir		
	Average percent of explanatory variables falling outside…			Average percent of explanatory variables falling outside…		
Scenario	Abs Current Range	5% of Current Range	10% of Current Range	Abs Current Range	5% of Current Range	10% of Current Range
RCP 4.5 - 2050's	7%	3%	1%	7%	3%	1%
RCP 4.5 - 2080's	15%	7%	3%	14%	7%	4%
RCP 8.5 - 2050's	17%	8%	4%	16%	9%	5%
RCP 8.5 - 2080's	45%	31%	21%	46%	34%	25%

Projections of future climate are impacting modelled stand carrying capacity in significant ways. Across the study region a majority of the landscape is seeing a downward shift in the SDI_{MAX} (Figure 3.3 and 3.4). This change is driven by changes in temperature (Table 3.12) and precipitation (Table 3.13). While the total amount of mean annual precipitation is projected to remain fairly constant or increase slightly under all future scenarios, the timing of precipitation is shifting away from the growing season. The balance of precipitation in the growing season relative to the entire year (PRATIO) is declining across the region while at the same time the frost-free period (FFP) and both summer and winter temperatures are increasing. Average temperatures in both the coldest and warmest months are projected to increase by 2 to 3 °C under the RCP 4.5 – 2050's projection, and by as much as 4 to 6 °C under the RCP 8.5 – 2080's projection. Forests are being exposed to an earlier, longer, warmer growing season with access to a smaller amount of precipitation. Water storage in the form of snowpack is extremely important for forests growing in droughty summer conditions (Waring and Franklin, 1979). The amount of precipitation falling as snow (PAS) is projected to dramatically decline (Klos et al., 2014), further exacerbating the limited amount of water these forests have access to during the low precipitation summers. Stand carrying capacity is almost exclusively determined by competition to water resources while under severe drought (Deng et al., 2006) and with future conditions expected to become more water limiting for Pacific Northwest forests, a drop in SDI_{MAX} is expected.

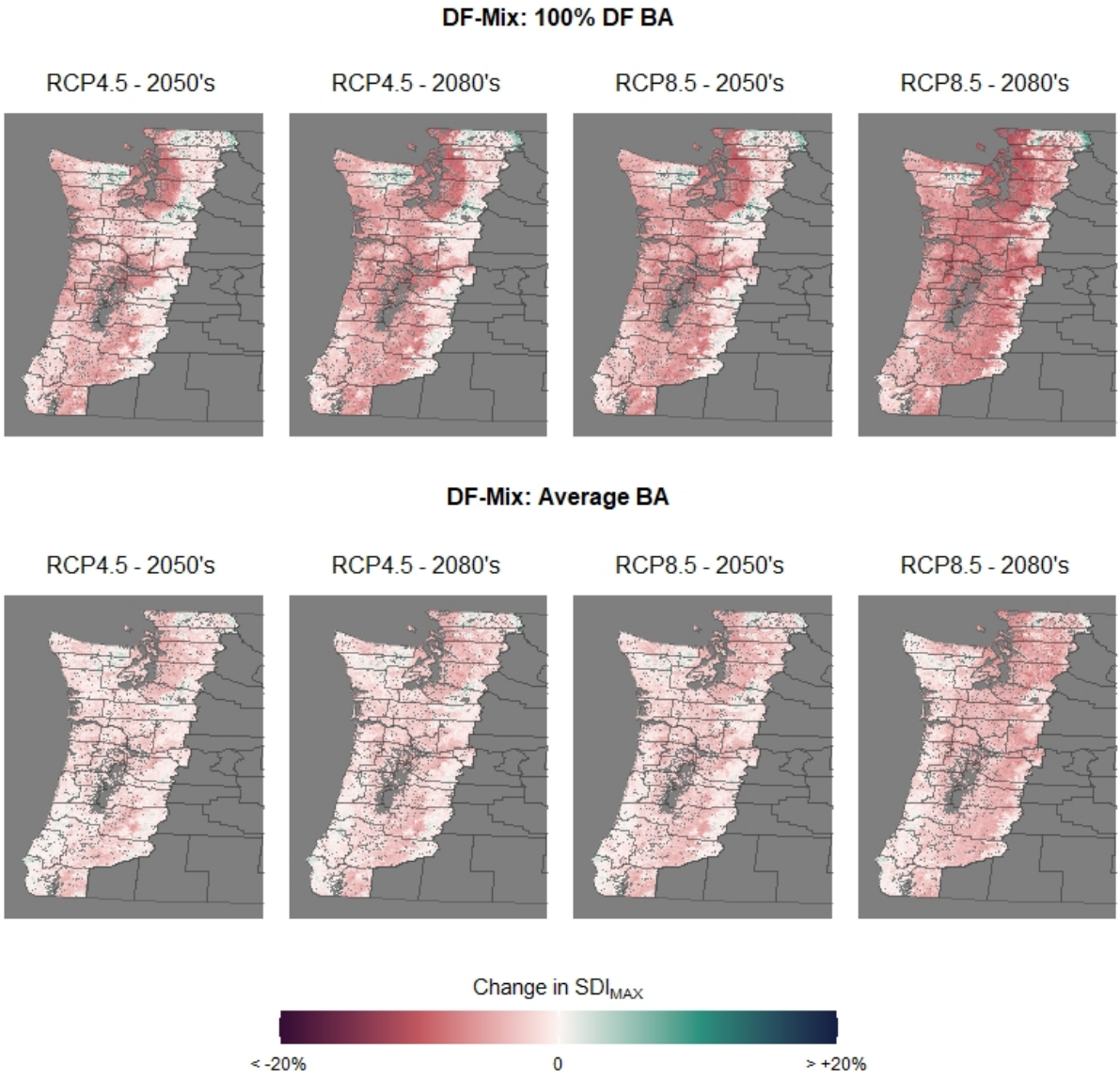

Figure 3.3 Percent change in SDI_{MAX} for regionwide DF-Mix range under future climate scenarios relative to current. Resolution of 1km hexagonal raster tiles.

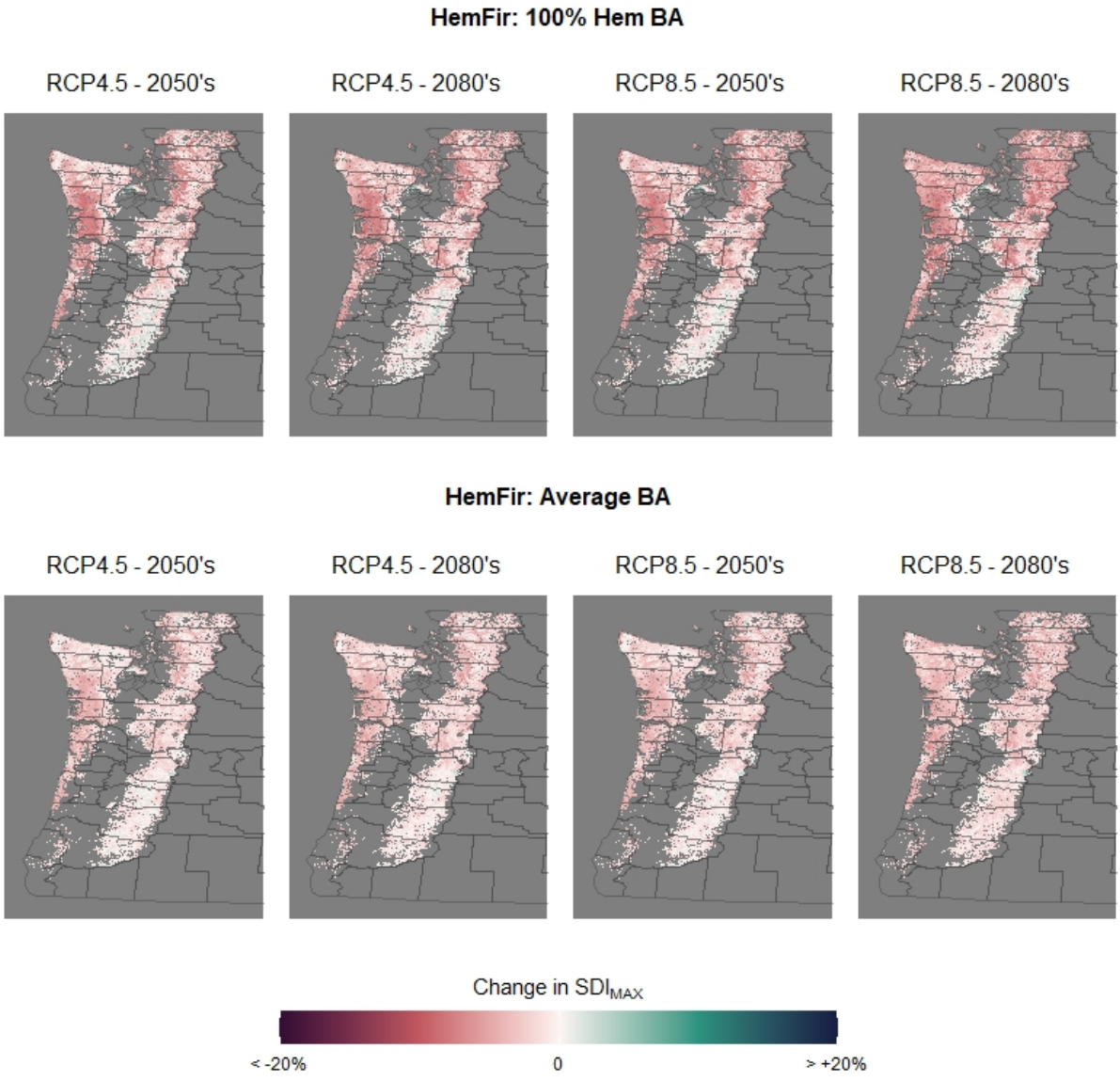

Figure 3.4 Percent change in SDI_{MAX} for regionwide HemFir range under future climate scenarios relative to current. Resolution of 1km hexagonal raster tiles.

Table 3.12 Absolute change in temperature (°C) under future climate scenarios relative to historic for the current range of DF-Mix and HemFir. MCMT – mean coldest month temperature and MWMT – mean warmest month temperature

		DF-Mix						HemFir					
Scenario	Variable	Min	1%	Med	Mean	99%	Max	Min	1%	Med	Mean	99%	Max
RCP 4.5 - 2050's	MCMT	1.6	1.7	2.0	2.0	2.5	2.6	1.6	1.8	2.1	2.1	2.5	2.6
	MWMT	2.2	2.3	2.7	2.7	3.1	3.2	2.2	2.3	2.9	2.8	3.1	3.2
RCP 4.5 - 2080's	MCMT	2.0	2.1	2.5	2.5	3.0	3.2	2.0	2.1	2.5	2.6	3.0	3.1
	MWMT	2.8	2.9	3.4	3.4	4.0	4.1	2.8	2.9	3.6	3.5	4.0	4.1
RCP 8.5 - 2050's	MCMT	2.0	2.1	2.4	2.5	3.1	3.2	2.0	2.1	2.5	2.6	3.1	3.2
	MWMT	2.9	3.0	3.6	3.6	4.2	4.3	2.9	3.0	3.8	3.7	4.2	4.3
RCP 8.5 - 2080's	MCMT	3.4	3.5	4.0	4.0	4.9	5.1	3.4	3.6	4.1	4.2	4.9	5.1
	MWMT	4.6	4.9	5.8	5.8	6.8	6.9	4.7	4.9	6.2	6.0	6.8	6.9

Table 3.13 Percent change in important climate variables under future climate scenarios for the current ranges of DF-Mix and HemFir relative to historic climate conditions. MAP – mean annual precipitation, PRATIO – proportion of precipitation falling during the growing season, PAS – precipitation as snow, DD5 – degree days above 5°C and FFP – frost free period.

		DF-Mix						HemFir					
Scenario	Variable	Min	1%	Med	Mean	99%	Max	Min	1%	Med	Mean	99%	Max
RCP 4.5 - 2050's	MAP	-2%	-1%	1%	1%	4%	4%	-2%	-1%	1%	1%	4%	4%
	PRATIO	-14%	-12%	-10%	-10%	-8%	-7%	-13%	-11%	-9%	-9%	-8%	-7%
	PAS	-64%	-61%	-54%	-54%	-36%	-15%	-63%	-61%	-55%	-55%	-41%	-26%
	DD5	20%	23%	30%	33%	57%	96%	23%	27%	34%	36%	53%	69%
	FFP	17%	21%	26%	27%	42%	86%	18%	22%	27%	27%	37%	49%
RCP 4.5 - 2080's	MAP	-1%	0%	2%	3%	6%	7%	-1%	0%	3%	3%	6%	7%
	PRATIO	-15%	-13%	-11%	-11%	-9%	-8%	-15%	-13%	-11%	-11%	-9%	-8%
	PAS	-70%	-68%	-61%	-61%	-43%	-18%	-69%	-67%	-62%	-62%	-49%	-31%
	DD5	26%	29%	39%	42%	74%	129%	29%	34%	43%	45%	68%	86%
	FFP	21%	26%	33%	34%	53%	117%	22%	28%	34%	35%	46%	63%
RCP 8.5 - 2050's	MAP	-2%	-1%	2%	2%	5%	6%	-2%	-1%	3%	2%	5%	6%
	PRATIO	-16%	-14%	-12%	-12%	-10%	-9%	-15%	-14%	-12%	-12%	-10%	-9%
	PAS	-71%	-70%	-63%	-63%	-45%	-20%	-71%	-69%	-64%	-64%	-51%	-34%
	DD5	27%	31%	40%	44%	79%	139%	30%	36%	45%	48%	72%	92%
	FFP	21%	26%	35%	35%	55%	124%	23%	30%	35%	36%	48%	65%
RCP 8.5 - 2080's	MAP	0%	1%	4%	4%	8%	10%	0%	1%	5%	5%	8%	10%
	PRATIO	-19%	-18%	-15%	-15%	-13%	-12%	-19%	-17%	-15%	-15%	-13%	-12%
	PAS	-87%	-85%	-80%	-80%	-67%	-38%	-87%	-84%	-80%	-80%	-71%	-56%
	DD5	44%	50%	67%	73%	136%	244%	49%	58%	74%	79%	124%	160%
	FFP	27%	39%	57%	57%	87%	210%	32%	46%	59%	59%	77%	103%

Discussion

Higher elevation sites and those closer to the Pacific Northwest coast are not seeing as dramatic a shift in predictions compared to the lower elevation, inland sites found in the Willamette Valley, which are almost exclusively in the negative direction. The magnitude of change projections in temperature, precipitation timing, and precipitation as snow is buffered by higher elevation. Competition for water resources will not be as extreme in these areas and in fact may see an increase in stand carrying capacity due to the increase in growing season length. Way and Oren (2010) suggest that high altitude tree communities may benefit from some degree of warming opposed to warm-adapted species often found at the edges of moisture limited environments. The results found in this study seem to agree with this and other projections of general range shifts upward in elevation with anticipated changes in climate (Parmesan, 2006; Reheldt et al., 2006). The impact of future climate changes on stand carrying capacity will be location dependent and any management decisions need to account for the specificity.

The impact of future climate on stand carrying capacity is shown to be greater in pure stands of Douglas-fir and western hemlock relative to mixed species stands. Species mixing in general has shown to lead to increased packing density within a canopy space due to complementary ecological traits and crown geometry (Pretzsch and Biber, 2016). The modeled carrying capacity of mixed species stands appear to be more resilient to projected changes in climate. Exploring the inventory datasets, records showing projected increases in SDI_{MAX} had more diversity of species basal area proportions. For example, under RCP 8.5 - 2080's scenario the DF-MIX dataset showed average Douglas-fir basal area was 78% for plots with a decrease in SDI_{MAX} and 71% for plots with an increase; and for the HemFir dataset, average western hemlock basal area was 69% for records with a decrease in SDI_{MAX} and 62% for those with an increase. This relationship held for all future climate scenarios. While this in part may be attributed to the GBM model, which showed more diverse plots as

having overall higher SDI_{MAX}, it also shows that given changes in important climate variables, more diverse stands have a greater resiliency to the impact of these changes compared to purer stands.

That said, exploring the regionwide datasets, the pure basal area scenarios showed the greatest magnitude shifts in SDI_{MAX} relative to the mixed species in either direction, positive and negative. Locations under pure basal area scenarios, for both the DF-Mix and HemFir datasets, which showed increases in SDI_{MAX} under future climate projections, had greater increases relative to mixed species scenario, as well as the opposite, where records with decreases where greater under pure basal area scenarios. For example, under RCP 8.5 – 2080's, the average positive shift was 2.9 and 1.1% greater for the DF-Mix and HemFir datasets respectively under the pure basal area scenarios relative to the average basal area scenarios. Conversely, the average negative shift was -6.7% and -3.8% greater for the pure basal area scenarios relative to the average basal area scenarios for the DF-Mix and HemFir datasets respectively.

The management implications of moving toward mixed species management with varying forest structure should allow for greater resilience to a changing climate. Under projected future conditions, mixed stands may be able to carry a greater density longer into the rotation before the impact of density dependent mortality. Puettmann (2011) describes this as the 'insurance hypothesis' (attributed to Yachi and Loreau, 1999) under which a diversity of species and vegetation conditions may buffer the impact of a changing climate. A more diverse forest allows for complementary facilitation, where the presence of one species increases the availability of a limiting resource, and resource portioning, with more efficient sharing of limited resources between different species (Pothier, 2019).

Projected future climate scenarios fall into extramural conditions across all scenarios. Utilizing any statistical model to extrapolate or predict outside the range of the input data is not appropriate. Nonetheless, general interpretations of the overall direction and magnitude of these shifts should be considered to understand what impact future climate may have on stand carrying capacity.

The impact of environmental conditions is reflected in underlying physiographical processes of these forest communities. The influence of climate on stand carrying capacity has been shown through many empirical studies (Kimsey et al., 2019; Aguirre et al., 2018; Andrews et al., 2018). General interpretations of the model projections are justified with the acknowledgment of the uncertainties involved in climate projections. In particular, the consistency of the modeled relationship between climate variables and SDI_{MAX} beyond the range of input data, as well as the unknown impact of elevated CO_2 concentrations on plant growth.

Conclusion

Climate projections show forest communities of the Pacific Northwest may be facing a longer, warmer, droughtier growing season in the future. Snow pack to provide water in some more precipitation-limited areas will be both increasingly significant and inadequate. Spatial knowledge of where these impacts will be felt the most is important for silivicultural planning. Management approaches need to consider the impacts of these changes on the forest stand's ability to handle the increase in density dependent competition, in particular for what may be an even more limited water supply. Planting and thinning to lower densities may provide resilience and capture the projected increases in density related mortality. Although many unknowns remain, for example the impact of global change on disease and insect patterns (Bentz et al., 2010) or wildfire behavior (Loehman et al., 2020), density management guidelines need to consider the influence a changing environment will have on density driven interactions among forest communities. These results present forest managers and policy makers with the ability to make location specific interpretations of the magnitude and variability of potential shifts in forest stand carrying capacity.

References

Andrews, C., Weiskittel, A., Amato, A. W. D., and Simons-legaard, E. 2018. Variation in the maximum stand density index and its linkage to climate in mixed species forests of the North American Acadian Region. *Forest Ecology and Management*, 417, 90–102. https://doi.org/10.1016/j.foreco.2018.02.038

Aguirre, A., del Río, M and Condes, S. 2018. Intra- and inter-specific variation of the maximum size-density relationship along an aridity gradient in Iberian pinewoods. *Forest Ecology and Management*, 411, 90-100. https://doi.org/10.1016/j.foreco.2018.01.017

Bentz, B., Regniere, J., Fettig, C., Hansen, E., Hayes, J., Hicke, J., Kelsey, R., Negron, J. and Seybold, S. 2010. Climate change and bark beetles of the Western United States and Canada: Direct and Indirect Effects. *BioScience*. 60:8, 602-613. https://doi.org/10.1525/bio.2010.60.8.6

Brunet-Navarro, P., Sterck, F., Vayreda, J, Martinez-Vilalta, J. and Mohren, G. 2016. Self-thinning in four pine species: an evaluation of potential climate impacts. *Annals of Forest Science*, 733, 1025-1034. https://doi.org/10.1007/s13595-016-0585-y

Chmura, D., Anderson, P., Howe, G., Harrington, C., Halofsky, J., Peterson, D., Shaw, D. and St.Clair, J. 2011. Forest responses to climate change in the northwestern United States: Ecophysiological foundations for adaptive management. *Forest Ecology and Management*. 261, 1121–1142. doi:10.1016/j.foreco.2010.12.040

Deng, J., Wang, G., Morris, C., Wei, X., Li, D., Chen, B., Zhao, C., Liu, J. and Wang, Y. 2006. Plant mass-density relationship along a moisture gradient in north-west China. *Journal of Ecology*. 94, 953-958. https://doi.org/10.1111/j.1365-2745.2006.01141.x

Dolanc, C., Thorne, J. and Safford, H. 2013. Widespread shifts in the demographic structure of subalpine forests in the Sierra Nevada, California, 1934 to 2007. *Global Ecology and Biogeography.* 22, 264-276. https://doi.org/10.1111/j.1466-8238.2011.00748.x

Elith, J., Leathwick, J. and Hastie, T. 2008. A working guide to boosted regression trees. *Journal of Animal Ecology*. 77, 802-813. https://doi.org/10.1111/j.1365.2656.2008.01390.x

Franklin, J. and Waring, R. Distinctive features of the Northwestern coniferous forest: Development, structure, and function. *Ecosystem Analysis: Proceedings, 40th Annual Biological Colloquim*. Oregon State University Press. 59-86.

Friedman J. 2001. Greedy function approximation: a gradient boosting machine. *Annals of Statistics*. 29:5, 1189-1232. https://doi.org/10.1214/aos/1013203451

Geraci, M. 2014. Linear Quantile Mixed Models: The 'lqmm' package for Laplace Quantile Regression. *Journal of Statistical Software*. 57(3), 1-29. http://dx.doi.org/10.18637/jss.v057.i13

Greenwell, B., Boehmke, B., Cunningham, J. and GBM Developers. 2020. gbm: Generalized Boosted Regression Models. R Package version 2.1.8. https://CRAN.R-project.org/package=gbm

Harpold, A. 2016. Diverging sensitivity of soil water stress to changing snowmelt timing in the Western U.S. *Advances in Water Resources*. 92, 116-129. https://doi.org/10,1016/j.advwatres.2016.03.017

Hastie, T., Tibshirani, R. and Friedman, R. 2008. The elements of statistical learning: Data mining, inference, and prediction 2nd edition. Springer. Stanford, CA ISBN: 0387848576

Hijmans, R. 2020. 'raster': Geographic data analysis and modeling. R package version 3.3-13. https://CRAN.R-project.org/package=raster

IPCC, 2013: *Climate Change 2013: The Physical Science Basis. Contribution of Working Group I to the Fifth Assessment Report of the Intergovernmental Panel on Climate Change* [Stocker, T.F., D. Qin, G.-K. Plattner, M. Tignor, S.K. Allen, J. Boschung, A. Nauels, Y. Xia, V. Bex and P.M. Midgley (eds.)]. Cambridge University Press, Cambridge, United Kingdom and New York, NY, USA, 1535 pp, doi:10.1017/CBO9781107415324.

Iverson, L., Prasad, A., Matthews, S. and Peters, M. 2008. Estimating potential habitat for 134 eastern US tree species under six climate scenarios. *Forest Ecology and Management*. 254, 390–406. https://doi.org/10.1016/j.foreco.2007.07.023

Kimsey, M., Shaw, T. and Coleman, M. 2019. Site sensitive maximum stand density index models for mixed conifer stands across the Inland Northwest, USA. *Forest Ecology and Management*, 433, 396-404. https://doi.org/10.1016/j.foreco.2018.11.013

Klos, P., Link, T. and Abatzoglou, J. 2014. Extent of the rain-snow transition zone in the western U.S. under historic and projected climate. Geophysical Research Letters. 41, 4560-4568. http://doi.org/10.1002/2014GL060500

Kuhn, M. 2020. caret: Classification and Regression Training. R package version 6.0-86. https://CRAN.R-project.org/package=caret

Loehman, R., Keane, R. and Holsinger, L. 2020. Simulation modeling of complex climate, wildfire, and vegetation dynamics to address wicked problems in land management. *Frontiers in Forests and Global Change*. 3, 1-13. https://doi.org/10.3389/ffgc.2020.00003

Millar, C., Stephenson, N. and Stephens, S. 2007. Climate change and forests of the future: Managing in the face of uncertainty. *Ecological Applications*. 17:8, 2145-2151. https://doi.org/10.1890/06-1715.1

Parmesan, C. 2006. Ecological and evolutionary responses to recent climate change. *Annual Review of Ecology, Evolution, and Systematics*. 37, 637-669. https://doi.org/10.1146/annurev.ecolsys.37.091305.110100

Pretzsch, H. and Biber, P. 2016. Tree species mixing can increase maximum stand density. *Canadian Journal of Forest Research*, 46:10, 1179-1193. https://doi.org/10.1139/cjfr-2015-0413

Puettmann, K. 2011. Silvicultural challenges and options in the context of global change: "Simple" fixes and opportunities for new management approaches. *Journal of Forestry*, 109:6, 321-331. https://doi.org/10.1093/jof/109.6.321

Pothier, D. 2019. Analysing the growth dynamics of mixed stands composed of balsam fir and broadleaved species of various shade tolerances. *Forest Ecology and Management*. 444, 21-29. https://doi.org/10.1016/j.foreco.2019.04.035

R Core Team. 2020. R: A language and environment for statistical computing. R Foundation for Statistical Computing, Vienna, Austria. https://www.R-project.com

Rehfeldt, G., Crookston, N., Warwell, M. and Evans, J. 2006. Empirical analyses of plant-climate relationships for the western United States. *International Journal of Plant Sciences*, 167:6, 1123-1150. https://doi.org/10.1086/507711

Reineke, L. 1933. Perfecting a stand-density index for even-aged forests. *Journal of Agricultural Research*, 46:7, 627-638.

Roise, J and Betters, D. 1981. An aspect transformation with regard to elevation for site productivity models. *Forest Science*, 27:3, 483-486. https://doi.org/10.1093/forestscience/27.3.483

Salas-Eljatib, C and Weiskittel, A. 2018. Evaluation of modeling strategies for assessing self-thinning behavior and carrying capacity. *Ecology and Evolution*, 8, 10768-10779. https://doi.org/10.1002/ece3.4525

Vuuren, D., Edmonds, J., Kainuma, M., Riahi, K., Thomson, A., Hibbard, K., Hurtt, G., Kram, T., Krey, V., Lamarque, J., Masui, T., Meinshausen, M., Nakicenovic, N., Smith, S. and Rose, S. 2011. The representative concentration pathways: an overview. *Climate Change*. 109, 5-31. http://doi.org/10.1007/s10584-011-0148-z

Waring, R. and Franklin, J. 1979. Evergreen coniferous forests of the Pacific Northwest. *Science*. 204, 1380-1386. https://doi.org/ 10.1126/science.204.4400.1380

Wang, T., Hamann, A., Spittlehouse, D. and Carroll, C. 2016. Locally downscaled and spatially customizable climate data for historical and future periods for North America. PLoS ONE. 11:6, 1-17. https://doi.org/10.1371/journal.pone.0156720

Way, D. and Oren, R. 2010. Differential responses to changes in growth temperature between trees from different functional groups and biomes: a review and synthesis of data. *Tree Physiology*. 30, 669-688. https://doi.org/10/1093/treephys/tpq015

Yachi, S. and Loreau, M. 1999. Biodiversity and ecosystem productivity in a fluctuating environment: The insurance hypothesis. *PNAS*. 96:4, 1463-1468. https://doi.org/10.1073/pnas.96.4.1463

Yue, C., Kahle, H., von Wilpert, K. and Kohnle, U. 2016. A dynamic environment-sensitive site index model for the prediction of site productivity potential under climate change. *Ecological Modelling*, 337, 48-62. https://doi.org/10.1016/j.ecolmodel.2016.06.005

Chapter 4: Impact of Simulated Field Plot Location Errors on Maximum Stand Density Index Model Development and Performance

Introduction

Spatially explicit data are prominently used in many environmental modelling applications. Site-specific variables are extracted from spatial data layers at field plot locations to build statistical relationships with a response variable of interest. Modelling of forest productivity (Latta et al., 2009), stand density index (Andrews et al., 2019; Kimsey et al., 2019), site index (Hemingway and Kimsey, 2020) and species distribution (Franklin, 2010) all utilize spatially explicit information to describe important ecological relationships across the landscape. These data are often topographic (i.e. slope, aspect, elevation), climatic (mean annual temperature and precipitation), geographic (county, state, water district, national forest, etc.) or innumerable other environmental characteristics such as vegetative cover, soil descriptions and land use or habitat classifications. Remote sensing products often rely on accurate registration of data, the linking of field plot locations with remotely sensed data. Forest productivity assessment utilizing satellite imagery (Coops et al., 1998), synthetic aperture radar (SAR) (Askne et al., 2018) and light detection and ranging (LiDAR) (Falkowski et al., 2009) are driven by the spatial linkage of metrics found within the remotely sensed data to the field data collected at the precise plot location. A primary driver of accuracy in all these models comes from precise location information to minimize error in variable extraction and data linkages.

Positional coordinates are required to identify the data point location on the three dimensional surface of the landscape. Positional uncertainties inevitably exist in GPS data points (Hong and Vonderohe, 2014). These positional uncertainties may be attributed to positional error inherent in the GPS or GNSS technology or a host of user errors related to how the location information was recorded. Positional error may be caused by outdated technology, poor satellite signal reception or by errors in data processing associated with conversions between coordinate systems or rounding of coordinate values (Gabor et al., 2020). Tree canopies mask and block the direct line of sight between the GPS receiver antenna and the satellite, affecting the quality of the computed position (Pirti, 2005).

Given the many sources of positional error that may be involved before the data is processed, identification of the presence and subsequent effects of these errors on model performance should be considered.

Exploring forest area classification from satellite imagery, McRoberts (2010) found that as many as half the ground plots used in the study were assigned to incorrect pixels due to GPS positional errors, leading to obscured relationships between field data and spectral information from imagery. Patterson and Williams (2003) found a loss in classification accuracy and large increases in forest area estimator variance with registration errors being off by only one or two 28.5 meter Landsat pixels. Frazer et al. (2011) performed positional accuracy manipulations within LiDAR point clouds and found median and range of mean differences in point cloud metrics increased markedly as GPS error increased. Zald et al. (2014) also examined the impact of plot location on LiDAR point cloud metric extraction and, in contrast to Frazer et al. (2011) and McRoberts (2010), found little impact of forest composition and structure mapping. Although, positional error in the Zald et al. (2014) study was on average only 18.18 m, less than the width of a single Landsat pixel but larger than the positional errors of typical GPS receivers.

Forest Inventory and Analysis (FIA) plot locations use a process of "fuzzing and swapping" to address privacy issues of forest land owners. Under amendments made in 2000 to the Food Security Act of 1985 new restrictions were put in place regarding the privacy concerns of forest land owners on which FIA plots fell. The new regulations called for specific procedures needed to insure confidentiality. The true plot locations are shifted randomly in x and y coordinate directions to meet these confidentiality concerns. Many studies utilize this rich source of data to perform spatial interpolations of important forest and ecological metrics. The effects these manipulations of coordinates have on spatial model accuracy is often unknown. Coulston and Reams (2004) explored the issues of interpolation accuracy when using fuzzed versus unfuzzed coordinates to generate forest biomass maps covering Minnesota and found model coefficients to be outside the 95% confidence

interval of the parameters found using actual plot locations. They suggested further exploration through simulation analyses.

Exploring the impact of positional error is an active topic in species distribution modelling. Graham et al. (2008), experimenting with species occurrence data, manipulated x and y coordinates of plot locations by shifting the position in a random direction and distance up to 5km, and found their modeling efforts to be rather robust to positional error. Conversely, Johnson and Gillingham (2008) experimenting with positional data of caribou, randomly manipulated positional error incrementally from 50 to 1000 meters and found non-overlapping 95% confidence intervals after 200 m of simulated error and concluded their model results to be rather sensitive to this introduced positional error. Osborne and Leitao (2009) also experimented with positional accuracy in species distribution modelling by deliberately introducing error through shifting habitat raster layers in a random direction and found a drop in model performance.

The primary objective of this study was to determine how sensitive the maximum stand density index models (SDI_{MAX}) derived in earlier chapters are to positional errors of field plot locations used in the variable extraction and model building process. This objective will be assessed through exploring changes in extracted variable values, model coefficients and predicted SDI_{MAX}.

Materials and Methods

Data

Plot data was obtained through a collaborative network of public and private forest land management organizations. Inventory and monitoring plot data represented a range of fixed and variable radius sampling methods, each geolocated to allow extraction of desired attributes from spatial layers containing various physiographic metrics. Plot location information, including United States Forest Service (USFS) Forest Inventory and Analysis (FIA) and Field Sampled Vegetation (FSVeg) records, was provided as unfuzzed coordinates. When exact plot location was unavailable, data was rolled up to the stand level (stand shapefiles supplied by data provider) and a stand centroid

location was utilized (<10% of the dataset). Each plot record included number of trees per hectare (TPH), quadratic mean diameter (QMD) and proportion of basal area (BA) by major species groups. Data screening removed plots with less than 2.54 cm QMD and 24.7 TPH to establish a consistent threshold of diameter and number of trees. Only trees marked as living were included in plot-level estimates. The final dataset (n=155,083) explored in this spatial sensitivity assessment consisted of only those plots containing at least 10% Douglas-fir basal area proportion.

Topographic attributes were derived from U.S. Department of Agriculture (USDA) and National Resource Conservation Service (NRCS) National Elevation Data 30-m digital elevation models. Slope and aspect were derived using the 'raster' package (Hijmans, 2020) available through R 4.0 (R Core Team, 2020). Spatial maps of soil parent materials were derived from USGS 1:24,000 geology maps and surficial volcanic ash mantles from the NRCS soil survey geographic database (SSURGO).

Thirty-year (1961-1990) annual, seasonal and monthly climate normals were obtained through the ClimateNA v6.11 (Wang et al., 2016) software package using plot-specific latitude, longitude and elevation. These climate data contained directly calculated and derived variables, as well as various interactions resulting in over 230 climate variables assigned to each record.

Plot Location Manipulation

To understand the influence of positional error on variable extraction and model performance, individual plot longitude and latitude coordinates were shifted in a random direction by 30, 60, 120, 500 and 1000 meters. While these distances are much larger than typical GPS accuracy error, they were chosen to allow for records to shift between adjacent pixels of the data source of highest resolution (30 m) and to see how error changes the further plot location shifts from the actual location. Each record was randomly assigned a -1 or +1 in both the x and y direction to determine the shift direction, resulting in four possible directional combinations. Once assigned to a record, the

directional shift remained constant for each distance interval. Variable data was then extracted for each record at the six plot locations (0 – actual location, 30, 60, 120, 500 and 1000 m).

Influence of Positional Adjustment on Data Extraction and SDI_{MAX} Model Performance

The finalized stochastic frontier regression (SFR) model developed in an early chapter was utilized to compare how coefficients and predicted SDI_{MAX} values changed with positional adjustments. The final model contained input variables describing number of trees, tree size and species basal area proportions, which will remain constant for each positional adjustment. Selected model input variables that will (potentially) change due to positional adjustments include latitude, elevation, topographic position, geologic and soil descriptors, and climatic variables relating to precipitation and temperature. The gamma statistic, which describes the validity of SFR to model a maximum boundary, as well as important model coefficients, will be used to compare model performance between positional adjustments.

Results

Model Parameters and Performance

The most influential drivers of the SDI_{MAX} model are the intercept and QMD slope coefficient. These two parameters overlapped under all positional scenarios at the 95% confidence interval (Figure 4.1). A comparison of the rest of the variables in the model showed similar results, with no significant differences between model coefficients at all positional adjustments. However, model performance as measured by the gamma statistic, showed decreasing model performance the further the positional adjustment (Figure 4.2).

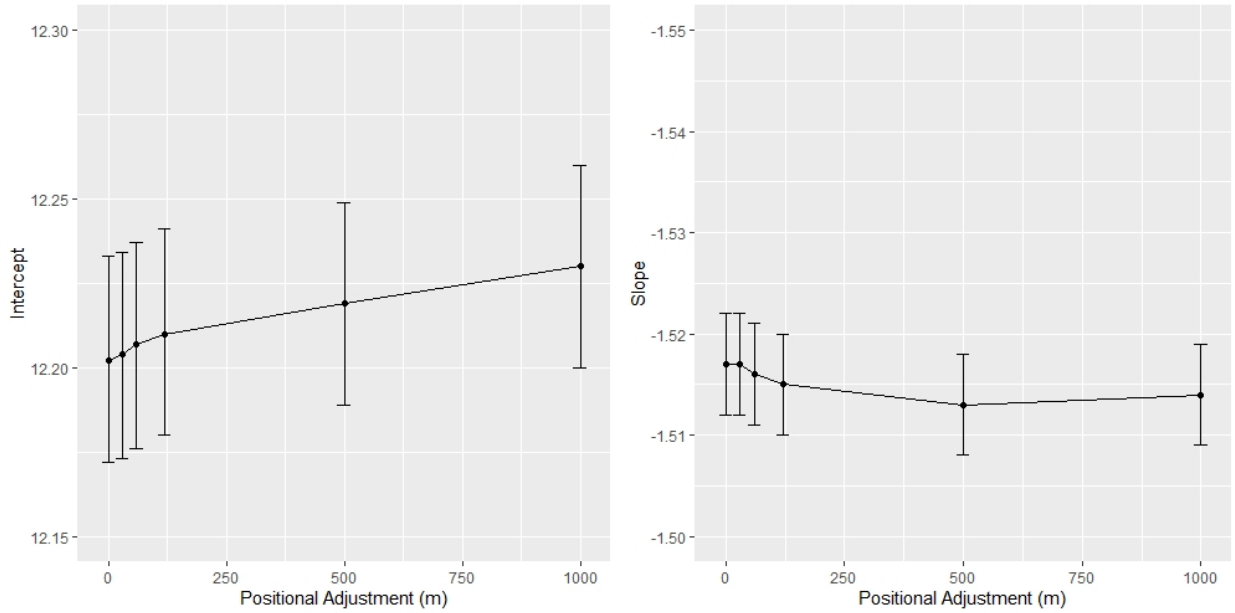

Figure 4.1 Intercept and slope parameters derived from the SFR model under increasing positional adjustments. Error bars represent 95% confidence intervals.

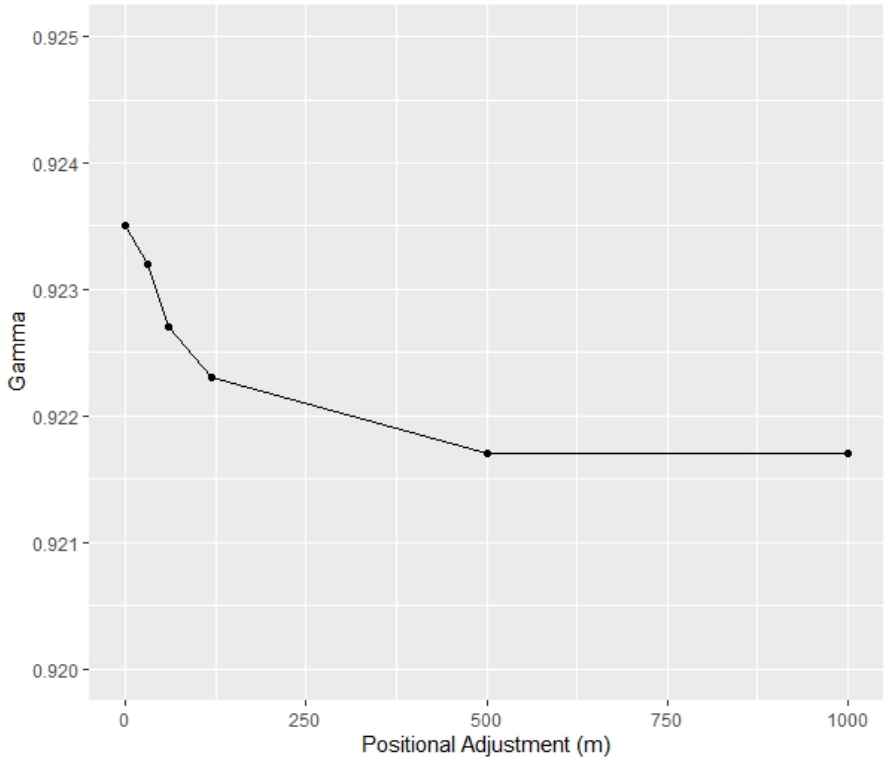

Figure 4.2 SFR gamma statistic for each position adjustment.

Predictive Performance

Under each positional adjustments scenario, SDI_{MAX} predictions for each record were made from the final SFR model. Increases in change at the 1 and 99 percentiles compared to actual location (0 m) increased with larger positional adjustment (Table 4.1). Average and median absolute change from actual location (0 m) increased the further the positional adjustment (Table 4.2). Standard deviations of change increased with larger positional adjustment. Average predicted SDI_{MAX} saw no obvious patterns with positional adjustments. However, an analysis of variance between group averages showed significant treatment (positional adjustment) differences at the 500 and 1000 m positional adjustments (Table 4.3).

Table 4.1 Change in SDI_{MAX} with positional adjustment relative to actual location.

	30m	60m	120m	500m	1000m
Min	-21.5%	-23.1%	-22.8%	-99.9%	-21.8%
1%	-3.95%	-4.83%	-5.25%	-6.49%	-7.20%
Mean	0.01%	-0.01%	-0.02%	-0.03%	0.00%
Median	0.0%	0.0%	-0.1%	-0.1%	0.0%
99%	4.01%	5.01%	5.43%	6.34%	7.23%
Max	22.7%	26.4%	29.1%	35.2%	34.1%
SD	1.4%	1.9%	2.3%	2.9%	3.1%

Table 4.2 Absolute change in SDI_{MAX} with positional adjustment relative to actual location.

	30m	60m	120m	500m	1000m
Min	0.00%	0.00%	0.00%	0.00%	0.00%
1%	0.01%	0.02%	0.04%	0.04%	0.04%
Mean	0.99%	1.47%	1.85%	2.26%	2.47%
Median	0.67%	1.14%	1.61%	1.99%	2.14%
99%	4.66%	5.69%	6.06%	7.31%	8.15%
Max	22.71%	26.42%	29.08%	99.91%	34.12%
SD	1.02%	1.26%	1.38%	1.75%	1.94%

Table 4.3 ANOVA of predicted SDI_{MAX}. Positional adjustments of 500m and 1000m showed significant departure from overall mean. Intercept was actual location.

	Estimate	Std. Error	t value	Pr(>|t|)
Intercept	1373.0896	0.4432	3097.972	<2e-16 ***
30m	-0.1815	0.6268	-0.29	0.7721
60m	-0.5921	0.6268	-0.945	0.3449
120m	-0.931	0.6268	-1.485	0.1375
500m	-1.488	0.6268	-2.374	0.0176 *
1000m	-1.2318	0.6268	-1.965	0.0494 *

Discussion

Overall the spatial sensitivity analysis showed this regional landscape level model developed for predicting SDI_{MAX} from spatially explicit site factors is robust to positional errors of plot locations for the majority of input records. The main driver of predicated carrying capacity is the self-thinning slope coefficient for QMD, which is not a spatially explicit variable. Model coefficients remained rather constant although the drop in model performance with increasing spatial adjustment was not unexpected. Site specific factors have been shown to influence carrying capacity. Therefore, as plot coordinates move away from true location, these correlations with real, underlying conditions found where the trees were actually measured become less accurate.

The largest swings in predicted SDI_{MAX} were caused when a plot moved between geologic or soil classifications, which are binary variables in the model. For example, a site on underlying geography classified as sandstone had a negative impact on predicted SDI_{MAX} and therefore a shift of the plot location into or out of an area classified as sandstone caused a significant fluctuation in the predicted value. While many geological and soil spatial layers are the result of interpolations, the influence of these characteristics is real and must be accounted for. This underscores the importance of both the need for accurate spatial layers, as well as field verification of the characteristics being mapped.

Another source of change within predicted SDI_{MAX} was the result of topographic position and elevation fluctuations caused with plot location adjustment. The forested landscapes of the Pacific

Northwest are often in mountainous terrain with variable topography. A plot on a gentle sloping, southern facing aspect could easily switch to a completely different aspect and slope grade with the wrong positional location. Elevation just as well could see large fluctuations in areas with more rugged topography, where a plot location could drop off a cliff due to positional error. Some of the more egregious examples of this phenomenon with the analyzed dataset were found in the Northern Cascades region, where plot location adjustment by only 30 meters saw some elevation changes of up to and exceeding 100 meters. Even further positional adjustments saw up to 1000 meters in elevation change. While the model contains an elevation variable, it does not have as strong an influence on predictions as the tree specific variables: however, a large enough shift can produce a significant change in prediction.

Conclusion

This spatial sensitivity analysis showed the developed maximum stand density index model was robust to positional error. The biggest issue came when the positional error caused true location to shift into or out of a binary classifier such as the underlying geologic or soil classification. Climate variables in the model do not vary widely with positional changes analyzed here. Although the most common and varied changes were found in topographic position and elevation, which caused predictions of individual records to swing due to positional adjustment, overall these changes had minimal effect on model parameters and regional SDI_{MAX} predictions. This analysis underscores the importance of accurate tree measurements, which have a much larger influence on model parameters compared to positional error of plot locations.

References

Andrews, C., Weiskittel, A., Amato, A. and Simons-legaard, E. 2018. Variation in the maximum stand density index and its linkage to climate in mixed species forests of the North American Acadian Region. *Forest Ecology and Management*, 417, 90–102. https://doi.org/10.1016/j.foreco.2018.02.038

Askne, J., Persson, H. and Ulander, L. 2018. Biomass growth from multi-temporal TanDEM-X interferometric synthetic aperture radar observations of a boreal forest site. *Remote Sensing*. 10:603, 1-18. https://doi.org/10.3390/rs10040603

Coops, N., Waring, R. and Landsberg, J. 1998. Assessing forest productivity in Australia and New Zealand using a physiologically-based model driven with averaged monthly weather data and satellite-derived estimates of canopy photosynthetic capacity. *Forest Ecology and Management*. 104, 113-127. https://doi.org/10.1016/S0378-1127(97)00248-X

Coulston, J and Reams, G. 2004. The effect of blurred plot coordinates on interpolating forest biomass: a case study. In: Proceedings of the joint meeting of the 15th annual conference of the International Environmetrics Society and the 6th international symposium on spatial accuracy assessment in natural resources and environmental sciences.

Falkowski, M., Evans, J., Martinuzzi, S., Gessler, P. and Hudak, A. 2009. Characterizing forest succession with lidar data: An evaluation for the Inland Northwest, USA. *Remote Sensing of Environment*. 113, 946-956. https://doi.org/10.1016/j.rse.2009.01.003

Franklin, J. 2010. Mapping Species Distributions: Spatial Inference and Prediction. Cambridge University Press. ISBN: 9780511810602. https://doi.org/10.1017/CBO9780511810602

Frazer, G., Magnussen, S., Wulder, M. and Niemann, K. 2011. Simulated impact of sample plot size and co-registration error on the accuracy and uncertainty of LiDAR-derived estimates of forest stand biomass. *Remote Sensing of Environment*. 115, 636-649. https://doi.org/10.1016/j.rse.2010.10.008

Gabor, L., Moudry, V., Lecours, V., Malavasi, M., Bartak, V., Fogl, M., Simova, P., Rocchini, D. and Vaclavik, T. 2020. The effect of positional error on fine scale species distribution models increases for specialist species. *Ecography*. 43, 256-269. https://doi.org/10.1111/ecog.04687

Graham, C., Elith, J., Hijmans, R., Guisan, A., Peterson, A., Loiselle, B. and the NCESA predicting species distributions working group. 2008. The influence of spatial errors in species occurrence data used in distribution models. *Journal of Applied Ecology*. 45, 239-247. https://doi.org/10.1111/j.1365-2664.2007.01408.x

Hemingway, H. and Kimsey, M. 2020. Estimating forest productivity using site characteristics, multipoint measures, and a nonparametric approach. *Forest Science*. Fxaa023, 1-8. https://doi.org/10.1093/forsci/fxaa023

Hijmans, R. 2020. 'raster': Geographic data analysis and modeling. R package version 3.3-13. https://CRAN.R-project.org/package=raster

Hong, S. and Vonderohe, A. 2014. Uncertainty and sensitivity assessments of GPS and GIS integrated applications for transportation. *Sensors*. 14, 2683-2702. https://doi.org/10.3390/s140202683

Johnson, C. and Gillingham, M. 2008. Sensitivity of species-distribution models to error, bias, and model design: An application to resource selection functions for woodland caribou. *Ecological Modelling*. 213, 143-155. https://doi.org/10.1016/j.ecolmodel.2007.11.013

Kimsey, M., Shaw, T. and Coleman, M. 2019. Site sensitive maximum stand density index models for mixed conifer stands across the Inland Northwest, USA. *Forest Ecology and Management*, 433, 396-404. https://doi.org/10.1016/j.foreco.2018.11.013

Latta, G., Temesgen, H. and Barrett, T. 2009. Mapping and imputing potential productivity of Pacific Northwest forests using climate variables. *Canadian Journal of Forest Research*. 39:6, 1197-1207. https://doi.org/10.1139/X09-046

McRoberts, R. 2010. The effect of rectification and global positioning system errors on satellite image-based estimates of forest area. *Remote Sensing of Environment*. 114, 1710-1717. https://doi.org/10.1016/j.rse.2010.03.001

Osborne, P. and Leitao, P. 2009. Effects of species and habitat positional errors on the performance and interpretation of species distribution models. *Diversity and Distributions*. 15, 671-681. https://doi.org/10.1111/j.1472-4642.2009.00572.x

Patterson, P. and Williams, M. 2003. Effects of registration errors between remotely sensed and ground data on estimators of forest area. *Forest Science*. 49:1, 110-118. https://doi.org/10.1093/forestscience/49.1.110

Pirti, A. 2005. Using GPS near the forest and quality control. *Survey Review*. 298, 286-298. https://doi.org/10.1179/sre.2005.38.298.286

R Core Team. 2020. R: A language and environment for statistical computing. R Foundation for Statistical Computing, Vienna, Austria. https://www.R-project.com

Wang, T., Hamann, A., Spittlehouse, D. and Carroll, C. 2016. Locally downscaled and spatially customizable climate data for historical and future periods for North America. PLoS ONE. 11:6, 1-17. https://doi.org/10.1371/journal.pone.0156720

Zald, H., Ohmann, J., Roberts, H., Gregory, M., Henderson, E., McGaughey, R. and Braaten, J. 2014. Influence of lidar, Landsat imagery, disturbance history, plot location accuracy, and plot size on accuracy of imputation maps of forest composition and structure. *Remote Sensing of Environment*. 143, 26-38. https://doi.org/10.1016/j.rse.2013.12.013

Chapter 5: Sensitivity of Stand Density Index to Diameter Calculations and Cutoffs

Introduction

Reineke's stand density index (SDI) was originally developed as the relationship between number of trees per unit area and the average diameter by basal area (Reineke, 1933). This diameter measure used in the original form presented by Reineke is known as the quadratic mean diameter (QMD). That is the classic definition of a quadratic mean (Iles and Wilson, 1977) where QMD is calculated as the "root-mean-square" and expressed as follows:

[1] $$QMD = \sqrt{\frac{\sum_{i=1}^{n}(d_i{}^2)}{n}}$$

Where *d* is the *n*th diameter of an individual tree and *n* is the total number of trees. When determining QMD from inventory data, it is often necessary to account for expansion factors and should be calculated as follows:

[2] $$QMD = \sqrt{\frac{\sum_{i=1}^{n}(d_i{}^2 * TPA_i)}{\sum_{i=1}^{n}(TPA_i)}}$$

Where *d* is the *n*th diameter of an individual tree and *TPA* is the number of trees represented by that tree. QMD is equivalent to the diameter of the tree of average basal area and can be calculated as follows:

[3] $$QMD = \sqrt{\frac{\overline{BA\_AC}}{\overline{TPA} * 0.005454}}$$

Where $\overline{BA\_AC}$ is average basal area per acre, $\overline{TPA}$ is average number of trees per acre and 0.005454 is the constant relating inches to square feet. The quadratic mean diameter is necessarily greater than or equal to the arithmetic mean diameter (AMD), as it gives greater weight to larger trees. The difference between QMD and AMD grows as the stand structure diverges from a tight, unimodal diameter

distribution of an even-aged stand, to that of a more skewed or reverse-J shaped distribution of an uneven-aged stand.

For expressing stand attributes, QMD has both mensurational advantages (i.e. the exact relationship to basal area) and historical precedent (Curtis and Marshall, 2000). Reineke developed SDI from even-aged stands where variance of diameters was low and thus was sufficient for describing 'average diameter'. The original equation of Reineke SDI was the following:

[4] $$SDI = TPA \left(\frac{QMD}{10}\right)^b$$

Where *TPA* is the number of trees per unit area, *QMD* is the classic 'root-mean-square' diameter and *b* is the slope of the self-thinning line. Reineke found this slope, in the linear form of the equation, to be -1.605.

Stage (1968) found the disadvantage of SDI in that there was no way to describe the contributions of various diameter classes of trees in the stand to the total index for the stand, and therefore computed SDI as a summation, hereafter referred to as SDI*. The summation method computes SDI* tree by tree within a stand as follows:

[5] $$SDI^* = \sum \left(\frac{DBH_i}{10}\right)^b$$

Where DBH_i is the diameter of the *ith* tree in the stand and *b* is the slope of the self-thinning line, using 1.6 a good approximation. If SDI* is to be calculated via the summation method from a stand table containing only diameter classes and number of trees, it can be calculated as follows:

[6] $$SDI^* = \sum \left(TPA_j * \left(\frac{DBH_j}{10}\right)^b\right)$$

Where DBH_j is the diameter of the *jth* diameter class in the stand, *TPAj* is the number of trees in the *jth* diameter class and *b* is the slope of the self-thinning line, 1.6 has been a standard approximation. At

the plot level, this summation formula is used with each "in" tree's diameter, and expansion factor as TPA. The plot total is the summation, where the stand total is the average of all plots in the stand.

Zeide (1983) describes how the 'average diameter' in Reineke's equation is technically neither the quadratic nor the arithmetic mean, but rather a function of the slope of the self-thinning line, and coined yet another diameter, which he called Reineke's diameter (D_R), calculated as:

[7] $$D_R = \left(\frac{1}{N}\sum {d_i}^b\right)^{\frac{1}{b}}$$

Where *N* is the total number of trees, *d* is the diameters of the *i*th tree and *b* is the slope of the self-thinning line, with 1.6 as a good approximation. In application, this equation, like that of the summation SDI, needs to be weighted by expansion factors for each tree and should be calculated as follows:

[8] $$D_R = \left(\frac{1}{\sum TPA_i}\sum TPA_i * {d_i}^b\right)^{\frac{1}{b}}$$

Where TPA_i is the number of trees represented by the *i*th "in" tree's diameter. The Reineke diameter can then be used in the classic SDI form in place of QMD, which has been shown to be equal to the summation SDI* (Shaw, 2000).

Zeide (1983) goes on to present another equation for D_R, developed using the first three terms of Taylor expansion, as a function of the arithmetic mean and its variability, represented by the coefficient of variation, as the following:

[9] $$D_R = \bar{d}\left[1 + \frac{(b-1)b}{2} * C^2\right]^{1/b}$$

Where $\bar{d}$ is the arithmetic mean, b is the slope of the self-thinning which should lie somewhere between 1, which would produce the arithmetic mean, and 2, which would produce the quadratic mean (1.6 is a good approximation for b), and C^2which is the squared coefficient of variation of the

diameter distribution. This form of the D_R equation is sometimes written without the coefficient of variation squared (Weiskittel and Kuehne, 2019; Andrews et al., 2018). The calculated D_R then replaces QMD in Reineke's SDI equation (Equation [4]) to get at a D_R derived SDI.

Shaw (2000) demonstrated the significance which stand structure (i.e. shape of the diameter distribution) has on the calculation of SDI. Reineke originally developed the SDI equation from even-aged stand data with normal diameter distributions. The QMD and summation methods produce similar results when applied to even-aged stands but as the diameter distribution becomes more irregular (greater variance about the mean diameter), as found in uneven-aged or multi-cohort stands, these two calculations diverge. Shaw (2000) comes to a similar conclusion of that of Zeide (1983), that using QMD is not "technically" correct and that the summation method yields the correct result.

Ducey and Larson (2003) when attempting to determine if there is a truly "correct stand density index", concluded that the summation and Reineke's original SDI should be considered different indices with different properties. Using a two-parameter Weibull function to simulate different diameter distributions with equal number of trees, basal area and QMD, they showed the summation SDI and Reineke SDI are 'remarkably consistent' over most of the diameter distributions until the distribution becomes heavily dominated with small trees.

Curtis (2010), using real stand data, demonstrated not only how these SDI calculation methods differ with stand structure, but how the diameter cutoff of the input data has a significant impact as well. He concludes that the minimum diameter limit has major effects on calculated density values and that in general trees smaller than 1.6 inches, or all trees of a clearly distinguishable understory, should be excluded from computations.

The overall goal of this analysis is to evaluate the impact of various diameter and SDI equations, as well as diameter cutoffs, on real forest inventory data which produced the maximum SDI

model used in previous chapters. In keeping with the tradition of the many papers cited in this introduction, English units will be used throughout this chapter.

Methods

Data

The forests of western Oregon and Washington will again serve as the study area for this analysis. Due to the requirement of the summation SDI and D_R equations for individual tree information, rather than plot or stand level summaries, this analysis utilized data from the U.S. Forest Service Inventory and Analysis (FIA) Program from Oregon and Washington, resulting in 10,432 records. FIA subplot data was summarized to the plot level. Tree level information included diameter at breast height (DBH) and number of trees per acre (TPA) represented by each individual tree.

The FIA dataset was summarized to the plot level under three diameter truncations. The first was no diameter cutoff, where all trees with associated expansion factors were included in plot level summaries. The second was the 1.6 inches which Curtis (2010) suggested as a reasonable cutoff to reduce issues associated with very large numbers of small trees in the understory. The third cutoff was a larger 5-inch cutoff, although subjective, represents a common small diameter cutoff within forest inventory.

Calculated Metrics

For each plot record, arithmetic mean diameter (AMD), quadratic mean diameter (QMD) and Reineke's Diameter (D_R) via the summation method (Equation [8]), as well as D_R via the Taylor expansion (Equation [9]) using both CV and CV^2, were calculated. SDI was then calculated utilizing the QMD (Equation [4]) and the three methods for Reineke's diameter within the classic SDI form (Equations [8], and [9] using both CV and CV^2, placed in Equation [4]) as well as SDI* calculated via the summation method (Equation [6]). Ratios of the various calculations were determined for each record under each diameter cutoff.

Results and Discussion

The two diameter cutoffs of 1.6 and 5 inches reduced the number of plots from 10,432 records to 10,423 and 10,285 respectively due to the removal of plots containing only small diameter trees. As expected, all mean values of the three calculated diameters increased and number of trees decreased with increasing small tree diameter cutoff (Table 5.1). The variability in tree diameters, as indicated by the coefficient of variation, decreased with increasing diameter cutoff.

Table 5.1 Calculated metrics using the various diameter calculations for the different diameter cutoff scenarios.

	No Cutoff	>= 1.6	>= 5
DBH (mean)	8.99	9.68	12.51
D_R (summation)	10.06	10.68	13.33
D_R (CV^2)	10.18	10.79	13.39
$\mathbf{D_R}$ (CV)	10.52	11.23	14.14
QMD	10.77	11.36	13.89
CV	0.70	0.62	0.43
TPA	404	331	155
SDI	282	274	234
SDI*	244	242	219
SDI (CV^2)	252	248	221
SDI (CV)	261	242	252

The increased diameter cutoff causes QMD and AMD to become closer in value. The 50^{th}, 75^{th} and 95^{th} percentiles of the ratio between QMD and AMD get lower as the cutoff increases (Table 5.2). With a diameter cutoff of 5 inches this ratio stays much closer to 1 with a maximum value of 1.67 compared to the lower and no cutoffs reaching 2.5 and 3 times the difference between QMD and the arithmetic mean.

Table 5.2 Ratio of QMD to AMD for the different diameter cutoff scenarios.

	Percentile			
Dataset	50%	75%	95%	Max
No Cutoff	1.20	1.36	1.70	3.02
>=1.6	1.16	1.29	1.56	2.52
>=5	1.08	1.14	1.27	1.67

As expected SDI* was always lower than SDI (Table 5.3), with all diameter cutoffs having a median (50th percentile) ratio between the summation and the QMD (i.e. SDI*:SDI) method of 90% or above. This ratio increased overall as the diameter cutoff increased. This finding is in agreement with Ducey and Larson (2003) who concluded the ratio is relatively insensitive to changes to the shape of the diameter distribution until the distribution becomes heavily dominated by small trees. Forest inventories with a minimum merchantability diameter cutoff will decrease sensitivity to small trees with large expansion factors and lead to a ratio of SDI*:SDI close to 1.

Table 5.3 Ratio of SDI to SDI for the different diameter cutoff scenarios.*

	Percentile			
Dataset	Min	50%	75%	95%
No Cutoff	0.55	0.90	0.95	0.98
>=1.6	0.57	0.91	0.96	0.99
>=5	0.70	0.95	0.97	0.99

Ducey (2009) demonstrated that the most extreme ratio of SDI* to SDI comes when trees are in two distinct diameter classes, such as those in a two-cohort stand like that of a shelterwood. These are stands where there are large numbers of small trees, yet, with majority of the basal area found in the large diameter classes. The most extreme ratios found in this analysis were between 0.55 and 0.60, with only 0.1% or 11 records, falling in this range. For example, the record with the lowest ratio of SDI* to SDI was a plot which contained 14 tree records with six large trees ranging from 30 to 56 inches and 8 trees less than 2.5 inches, fitting with the criteria laid out by Ducey (2009) and others describing a stand structure which would have an extreme ratio. In this example the QMD derived SDI

was 175, and the summation derived SDI* was 96. This same record, with the diameter cutoff of less than 5 inches, SDI and SDI* are almost identical with each at 62. In this extreme example, both the method of calculating SDI and the diameter cutoff are important with regard to any interpretation of what these metrics represent or tell about this stand. Overall, with no diameter cutoff there is a greater amount of records tailing to the lower end whereas the larger diameter cutoff concentrates the distribution closer to 1 (Figure 5.1).

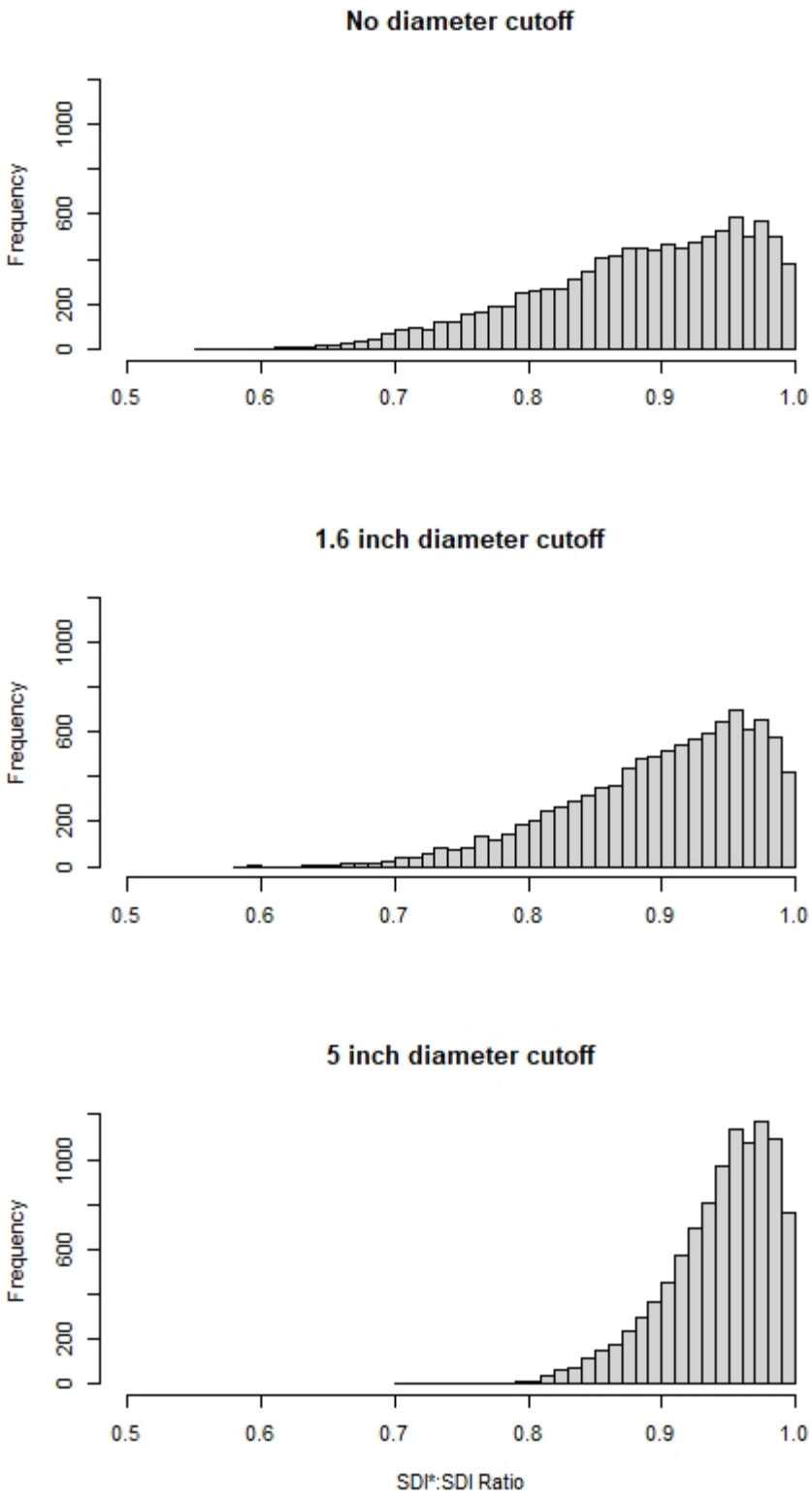

Figure 5.1 Histograms of SDI to SDI ratio for each of the diameter cutoff scenarios.*

D_R calculated from Zeide's (1983) Taylor expansion (Equation [9]) should have the CV squared, proof being that when the b coefficient is 1 D_R equals AMD and when b is 2 D_R equals the QMD (Figure 5.2). This proof is only true for QMD when the CV is squared. Although, an investigation into whether D_R derived via this method is equal to the summation derived D_R, has exposed some issues. First, the assertion and proof shown by Shaw (2000), that the summation SDI* (Equation [6]) and the SDI calculated when utilizing the summation derived D_R (Equation [8] used in Equation [4]) are equal, is correct. However, D_R calculated via the Taylor expansion, as shown in the equations of Zeide (1983) where CV is squared or for Weiskittel and Kuehne (2019) where CV is not squared, is not exactly equivalent to the D_R calculated by the summation method (Figure 5.3). In particular, as the coefficient of variation about arithmetic mean diameter increases, D_R via Taylor expansion increases in proportion to D_R calculated via the summation method. Perhaps, the early findings when utilizing D_R were developed with stand data having low variability in diameter distribution, where these two calculations are indeed approximately equal. Zeide (1983) made use of the stand table in Gingrich (1967 – Table 5, p48), which had a coefficient of variation for the smallest and largest diameter classes of 45 and 29 respectively, to calculate D_R via Taylor expansion (Equation [9]), which would show close agreement with the summation D_R (Equation [8]).

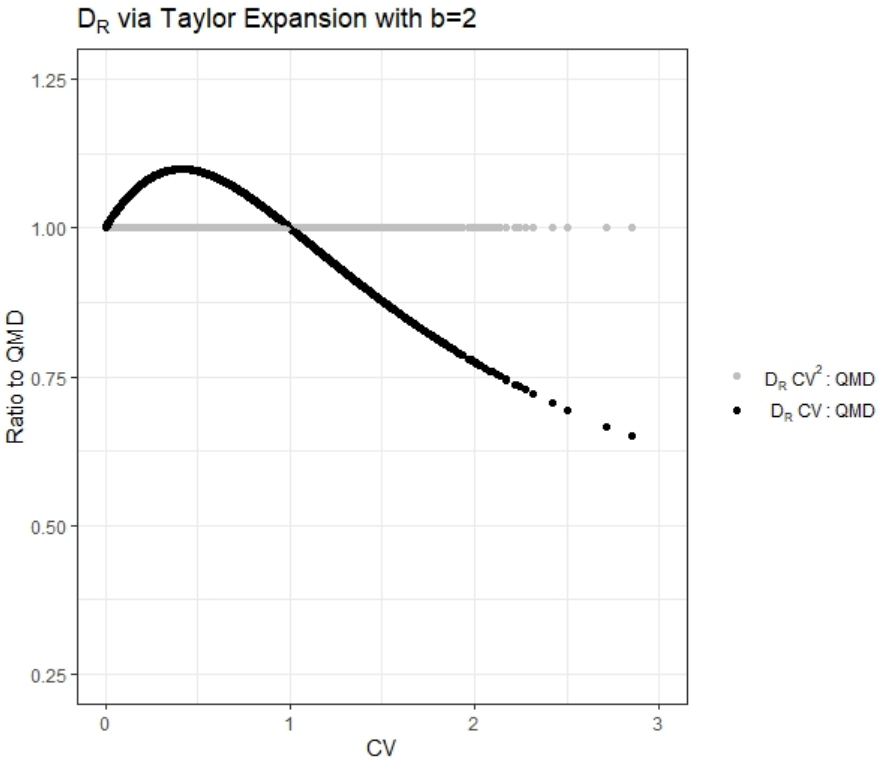

Figure 5.2 D_R via the Taylor expansion (Equation[9]) when b=2 should be equal to QMD. Coefficient of variation in this equation should be squared. CV on the x-axis is coefficient of variation. Dataset with no diameter cutoff shown.

Likewise, the SDI found with input of the Taylor expansion D_R in place of QMD (Equation [9] using both CV and CV^2, placed in Equation [4]) is not equivalent to the SDI* (Equation [6]) found via the summation method (Figure 5.4). Although, as the diameter cutoff increases there is greater agreement between the summation SDI* and the SDI calculated with D_R via the Taylor expansion using CV^2, in particular when the coefficient of variation is low. SDI calculated with CV not squared has already been shown to be incorrect, nonetheless it is interesting how the calculated SDI begins to fall in line with the summation SDI* at higher levels of variance. To avoid any confusion about what this diameter calculation is actually representing when calculating SDI*, D_R calculated via Taylor expansion should not be utilized. It is recommended to either utilize QMD to calculate SDI, or if an area-based metric is desired, use the summation method to calculate SDI*.

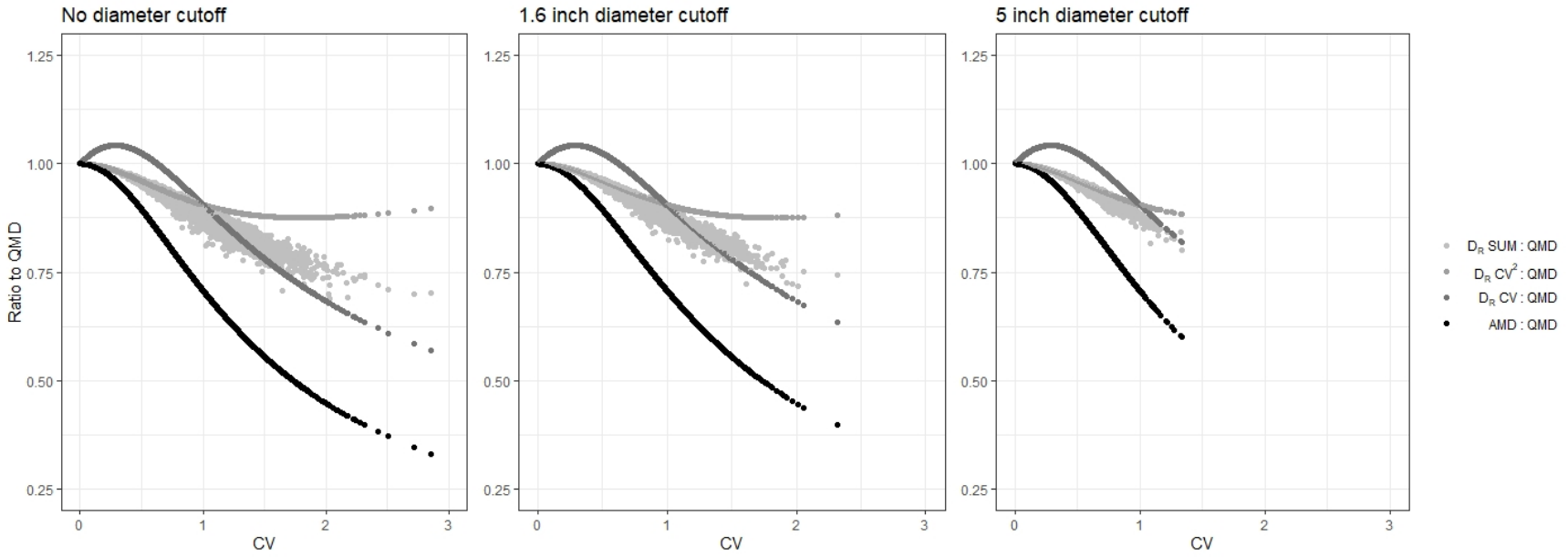

Figure 5.3 Ratio of diameter calculations relative to QMD. CV on the x-axis is coefficient of variation.

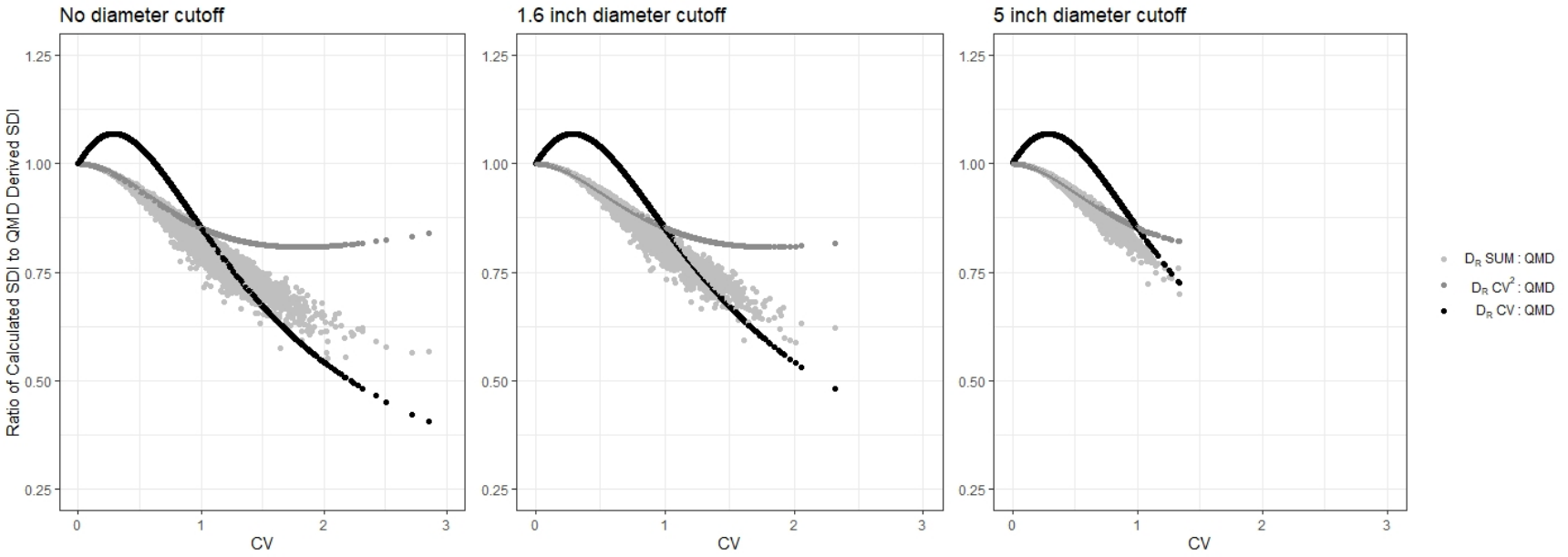

Figure 5.4 Ratios of SDI calculated by summation D_R (equivalent to SDI), D_R with CV^2 and D_R with CV relative to SDI calculated with QMD for each diameter cutoff scenario. There is no SDI calculation from AMD. CV on the x-axis is coefficient of variation.*

Conclusion

The major conclusion of this analysis is that forest structure and any diameter cutoffs used during forest inventory sampling have a significant impact on SDI or SDI* calculation. Any application of either SDI or SDI* for density management should understand how diameter distributions and truncation could impact the interpretation of these indices, in particular, when dealing with irregularly structured forest types. While the use of D_R via Taylor expansion has interesting mathematical properties, the findings of this analysis do not support the use of this particular diameter calculation when applying to the stand density index. If a tree-by-tree, or area-based SDI* is desired, then the summation method, or calculating D_R via the summation method, should be utilized. Ducey and Larson (2003) ask whether sensitivity of SDI* to the shape of the diameter distribution enhances the meaning of the index or whether it is meaningless noise. The utility of any density index can only be set by the management objectives it will guide and the meaning it will have on any planned silvicultural activities. Moreover, the structure of the forest will ultimately dictate how the density index will be utilized and interpreted.

References

Andrews, C., Weiskittel, A., Amato, A. and Simons-legaard, E. 2018. Variation in the maximum stand density index and its linkage to climate in mixed species forests of the North American Acadian Region. *Forest Ecology and Management*, 417, 90–102. https://doi.org/10.1016/j.foreco.2018.02.038

Curtis, R. 2010. Effects of diameter limits and stand structure on relative density indices: a case study. *Western Journal of Applied Forestry*, 25:4, 169-175. http://doi.org/10.1093/wjaf/25.4.169

Curtis, R. and Marshall, D. 2000. Why quadratic mean diameter? *Western Journal of Applied Forestry*. 15:3, 137-139. https://doi.org/10.1093/wjaf/15.3.137

Ducey, M. 2009. The ratio of additive and traditional stand density indices. *Western Journal of Applied Forestry.* 24:1, 5-10. https://doi.org/10.1093/wjaf/24.1.5

Ducey, M. and Larson, B. 2003. Is there a correct stand density index? An alternate interpretation. *Western Journal of Applied Forestry*, 18:3, 179-184. https://doi.org/10.1093/wjaf/18.3.179

Gingrich, S. 1967. Measuring and Evaluating Stocking and Stand Density in Upland Hardwood Forests in the Central States. *Forest Science*. 13:1, 38-53. https://doi.org/10.1093/forestscience/13.1.38

Iles, K. and Wilson, L. 1977. A further neglected mean. *Mathematics Teacher*. 70, 27-28.

Reineke, L. 1933. Perfecting a stand-density index for even-aged forests. *Journal of Agricultural Research*, 46:7, 627-638.

Shaw, J. 2000. Application of stand density index to irregularly structured stands. *Western Journal of Applied Forestry*, 15, 40-42. https://doi.org/10.1093/wjaf/15.1.40

Stage, A. 1968. A tree-by-tree measure of site utilization for grand fir related to stand density index. USDA Forest Service Research Note INT-77, Intermountain Forest and Range Experiment Station, Ogden, Utah

Weiskittel, A. and Kuehne, C. 2019. Evaluating and modeling variation in site-level maximum carrying capacity of mixed-species forests stands in the Acadian Region of northeastern North America. *The Forestry Chronicle*. 95:3, 171-182. https://doi.org/10.5558/tfc2019-026

Zeide, B. 1983. The mean diameter for stand density index. *Canadian Journal of Forest Research*, 13:5, 1023-1024. https://doi.org/10.1139/x83-135